# IMPACT OF LAND COVER TYPE ON TEMPERATURE

*Thesis submitted to Jawaharlal Nehru University*

*for the award of the degree of*

## DOCTOR OF PHILOSOPHY


## NAHID ARABI

CENTRE FOR THE STUDY OF REGIONAL DEVELOPMENT

SCHOOL OF SOCIAL SCIENCES

JAWAHARLAL NEHRU UNIVERSITY

NEW DELHI-110 067


2017

जवाहरलाल नेहरू विश्वविद्यालय
JAWAHARLAL NEHRU UNIVERSITY
Centre for the Study of Regional Development
School of Social Sciences
New Delhi-110067

# CETIFICATE

This is to certify that the thesis entitled "**Impact of Land Cover Type on Temperature**" is submitted by **Nahid Arabi,** for the award of the degree of **Doctor of Philosophy** from **Jawaharlal Nehru University**, New Delhi, is bona fide record of research work carried out by her under my supervision. The content of this thesis, is full or in parts full, have not submitted to any other Institution or University for the award of any degree or diploma in this or any other university in India or outside.

We recommend that this thesis is placed before the examiners for evaluation.

**Dr. S. Sreekesh**
(Supervisor)

**Prof. Sachidanand Sinha**
29.9.17
(Chairperson)

Tel.: 26704463, Gram : JAYENU Fax : 91-11-26742586, 26741504

I dedicate this thesis to my dearest, beloved and caring husband Abolfazl Sadeghnezhad for all his support and encouragement

and my parents for their patience

# ACKNOWLEDGEMENT

In the name of God

First and foremost I would like to thank God for giving me the ability and the intellect to carry out this research until completion.

I would like to thank all faculty members for all their co-operations, help and efforts and again my special thanks go to the CSRD chairperson, Professor Sinha for his immense and unforgettable understanding of my circumstances and his help and also professors Deepak K. Mishra, Atul Soud and Milap Sharma, for their help and efforts.

I would like to thank all the staff in the Department for helping me in one way or another and specially Mr. Sherma in the CSRD office for all his help and kindness.

I would also like to thank all my friends everywhere for the encouragements.

Finally I would especially like to thank my husband who has supported me in every step of completing my thesis and without his help, patience and encouragements; this work would never be completed.

My deepest gratitude goes to my parents and family members for their support during the years of my study and their perseverance.

Nahid Arabi

# CONTENTS

# LIST OF TABLES AND FIGURES

# Chapter 1

**Background, Data and Methodology**

## Introduction

One of the important issues in climate studies is temperature and the factors that affect it. Temperature attracts the attention of researchers more than any other climatic factor as its impact on the climate is more visible. Various environmental factors affect the temperature and one of these factors is land cover. The magnitude of the impact of this factor on temperature varies depending on the type of coverage and characteristics of each area. That is why the outcome of a research on any region cannot be generalized and applied to all areas and each area needs its own studies. Investigating the type of land cover and its effect on temperature requires understanding of land cover change over different periods. For this reason, the study of climate and its effect on human life during various periods of land cover change has been considered and many efforts have been made to study climate change from the past to the present time and its possible future changes to be predicted. (Otieno el 2012).In recent years the possible factors influencing temperature have been investigated and the results have shown that land cover and greenhouse gases are the most important factors affecting temperature changes. (Nayak et.al2008). Land cover change particularly in cities has affected the range of maximum and minimum temperatures. (kalnay 2003).

In their studies, climate researchers measure any environmental changes with the magnitude of impact of these changes on temperature. The reason for this is that many scientists have predicted the temperature of planet Earth will increase by 2˚C by 2040 and in 2100 this increase will be at 5˚C Alijani, (2000). Also, Koziov & et al (2002), believe the global mean temperature has increased over the past 100 years by 0.3–0.6 ◦C and a further increase of 0.9 to 3.5 ◦C is predicted by the year 2100. The current Scientific Consensus is that according to the NASA, statement from 18 scientific associations on climate change is ”ninety-seven percent of climate scientists agree that climate-warming trends over the past century are very likely due to human activities” and most of the leading scientific organizations worldwide have issued public

statements endorsing this position. Human activities in his surrounding environment have affected temperature and subsequently the climate, locally, regionally and even globally. The above observations and predictions seem to be realistic in populated areas such as cities where by changing land cover type as a result of human activity related developments we lay the path for temperature increase. In fact, the resulting effects of human activities and accomplishments on Earth appear in the form of land cover change which may be one of the effective causes of temperature change.

In order to understand the extent of impact of land cover on temperature, we first need to understand how land cover type can have any impact on temperature. To appreciate this, generally, land cover is divided into two main groups of the utilized and unutilized lands. Utilized lands are those which include civil structures, residential, commercial, industrial, cultural, educational, recreational and official buildings. We must not forget the huge portion of this type of land being utilized by the transport industry in the form of parking spaces, highways and railways. Unutilized lands are empty lands and those naturally created and maintained without much of interaction or influence by human activities. Deserts, forests or woods, beds of rivers and lakes, derelict and barren and empty lands are examples of this type of lands.

In either case the type of Land cover such as vegetation, constructed dams and artificial lakes, residential buildings, industrial complexes and created civic green spaces each contribute to absorption and re-radiation of the solar rays which affect the temperature.

Solar radiation absorption and reflection level of a built-up area is not the same as that of a vegetation cover. Either of these responds differently to radiation, resulting in different levels of temperature. This phenomenon can be more clearly understood if we imagine the difference in a larger proportion such as an area of 100s of acres of land covered with ceramic roof tiles. These tiles absorb a huge amount of solar radiation converted into solar heat. Throughout the day the absorbed and dissipated hate obviously affects the temperature of the whole area creating a micro climate.

In contrast, with solar radiation absorption level of vegetation cover being lower than that of ceramic tiles, we can see why the temperature of cities are normally higher than the green suburbs without accounting for other factors such as air circulation difference in built up and open areas or many human related activities such as city transportation, use of heating/cooling and cooking appliances, etc., etc. Population increase and urban life and area expansion has

changed all types of land cover in urban and surrounding areas and this has resulted in a varying climate change which is called city climate, (Rose et al. 2009).

This is how cities as the most important centers of human activities have the most influence on changes in land cover as a result of residential and industrial developments. Although cities, towns and settlements cover only a tiny fraction of the world's surface, urban areas are the nexus of human activity, (70–90% of economic activity with more than 50% of the population (Schneider et al, 2010).

In general, the root of city climate investigation goes as far back as the beginning of the 19th century, when Howard published his first active study entitled "London weather" based on the 1813 climate findings. Since then, research in this area has much increased, particularly in the U.S, Europe and Japan. So far, various studies have taken place to show the effect of human environmental activities on temperature change. In all these studies, there is a very close relationship between land cover and the city area temperatures.

My city of Tehran in Iran has been no exception to this phenomenon and studies have been done in this area to investigate this. The reason for these studies has been the fact that industrialization is the result of human developments, wants and needs as well as population increases globally. Iran's population has now doubled over the last few decades with increasing concentration in major cities like Tehran. This, as well as the consequential impact of it on land use and the resulting land cover changes and environmental complications were the reason for choosing this topic to investigate the relationship of temperature with land cover and its possible impact on temperature.

In this research, changes in land cover in Tehran over 35 years, and its impact on the temperature of this city are studied. As a political center and the focus of human activities, Tehran is very important as the largest city of Iran. Expansion of Tehran, like many other major cities in the world, has caused extensive changes in land cover and these changes have been accompanied by environmental changes. Therefore, the study and recognition of these changes by researchers who seek sustainable development is important as they have found that sustainable development in each country is achieved through the recognition of all environmental capabilities and for this purpose the full recognition of the environmental factors and their influencing elements will be essential.

## 1.2. Literature review

Many researches have been undertaken to understand the changes in air temperature, land surface temperature and effects of land cover type on temperature. On the basis of the title of this thesis, the above three subjects have been reviewed in pre-research literatures and some of the studies that are more relevant for the present work have been mentioned in this section.

### 1.2.1. Studies based on air temperature

Narisma et.al (2002) in a paper titled "The Impact of 200 Years of Land Cover Change on the Australian Near-Surface Climate", in their study of 200 years they investigated changes in minimum and maximum temperatures over the months of January and July, using meteorological stations data. This study was carried out in Australia for the period of 1788-1988 to investigate the impact of land cover changes on temperature. Results show the impact of land cover change on local air temperature. Ahmed et.al (2000) studied temperature and rainfall and their impact on environmental degradation in Sudan. They used monthly data for each location, which were combined to obtain seasonal and annual mean time series. The linear trend was used to measure the rate of change. The changes in the variability have been considered on monthly basis. . Temperature and its changes, not only in the hot deserts of Africa, but also in the cold northern areas have been subject of investigations. Kozlov et.al (2002) assessed temperature of North Taigo. The annual, seasonal and the monthly mean temperatures have shown directional changes between the years1936-1998. The use of more accurate statistical methods that can in the Long-term show the temperature change process has an important position in the temperature studies. Amongst these methods is the Mann-Kendall method that Tcrkes used to study the trend of temperature changes in Turkey. Tcrkes et.al (2002) studied re-evaluation of trends and changes in low, average and minimum temperatures of Turkey for the period of 1929-1999. In this study, Mann-Kendall method was used to show most of the temperature series on the basis of increasing and decreasing trends of temperature in different seasons. In general, studies in this field have been very vast and it is not possible to mention them all and so some of these researches are mentioned below.

Garci et.al (2003) studied temperature predictability in the great Mediterranean area. Annual and seasonal average temperatures have been considered for this study during the period 1955 to1990. The spatial patterns derived from seasonal mean temperature and high variability.

Livingstone (2003) studied impact of secular climate change on the thermal structure of a large temperate central European lake. He used monthly mean temperature during the period of 1950 to 1990. His research showed that increase of temperature exists in central Europe Lake.

Xain et.al (2004) used the ETM & TM images taken in 2003, 2001, 2000, 1995, 1994, and based on ultra violet band and NDVI indicator of temperature of city investigated the effect of human activities and urbanisation on climate of Tampa bay in Florida. They calculate land surface temperature and then used data taken from 16 ground based stations including mean of yearly, monthly temperature & rainfall. According to their study during the 1970s, an increasing level of $0.02C^{\circ}$ was seen which was because of an increasing temperature of the city urban thermal islands. Rigo et.al (2006) by use of MODIS and ETM images taken in 2002 and also by use of the measured climatology data from ground based stations including temperature and moisture, studied the heat of the surface of baste. This kind of temperature measurement showed the variable temperature (satellite and ground based station) in similar places. Ulden et.al (2007) had studied climate in central Europe using mean temperature and mean precipitation. They found changes in the summer climate in the central Europe. Anisimov et.al (2007) studied mean annual and seasonal temperature. Their study surrounded the 'Analysis of changes in air temperature in Russia and empirical forecast for the first quarter of the $21^{st}$ century'. .

Bahak, (2012), studied the rain level and temperature changes in Kerman, using statistical data for the period of 1956-2000 and the Mann-Kendall method. He found sudden and fluctuating changes in the study area over the period. . Bandyopadhyay et.al. (2011), To study the temporal trend of meteorological parameters over 32 years (1971-2002), monthly meteorological data were collected from 133 selected stations over different agro-ecological regions of India. They employed the Man-Kendall method is their extensive study.

Bisai.D et al(2014), Statistical Analysis of Trend and Change Point in Surface Air Temperature Time Series for Midnapore Weather Observatory, West Bengal, India. They studied temperature time series data of the period from 1941-2010. Fluctuations and trends of annual mean temperature, annual mean maximum temperature and annual mean minimum temperature time series were statistically examined. The results showed that Midnapore experienced a cooling trend, in general.

### 1.2.2. Studies based on land surface temperature

In addition to statistical data and the analysis of data to study temperature, the use of satellite imagery has also been of utmost importance in the climate studies. Here are a few of the relevant researches.

Chen et.al 2001, in a study in Singapore and part of Malaysia which is considered a tropical area, using the Landsat TM and ETM images related to 1990 and 2000, calculated the emissivity and the surface temperature. They classified the images by unsupervised classification method into 8 classes to investigate the relationship between land cover and temperature. Xiao et.al (2004) studied the land surface temperature by use of TM images of 2001 in Beijing. They calculated the NDVI and emissivity to derive the land surface temperature. To analyse land cover they used a map scale of 1:10000. They analysed the city temperature model and the land cover type to identify the relationship between land cover and temperature. Stathopoulou et.al (2007) investigated 5 big cities of Greek by use of ETM images. In this research land surface temperature was calculated and showed that there is a relation between the type of land cover and the temperature and drawn its maps in GIS. Yuan et.al (2007) used ETM & TM images and NDVI indicator in order to study the land surface temperature in four seasons. They investigated the images for Minnesota on 21s May 2002, 16$^{th}$ July 2002, 12$^{th}$ September 2000, and 27$^{th}$ February 2001. Amiri et.al, (2009) studied Spatial–temporal dynamics of land surface temperature in relation to fractional vegetation cover and land use/cover in Tabriz city. Multi-temporal images acquired by Landsat 4, 5 TM and Landsat 7 ETM+ sensors on 30 June 1989, 18 August 1998, and 2 August 2001, were processed to extract LULC classes and land surface temperature (LST). Mbithi et.al, (2010), "The impact of land use and land cover changes on land sureface temperature". Landsat images of years 1986 (TM) and 2010 (TM) for Addisababa were used. They calculated the NDVI and emissivity to derive the land surface temperature. They specified 6 classes of land covers and investigated their impact on temperature. Widyasamratri et.al (2012) "A comparison of air temperature and land surface temperature to detect urbanization effect in Jakarta, Indonesia" They used two LandSat images for 1989 and 2006 to calculate the emissivity and the LST. Also, they used the data from two ground stations for 1980 to 2010 time series air temperatures to analyse the regression with the LST. Feizizadeh et.al (2012) in their study "Monitoring land surface temperature relationship to land use/land cover

from satellite imagery in Maraqeh County, Iran", ETM image from 31 August 2010 was used. They first calculated the NDVI then the emissivity before calculating the LST. Then, they classified the study area images into 6 classes of land cover. They selected some points from the classified area and measured the LST. Their aim was to compare the derived LST from satellite with the observed LST. They found that there was a 1.69C difference in temperature. Swadas pal et.al (2016), "Detection of land use and land cover change and land surface temperature in English Bazar urban center". They calculated the Earth's temperature using three Landsat satellite images of 1991, 2010, and 2014. They chose the months of January, April and October according to the winter season and the West Bengal Monson. They divided their study area into 6 classes and found that the increase in surface temperature was proportional and relative to the variation in land cover type.

### 1.2.3. Studies based on land cover changes

Weng. Q (2001) studied the effect of development of cities on the Earth temperature in the Zhujiang detta in China. He, by use of Landsat images TM, classified data related to 1989, 1994 and 1997 and supervised classification method, classified the lands to 7 classes. Mahiny (2002) "Accuracy assessment of land use and land cover change modeling results, a long neglected aspect of RS and GIS applications in Iran". In his study, a MSS scene of the year 1973 and a TM scene of the year 2000 were selected as the start and end dates. His study area was the city of Gorgan to investigate the land cover changes using classified satellite images. Alavipanah et.al (2003) used land cover classification in Varamin plain. They used TM satellite images in this study. In Varamin, they found 4 groups of land cover types of Vegetation; soil; water; civil area, using supervised classification method. Etudoyin (2011), using LandSat images for 1986 and 2000 investigated the land cover changes of river basin area of Nigeria and specified 7 types of land cover. Their paper was "GIS assessment of land use and land cover changes in OBIO/AKPOR L.G.A., rivers state, Nigeria". Rahman et.al (2012) in a paper titled "Assessment of Land use/land cover Change in the North-West District of Delhi Using Remote Sensing and GIS Techniques", using two satellite images and supervised classification for the time series of 1972-2003. They specified 4 land cover classes and that in the southern part of the study area farm lands over the past 30 years had been converted to built-up area. J.S.Rawat et.al (2015), "Monitoring land use/cover change using remote sensing and GIS techniques", Landsat satellite imageries of two different time periods of 1990 and 2010 were Supervised classified. The images

of the study area were categorized into five different classes. The results indicate that during the two decades, vegetation and built-up land were increased, while agriculture, barren land and water body were decreased.

## 1.3. Statement of the problem

Human's daily actions change the natural systems of the Earth's surface and consequently by changing the types of land cover, it changes the balance of energy and this in turn creates changes in the climate. Every region on Earth has experienced numerous variations in its land cover proportional to the increase of its population during the recent decades. So when we speak of land cover change or the temperature change, all the attention is drawn towards cities and highly populated areas. Cities as the largest center of population and industry in the world have experienced some sort of land cover shift during the recent decades. Changes to the Land cover and conversion of vegetation and barren lands to buildings and other constructions do not simply mean a superficial variation. These variations and conversions on the Earth's surface have direct and indirect or a combination of these impacts on the climatic factors. Among these, temperature is more volatile than any other factor and any change in that can influence other factors of the climate.

In civil environmental programming, it is necessary to investigate the contribution of every kind of land cover to temperature changes in particular. Hot and cold temperature extremes or thresholds can have major impact on the social, economic and the life style of a city population. An ideal living condition in an ideal environment along with a plan for a sustainable development requires environmental knowledge and awareness of its elements and the influencing factors. Therefore, it is important that researchers and scientists should help environmental planners and city managers through their studies of change trends and the influencing factors to control them. It was with regards to this importance and necessity that this research was chose for the purpose of investigating the land cover changes and its impact on the city of Tehran's temperature as my thesis.

Tehran is a city with a sensitive and special climate and geographical position in that it is situated in a sink shape area surrounded by mountains in the North, blocking moderate winds and has an annual rainfall less than the global average. Therefore, any unforeseen or unplanned

environmental change can affect its balance. This urban area has been through an extreme route of land cover change during the recent decades with its developing change trend being without any clear regulations or policies.

Until now, there has not been any complete and accurate study of land cover change and its relationship with air and surface temperature of Tehran. With regards to the importance of this city, the need for an investigation of land cover change status is unavoidable. For this purpose, familiarity with time series behavior of temperature and the identification of any possible changes through reliable statistical and graphical methods is necessary. The ultimate goal of this research is to produce a clear picture of these determinations through a long term data available.

## 1.4. Theoretical framework of thesis

A phenomenon in the world formed under the name of the global warming which was caused by the rise of temperature, causing climate change on Earth. Many theories have been suggested that some of the reasons for this phenomenon are attributed to the change in land cover, some to greenhouse gases, and some to the result of solar activity. Another theory is that this phenomenon is the result of all these factors. With the expansion of cities and the resulting land cover changes; this theory of the effect of the land cover on the change in temperature will be investigated; in fact, two important environmental variables, namely, land cover and temperature will be evaluated to serve the main purpose of this study to find the relationship between these two variables. So far, many studies have been conducted in order to consider the temperature of the air and its changes in the study area. There have also been separate studies on land cover change and how the city has expanded over time. However, no study has ever been done to examine the relationship between these two variables. Therefore, the examination of the effect of land cover on temperature is a point that highlights the subject of this thesis. To achieve this goal, the two variables should be studied in the longest available periods. For this purpose, the air temperature of the long-term periodic courses are obtained from ground stations and satellite data, and for the study of land cover change, the Landsat satellite imagery have been surveyed for at least thirty years.

For the temperature as one of the variables in this thesis the time series of annual mean temperature from the ground stations is processed by Mann- Kendall method. This is a suitable

method to show fluctuations, abrupt changes, and temperature trends that are done with Excel software. Using Landsat satellite imagery, surface temperature and land cover types are determined. The temperature of the air is calculated by processing the satellite thermal band. First, digital terrestrial satellite imagery thermal band are converted to DN then through stages are converted to Celsius. In order to calculate the surface temperature in the studied area, which is a metropolitan area, the PV and the emissivity is necessary to be calculated, before calculating the NDVI. The derived LST is then used to calculate the air temperature and these are then used to produce the related air temperature maps. All these steps are done in the GIS. Also, using Landsat satellite imagery in the ERDAS software, the classification and detection of land cover changes are determined. To validate all of the information derived from the above processes, an extensive field work is undertaken by selecting a number of samples points from each of the classes in the study area and recording their temperature. Also Satellite imagery of the time of these recorded temperatures is obtained and their air temperatures are calculated and ultimately, the results are compared.

For the land cover as another variable in the thesis, images from the Landsat are classified using the Erdas software by unsupervised classification method. These are then further processed to detect any changes in land cover types in the study area.

The results obtained from the analysis of the two variables and their relationships are measured together. Based on the subject and purpose of this thesis and the objectives of research questions, the content is designed in six chapters as follows:

The first chapter includes the overall layout of the thesis, namely, the introduction, literature review and the methodology. From chapter two up to chapter five the objectives will be addressed and assessed in the order described below. In chapter two, first the ground based stations data will be analysed. The two main purposes in this chapter are, firstly to specify the hottest and the coldest months in Tehran and select the satellite images for these months to assess the land surface temperature. The second is to assess the process of temperature change using ground station data. Chapter three will be devoted to satellite imagery preparation and their supervised classification to specify the land cover types of study area of Tehran. Land cover changes over the last 4 decades will be detected and their possible impact on temperature will be assessed. In chapter four, the thermal band of satellite images will be prepared to

calculate the surface temperature over the period of 1990-2015. For this purpose, the NDVI and the emissivity will also be calculated in this chapter. In chapter five the land surface temperature will be converted to air temperature, as the purpose of the temperature assessment in this thesis is to assess the air temperature. In the study area field work for this research, certain points will be specified and their air temperatures will be measured. Then the satellite images of the relative period will be retrieved to first calculate the surface temperature to be converted to air temperature. Ultimately, the derived temperatures from satellite images, the data from ground based stations (in chapter 2) and the field work will be compared and analysed. In chapter six, the results of land cover change detection and the temperature changes will be assessed and analysed in relation to one another. Then the final results will be obtained to answer the questions raised in this thesis.

A further point that is important to be mentioned in this thesis is the time difference and discrepancy in the study area calendar. According to the Iranian calendar which is not in line with the Georgian calendar and there is a lag in the seasonal months of each year, so that July of 1990 and January of 1991 are the months of summer and winter of the same year in the study area calendar. Therefore, for the purpose of this study the order of the months were chosen in this way.

## 1.5. Objectives

- To analyze the monthly variation in temperature through 1950-2011
- To analyze land cover changes in Tehran city
- To spatially map monthly temperature variability using satellite images
- To correlate the temporal changes in land cover with temporal changes in temperature.

This study aims to address the following research questions:

- To assess whether or not the temperature changes in Tehran are linked to any type of land cover change.
- To compare the data from the fieldwork ground observation with the data from satellite in the same region.

## 1.6. Methodology

The first objective of this research is the investigation and analysis of ground station statistical data from 5 stations as shown in the table below with the longest data period of over 40 years. The reason for choosing this objective to begin with, is that it is aimed to find the hottest and coldest months of the winter and summer seasons, based on the mean minimum and maximum temperatures respectively.

Then, selection of the satellite image dates will be based on the coldest and hottest months of this statistical period. Following this, using an appropriate method to show the temperature status with time series, trends, fluctuations and possible temperature changes are investigated.

### 1.6.1. Mann-Kendall Test

The purpose of the Mann-Kendall (MK) test (Mann 1945, Kendall 1975, Gilbert 1987) is to statistically assess if there is a monotonic upward or downward trend of the variable of interest over time. A monotonic upward/downward trend means that the variable consistently increases /decreases through time, but the trend may or may not be linear. The MK test can be used in place of a parametric linear regression analysis, which can be used to test if the slope of the estimated linear regression line is different from zero. The regression analysis requires that the residual from the fitted regression line is normally distributed; an assumption not required by the MK test, that is, the MK test is a non-parametric (distribution-free) test.

Hirsch, Slack and Smith (1982, page 107), indicate that the MK test is best viewed as an exploratory analysis and is most appropriately used to identify stations where changes are significant or of large magnitude and to quantify these findings.

Based on Kendall model, (u) and (u') in the diagrams provided show the time series. Lack of any confluence of two indicators is indicative of lack of any change in the time series Torkesh et al, (2002). The confluence of two graphs series1 (u) and series2 (u') indicate the point of change and trend. This is so, that if these lines intersect within the critical range of ±1.96 (u, u'), they mark the beginning of a sudden change in the datasets. However, periodical intersection of lines at this level denotes temperature fluctuation. In the case of critical intersect being outside of

the time series it is indicative of a trend. With the confluence of lines above or below the standard number of 1.96, the test probability level is 95%. (Alijani, 1998).

In this research the long-term statistics of average minimum and maximum temperatures obtained from each station will be reviewed using Mann-Kendall ratings.

### 1.6.2. Atmospheric Effects and Correction

The atmospheric characteristics and the surface characteristics affect the satellite imagery as the electromagnetic energy passes through the atmosphere twice. First from the sun to the Earth and then back to the sensor. The down welling radiation from the sun is Irradiance. Radiance is the upwelling radiation from the Earth to the sensor. The interpretation and pattern recognition accuracy of satellite images are affected by the structure of the Earth's atmosphere by three processes of, scattering, absorption and reflection of solar radiation. Atmospheric correction removes the scattering and absorption effects from the atmosphere. The removal of these effects is an important pre-processing step to convert at-satellite spectral radiances to at-surface radiance in order to produce accurate and realistic data and improve the image classification.

### 1.6.3. Land Cover Change

One of objective of my research is about analyzing the land cover changes in the city of Tehran. For this objective we try to develop a methodology to map and analyze land cover changes through supervised classification. This objective will be carried out by visual image interpretation. The following steps are involved in the classification procedure.

1. Stack layer in Erdas which are collected of Remote Sensing data from, LandSat 5,7,8.(1990-2015)
2. Training area definition, signature generation and supervised classification to various classes.
3. The overall accuracy of classification and the correction percentage will be calculated and its changes over the period of 40 years with 10 yearly intervals will be detected. All these processes will be implemented using the Erdas software.

### 1.6.4. Land surface temperature

To calculate the land surface temperature, the thermal band of the images will be prepared and the subsequent steps will be followed in the order listed.

#### 1.6.4.1. *Processing thermal bands*

In step one: The digital numbers (DN) of the images are converted into units of radiance and then reflectance.

(According to the LandSat user's guide):

$L\lambda$ = "gain" * (DN) + "offset"

In this formula, $L\lambda$ is the radiance of the pixel and is calculated by multiplying the gain of the sensor's band by the DN value. To cut a long-story short, this gain is calculated to account for the fact that there are different Landsat satellites and different Landsat formats.

To convert the image into radiance we need some information to find out whether each band was "high or low gain". This information can commonly be found in the header file.

$L\lambda = ((LMAX\lambda - LMIN\lambda)/(QCALMAX-QCALMIN)) * (QCAL-QCALMIN) + LMIN\lambda$

In step two: The thermal band is converted to Kelvin and then to centigrade.

$T = K2 / \ln(K1 / L\lambda + 1) – 273.15$

In the above formula, the kelvin value of the thermal band minus 273.15 will give the temperature value in centigrade. In step three: since in this research we aim to calculate the emissivity for accurate calculation of the land surface temperature, in this step we first calculate the NDVI and then the emissivity as this is necessary for its estimation.

#### 1.6.4.2. *Normal Difference Vegetation Index*

The NDVI is a vegetation index to monitor the density and condition of vegetation or vegetation health. The NDVI is the most commonly used vegetation index for monitoring vegetation globally. Here, the purpose of calculating the NDVI is merely to derive the figures to calculate the emissivity. Mathematically NDVI is calculated using the below formula:

$$\mathrm{NDVI} = \frac{p_{\mathrm{NIR}} - p_{\mathrm{red}}}{p_{\mathrm{NIR}} + p_{\mathrm{red}}}$$

The significance of NDVI value from -1 to 1 is interpretation of NDVI images. The variations of NDVI have pronounced effect on the seasonal variation of temperature.

#### 1.6.4.3. *Emissivity*

Emissivity describes a material's ability to emit or release the thermal energy which it has absorbed. The emissivity of a surface is controlled by such factors as water content, chemical composition, structure, and roughness (Snyder et al., 1998). For vegetated surfaces, emissivity can vary significantly with plant species, areal density, and growth stage (Snyder et al., 1998). In the meantime, emissivity is a function of wavelength, commonly referred to as spectral emissivity (Dash et al., 2002).

Estimation of emissivity for ground objects from passive sensor data is measured using different techniques such as the NDVI method, Valor & Casetles (1996), which will be used in this research to separate temperatures from emissivity, so that the effect of emissivity on estimated LST can be determined. In this research, due to the suitability of the data available, it has been preliminarily decided to use the classification based estimation and the NDVI method to estimate the required emissivity. One of the most powerful models for the estimation of emissivity is:

$$e = 0.004 * pv + 0.986$$

A number of researchers have used the above formula to calculate the emissivity including, (Sobrino, 2004) in his research titled "Land surface temperature retrieval from LANDSAT TM 5"; Also (Shah, 2015) in his study paper of "MaPPing Urban Heat Island Effect in Comparison with the Land Use/ Land Cover of Lahore District", made use of the same formula.

Proportion vegetation (Pv) is the fraction cover that could be directly obtained from the NDVI vegetation index, that is obtained from satellite measurements.

$$Pv= [(NDVI-〖NDVI〗_min)/(〖NDVI〗_max-〖NDVI〗_min )]2$$

#### 1.6.4.4. *Calculating land surface Temperature*

In the final step: using the below formula, we calculate land surface temperature.

$$T_s = \frac{T_B}{1+(\lambda \times T_B / \rho)\ln \varepsilon}$$

The calculation of land surface temperature will be carried out for all images related to the months of January and July during the period of 1990-2015. Having obtained the land surface temperature maps, the temperature of different periods and the level of changes will be assessed and analyzed. Since the temperature of the images will vary, these maps will be standardized so that their temperature will fall between 0-1 to allow the comparison of images with similar values.

N= (T-Tmax) / (Tmax –Tmin)

### 1.6.5. Air temperatures

One of the most important discussions in this thesis is the subject of temperature. As already mentioned, the main purpose of this thesis is to assess the impact of land cover on temperature, i.e. air temperature. Here, all land surface temperature maps will be converted to air temperature maps. One of the best line expressions to convert LST to air temperature is related to (Garcia – cuelo, 2000) as below:

Ta = 14.6 + 0.44 * LST where,

Ta, is the air temperature,

14.6 And 0.44 are constants,

In the chapter relating to air temperature, the surface temperatures of the satellite images related to the field work period, will also be converted to air temperatures, using the above formula.

### 1.6.6. Temporal Changes in Land Cover and Temperature

In the final stage of carrying out this research the air temperature maps, land cover change maps and the results obtained from assessing the air temperatures of the ground sources, (ground stations and the field work) will be compared and analysed. The final results will show whether or not there is a relationship between land cover change and temperature change. In other words, the proposed hypotheses will either be accepted or rejected.

## 1.7. Data

In line with the aims of this thesis and objectives mentioned, two sources of data have been used including ground data and satellite data as follows:

**Table 1.1 Tehran of city meteorology stations (1951-2011)**

| Station | High | Longitude | Altitude | Period |
|---|---|---|---|---|
| Mehrabad | 1191 | 51 18 34 | 35 41 36 | 1951-2011 |
| Dushan-TaPPeh | 1122 | 51 28 33 | 35 42 08 | 1972-2011 |
| Shemiran | 1708 | 51 29 07 | 35 47 56 | 1988-2011 |
| Geophysics | 1419 | 51 23 12 | 35 44 48 | 1991-2011 |
| Chitgar | 1067 | 51 10 19 | 35 44 57 | 1996-2011 |

### 1.7.1. Ground data

Meteorological data from the meteorological organization of Iran will include the monthly temperature data at various stations in Tehran, starting from 1950 to 2011. As well as these, air temperatures based on the land cover classes will be recorded during the field work study and these will be used in the air temperature analysis in chapter 5.

### 1.7.2. Satellite Data

The Landsat 5, 7 and 8 images for (1990-2015) used to assess the Land cover changes and their thermal bands used to determine the surface temperature. The Landsat Thematic Mapper (TM) 5, 7 satellite images used to understand and interpret the land cover and land surface

temperature in the area. The satellite images downloaded from USGS online websites, which are freely available to users. It endeavored to obtain the best satellite images of particularly cloud free quality. This was possible for all years with the exception of the images for 1990 or even the year before and after, relating to the coldest month. For the purpose of investigation and analysis of these data the following tables have been devised.

**Table 1.2 Landsat satellite images in July 1980-2014**

| Year | Month | Landsat | Image date |
|---|---|---|---|
| 1990 | July | LandSat 5 | 1990-07-31 |
| 2000 | July | LandSat 7 | 2000-07-18 |
| 2009 | July | LandSat 5 | 2009-07-19 |
| 2014 | July | LandSat 8 | 2014-07-01 |

**Table 1.3 Landsat satellite images in July 1991-2015**

| Year | Month | LandSat | Image date |
|---|---|---|---|
| 1991 | January | LandSat 5 | 1991-01-07 |
| 2001 | January | LandSat 7 | 2001-01-10 |
| 2010 | January | LandSat 5 | 2010-01-27 |
| 2015 | January | LandSat 8 | 2015-01-25 |

## 1.8. Study area

Tehran is between the orbits of 35˚ 36′ to 35˚ 49′ of northern latitude and 51˚ 4′ to 51˚ 33′ of eastern longitude. The huge city of Tehran with a surface area of 2300km squares (Center for



,

civil programming studies in Tehran, 1999), surrounded in the north and east by Tochal, Sepaye and Bibi-shahrbanoo and in the west and south by Shahriyar and Varamin plains. As a result, this city has both the advantages of a mountainous region and the problems and limitations of a desert region.

Etborz altitudes have separated Tehran from Caspian see shores and created the mountainous landscapes in the north of the city. Tehran is on the base of highest hills of Elborz which has a steep slope from north to the south, so, as the highest peak of this mountain is (Damavand) with the height of 5678 meters above sea level and the lowest part is the Kavir desert 800meters below sea level. This unique sink like situation of Tehran and the heights which surround it affect its atmosphere and local climate. The particular topographical situation of Tehran results in creating two systems of displacement of air as follows (Alijani, 1997):

### 1.8.1. Local circulation of mountain and plain

As a whole, the physical surface of the Earth because of the suns' radiation is hot and creates an atmospheric low pressure circulation in the low level of atmosphere and vice versa, during the night because of absence of sunshine, or ground irradiancy, physical surface of Earth is cold and accordingly creates an atmospheric high pressure of circulation in the low level of atmosphere and this variety of pressure creates wind.

The dark and uneven rocks in the north heights of Tehran gain more sunshine during the days, so the air adjacent to these surfaces is hotter than the air of the plains (the even lands and lower). As a result, there is an air circulation from plain to mount called plain breeze.

The opposite of this happens at night. After the sunset, the rocky body of mountains, because of air diluteness and low moisture and ground irradiancy, loses its heat quicker and gradually become colder than even lands and plain, then the cold air of these areas move to plain which have hotter air and result in creating mountain breeze. According to above statements, it can be said that in Tehran, there is south wind during days and north wind during nights. These circulations can have a crucial role in dispersion of atmospheric pollutions in Tehran.

### 1.8.2. Local circulation in valleys:

The presence of several valleys in the north of Tehran and the Toochal foots results in the cold and accumulated air of these valleys circulating to plain and low areas and create a cold and (mild) breeze. Of course, the level of the effects of these kinds of circulations depends on several factors such as the depth and extent of valley, the number of natural and artificial obstacles against them. The presence of such a tranquil circulation has a significant role in air pollution dispersion in Tehran and the time and place of this can be ever changing.

Another important point in Tehran topography which relates to air pollution is that, the north and northeast of Tehran is wholly surrounded by Elborz heights or in other words, Tehran is wind sheltered by Elborz heights. The result is that it does not benefit from the moisture and northern circulation of Caspian Sea. On the other hand these heights mimic a windbreaker action against the western winds which are the basic systems of air circulations especially in the cold months of the year and result in stagnation of the air and remain in the eastern and north eastern of the city and as a result this problem is very crucial in the subject of air pollution.

Three geographical factors which have an important role in climatology structure of Tehran are (Alijani, 1997):

A. *Kavir desert*: dry area such as Ghazvin Plains, Kavire Ghom, and dry areas of Semnan state which are neighbor to Tehran, all have negative effect on the air in this city and cause to heat and dry the air along with dust.

B. *Western moist and rainy winds*: most of the winds blows from west and northwest of the country and have an effective role in modulation of the torrid heat of desert.

C. *Elborz Range Mountains*: these mountains which separate Tehran from Caspian Seashores have large effects on modulation of Tehran air. Raining in Tehran usually depend on the factor, height, so as in the north area because of mountainous circumstances, the amount of rain compare with the southern part of it is much more.

### 1.8.3. Air mass

Geographical situation of Tehran is such a way that during a year it settles against northern and western air circulations in different forms. The basic aerial ranks which affect Tehran consist of:

**1.8.3.1. Siberian high pressure circulation**: this high pressure air which forms during the early autumn in Siberia, at the highest point of its activity enters Iran, resulting in heavy snow fall in Tehran. This haPPens when this circulation meets with Mediterranean and Jordanian low pressure systems, as well as causing a decline in temperature.

**1.8.3.2. Western migration of high pressure**: this high pressure usually moves from some parts of north or central Europe to Iran. This cold weather, In the case of encountering to relative warm weather of southern latitudes, may fall in the form of snow in the northern and southern margins of Elborz heights.

**1.8.3.3. Azoour high pressure**: this high pressure circulation which has formed on Azoour islands because of air dynamic subsiding, affect the southern margin of Elborz in summer along with the stable air.

**1.8.3.4. Mediterranean low pressure system:** much of winter fall in our country relates to this system. The precipitation result of this system in even land and plateau is rain and on the northern and northeast heights is snow.

**1.8.3.5. Jordanian low pressure system:** this system enter our country from the region of north of Jordan. Its way to our country is from west, southwestern and even south. If this system meet the cold air of northern latitudes it results in snow fall on the heights and rain in plains and plateaus in the neighborhood of mountains.

## Reference


1. Ahmed, N. E. and Mansell, M. G., 2000. Climate impacts of environmental degradation in Sudan geo journal, Vol.50 PP. 311–327.

2. Alavi Panah, S. K.Ch B Komaki, A Goorabi and H R Matinfar, 2007, Characterizing Land Cover Types and Surface Condition of Yardang Region in Lut Desert ( Iran ) Based upon Landsat Satellite Images, World APPlied Sciences Journal 2, Vol. 3, PP. 212-228.

3. Alijani, B., M. Kaviani 1998. The principles of climatology. Payam-e Noor publisher, Tehran.

4. Amiri, Reza Amiri., Qihao Weng, Abbas Alimohammadi& Seyed Kazem 2009. Spatial temporal dynamics of land surface temperature in relation to fractional vegetation cover and land use/cover in the Tabriz urban area, Iran, Remote Sensing of Environment, Vol. 14, PP. 2606-2617.

5. Anisimov .O .A, V. A. Lobanov, and S. A. Reneva 2007. Analysis of changes in air temperature in Russia and empirical forecast for the first quarter of the 21st century, meteorology and hydrology, Vol. 32, PP. 620–626.

6. Bahak,B 2013. Studied the rain level and temperature changes in Kerman, sarzamin Jornal,Iran, Vol 34.

7. Bandyopadhyay. A; A. Bhadra; N. S. Raghuwanshi; and R. Singh 2011. Temporal Trends in Estimates of Reference Evapotranspiration over India, Journal of Hydrologic Engineering, Vol 14.

8. Bisai.D, Chatterjee. S, KhanA. And Barman NK, 2014. Long Term Temperature Trend and Change Point: A Statistical APProach, journal of atmospheric and climate change, Vol. 1

9. Chen, X. L., Zhao, H. M., Li, P.X & Yin, Z.Y. 2006. Remote sensing image–based analysis of the relationship between urban heat island and urban use/cover changes. Remote sensing of Environment,Vol. 104 ,PP. 133-146.

10. Dash P. Dash, F.-M. Göttsche, F.-S. Olesen & H. Fischer 2002. Land surface temperature and emissivity estimation from passive sensor data: Theory and practice-current trends, International Journal of Remote Sensing, Vol 23.

11. Etudoyin 2011, “GIS assessment of land use and land cover changes in OBIO/AKPOR L.G.A., rivers state, Nigeria”.

12.Feizizadeh.B, Thomas Blaschke , Hossein Nazmfar, Elahe Akbari & Hamid Reza Kohbanani 2012., land surface temperature relationship to land use/land cover from satellite imagery in Maraqeh County, Iran, Journal of Environmental Planning and Management, Vol 56.

13. Garcia,.R, T. Mun˜oz, E. Herna´ndez, P. Ribera, and L. Gimeno 2003., Temperature predictability in the great Mediterranean area, theoretical applied climatology, Vol.75,PP. 179–187.

14. Kozlov Mikhail. V and Natalia G. Berlina 2002. Decline in length of the summer season on the Kola Peninsula Russia, climatic change, Vol. 54, PP. 387–398.

15. Livingstone David M 2003. Impact of secular climate change on the thermal structure of a large temperate central European lake, Climatic Change, Vol 57, PP. 205–225.

16. Mahiny 2002. "Accuracy assessment of land use and land cover change modelling results, a long neglected aspect of RS and GIS applications in Iran, Department of the Environmental Sciences, Gorgan University, Gorgan, Iran .

17. Mbithi.D, Ermias T. Demessie and, Tendai Kashiri 2010. The impact of Land Use Land Cover LULC. changes on Land Surface Temperature LST.; a case study of Addis Ababa City, Ethiopia, Kenya Meteorological Services.

18. Narisma G. T and A. J. Pitman 2002. ,The Impact of 200 Years of Land Cover Change on the Australian Near-Surface Climate, Journal of, hydrometeorology, Vol. 4, PP. 424-437.

19. Nayak. S and M. Manda 2008. Impact of land-use and land-cover changes on temperature trends over Western India, Centre for Oceans, Rivers, Atmosphere and Land Sciences, Indian Institute of Technology, Kharagpur,India.

20. Otieno.V, R. O. Anyah 2012. Effects of land use changes on climate in the Greater Horn of Africa, Contribution to CR Special 29 'The regional climate model RegCM4, Published March 22, Vol. 52, PP. 77–95.

21. Rahman. A, Sunil Kumar, Shahab Fazal, Masood A Siddiqui 2012. In a paper titled Assessment of Land use/land cover Change in the North-West District of Delhi Using Remote Sensing and GIS Techniques, Indian Soc Remote Sensing, DOI 10.1007/s12524-011-0165-4.

22. Rigo,G,. Parlow,E & Oesch, D.2006.Validation of satellite observed thermal emission with insitu measurements over an urban surface.Remote sensing of Environment,Vol.104,PP.201-210.

23. Rose.L, Monsingh D Devadas, 2009, Analysis of land surface temperature and land use/land cover types using remote sensing imagery-a case in chennai city, india, The Seventh International Conference on Urban.

24. Rawat. J.S, ,Manish Kumar 2015., Monitoring land use/cover change using remote sensing and GIS techniques: A case study of Hawalbagh block, district Almora, Uttarakhand India, The Egyptian Journal of Remote Sensing and Space Sciences , vol.18, PP. 77–84.

25. Shah. B, B Ghauri, 2015, MaPPing Urban Heat Island Effect in Comparison with the Land Use/ Land Cover of Lahore District, Journal of Meteorology Vol. 20.

26. Snyder.C, A. Joly 1998, Development of perturbations within growing baroclinic waves, Quarterly Journal of the Royal Meteorological Society, Vol. 124, PP. 1961–1983.

27. Stathopoulou, M, Cartalis, C 2007, Daytime urban heat islands from landsat ETM+and Corine land cover data: An aPPlication to major cities in Greece. Solar Energy,Vol. 81, PP. 358-368.

28. Sobrino.J.A,. C.Jiménez-Muñoz and L.Paolini2004, Land surface temperature retrieval from Landsat TM 5, Remote Sensing of Environment, Vol 90, Vol. 4, PP. 434-440.

29. Swadas pal and Sk.Ziaul 2016., Detection of land use and land cover change and land surface temperature in English Bazar urban center, The Egyptian Journal of Remote Sensing and Space Science, Vol 20, Vol 1, PP. 125-145.

30. Tcrkes Mcrat, Utkum Somer And Ismail Demir 2002., Re-evaluation of trends and changes in mean, maximum and minimum temperatures of turkey for the period 1929-1999, international journal of climatology, vol 22, PP 947-977.

31. Ulden Aad van & Geert Lenderink & Bart van den Hurk &Erik van Meijgaard, 2007, Circulation statistics and climate change in Central Europe: PRUDENCE simulations and observations, Climatic Change, Vol. 81, and PP.179–192.

32. Valor.E, V.CasellesOpens 1999, MaPPing land surface emissivity from NDVI: APPlication to European, African, and South American areas, Remote Sensing of Environment, Vol. 57, Vol. 3, PP. 167-184

33. Weindor ,D.C., M.H. Bahnassy, S.M. Marei& M.M. El-Badawi2010., Monitoring land cover changes in a newly reclaimed area of Egypt using multi-temporal Landsat data. APPlied Geography Vol. 30, Vol .4, PP. 592-605.

34. Weng, Q.2001. Effect of development of cities on the Earth temperature in the Zhujiang detta in China. INT. J. Remote sensing, Vol.10, PP.1999-2014.

35. Widyasamratri 2013, A comparison of air temperature and land surface temperature to detect urbanization effect in Jakarta, Indonesia, Atmosphere & Oceanography & Climate change, University of Yamanashi, Japan

36. Xian, G,. Crane, M. 2004. Evaluation of urbanization influences on urban climate with remote sensing and climate observations. SAIC/ USGS National Canter for Earth Resources Observation and Science, Sioux falls, SD 57198.

37. Yuan, F., Bauer, M. E. 2007. Comparison of impervious surface area and normalized difference vegetation index as indicators of surface urban heat island effects in Landsat imagery. Remote Sensing of Environment, Vol. 106, PP. 37 5-386.

# Chapter 2

**Analysis of Statistical Data**

---

## 2.1. Introduction

The study of temperature as the most important factor in climate change has attracted the attention of many scholars. Worldwide climatologists are investigating all possible activities to discover any possible relationship between the climate change and the anthropogenic behavior by studying trends in different climatic parameters, Mishra et. al (2014). Temperature has an important influence on the makeup of the planet Earth. The degree of temperature changes followed by climatic changes has immense and direct effects, not only on the natural environment of Earth but also on human life. Therefore, investigation of these changes being either fluctuating short term or long term change is unavoidable and indispensable.

Clearly, there are many reasons for temperature changes on Earth and a huge proportion of this may be blamed on human undertakings in cities. (The whys and hows of this statement have become general knowledge through primary education, various media and research literature with titles such as "anthropogenic causes of climate change" for decades. Regardless of this subject being rejected by certain guilty and irresponsible parties, no one can deny human irresponsibility in the environment has had a huge impact on global change with global pollution, land cover change, etc. The discussion of this subject is out of the scope of this research). Study of metropolises temperature makeup and its effective elements has considerable importance and helps city managers and planners in their programs of controlling planning permissions, manner of activities as well as the city land cover changes and its temperature status.

The importance of examining the climate in cities has imposed the necessity for many meteorological stations in major cities to record the status of climate parameters over time. In fact, long-term meteorological station data is considered as very important and reliable data for climatologists. In Tehran, 5 meteorological stations (Table 1.1), with good dispersion throughout the city (Fig. 2.1), record all climate parameters including temperature and provide a

valuable source of state of these parameters. In this chapter, temperature will be studied in the metropolis of Tehran during the last few decades and possible changes over a period of 60 years will be reviewed using data from the city ground based stations.

## 2.2. Data and Methodology

The following steps are involved in the monthly variation of temperature analysis using the ground temperature data collection for (1950-2011) from 5 meteorological stations), which have been obtained from the Meteorological Organization of Iran (table 1.1).

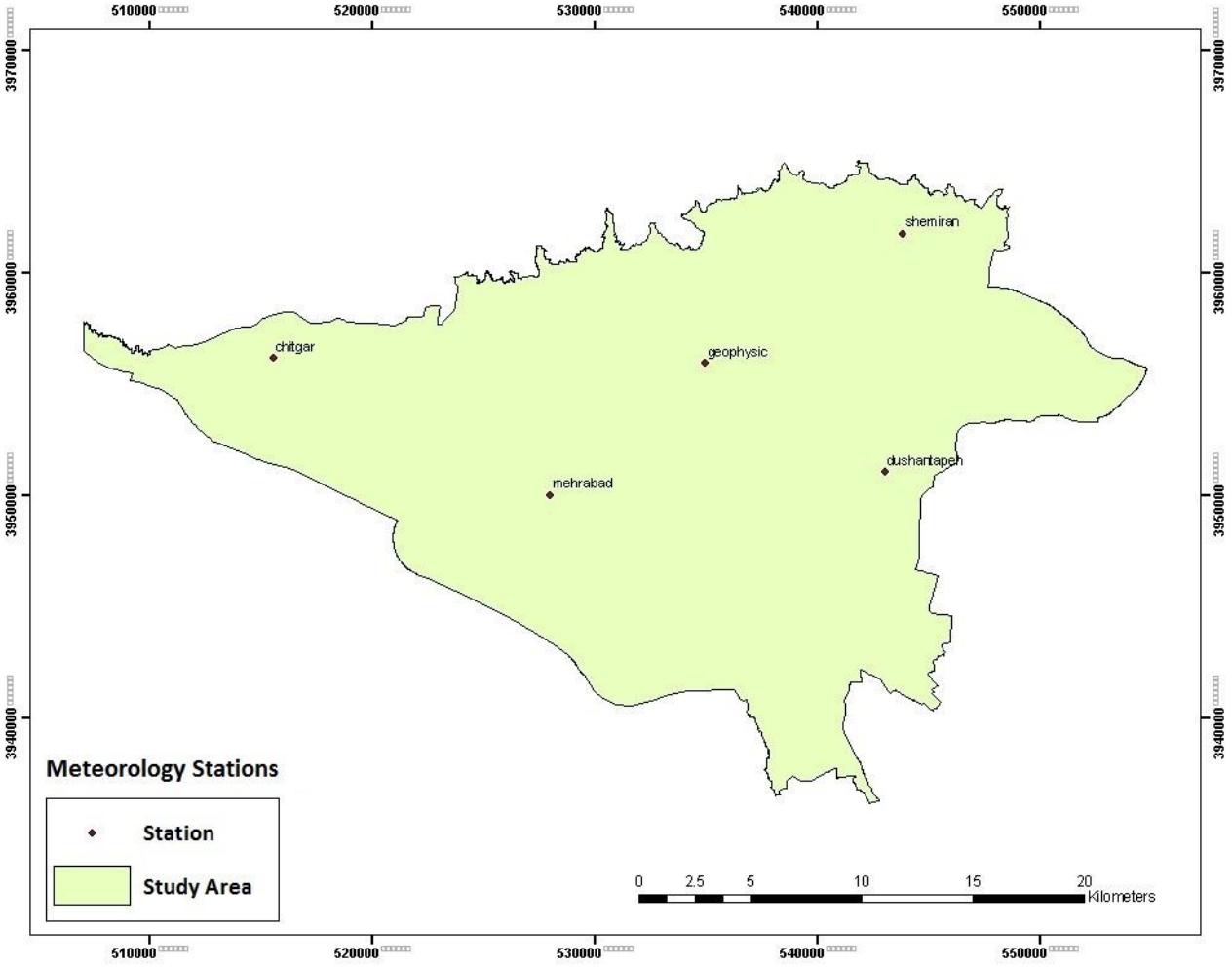


**Figure 2.1 Locations of meteorology stations in the city of Tehran**

It is worth mentioning that the history of statistical data period at these 5 stations are not the same. The data available from these stations range from 60 years at the Dushan-Tapeh station down to 15 years of data history at the Chitgar station. Shemiran station is located in the extreme north of Tehran in an area of relatively high in the southern slopes of the mountains. Chitgar station is located in the west of Tehran near the forest park and the Chitgar artificial lake. Dushan-Tapeh is considered one of the oldest stations that covers East by more than 40 years of statistical period. Mehrabad station is located near the airport with the same name as (Mehrabad airport of Tehran), holding the longest statistical data and being the most important and most reliable station. Lastly, data used in this study is from the Geophysics station which is situated near the Geophysics Institute of Tehran with statistical period data for the past 20 years. In figure 2.1, the location of the stations in the city is shown. Almost all stations are situated in proportionate and geographically appropriate directions in different directions across the city.

### 2.2.1. Assessment of temperature changes using the Man-Kendal method

In the first stage of air temperature assessment, the mean maximum/minimum temperatures from 5 ground based stations will be used with the Man-Kendal method. With this method the change, trend and fluctuations of temperature are assessed using long term statistical data. Mann-Kendall (MK) is one of the most commonly used non-parametric tests for detecting climatic changes in time series and trend analysis. The trend test is a rank correlation test for two groups of observations proposed by (Mann 1945; Kendall 1955). This test is able to suggest the significant trend in hydrological and climatological time-series data (Modarres and Silva 2007). Many scientists have studied climatic change in various areas, using long term ground data and time series. Among these, are Widyasamratri et.al (2012), who used the data from two ground based stations for 1980 to 2010 time series together with the average minimum and maximum air temperatures to compare Jakarta with its suburbs. Also, Bandyopadhyay et.al (2011) used the average temperature of the statistical data for India over the 1971-2002 period to assess temperature changes with the Mann Kendal method.

Since the purpose of this investigation is to study the changes or possible trends in temperature of coldest and hottest months in the year, therefore, July has been nominated as the hottest month to represent summer and January as the coldest, representing the winter of each year. In this research in addition to assessing temperature data from the ground based stations,

satellite images will also be used for assessing temperature changes. Therefore, selection of these images will be based on these hottest and coldest months.

### 2.2.2. Mann-Kendall Test

This test is for identifying trends in time series data around the Tehran city. One benefit of this test is that the data need not conform to any particular distribution. The test compares the relative magnitudes of sample data rather than the data values. In this method there is less chance of error than from other methods. The monthly variation of temperature plots are prepared for the u(t) and u'(t) values derived from the sequential analysis of the Mann-Kendall test where u(t) is a value that indicates the direction of trend in the time series. This procedure is formulated as follows:

First of all, the original observations are replaced by their corresponding ranks, which are arranged in ascending order. Then, for each term, the number $n_k$ of terms $y_j$ preceding it in the form of (i>j) and it is calculated with ($y_i > y_j$) and the test statistic $t_i$ is written as:

$$t_i = \sum_{k=1}^{i} n_k$$

The distribution of the test statistic $t_i$ has a mean and variance derived by

$E(t_i) = i(i-1)/4$ and $var(t_i) = [i(i-1)(2i+5)]/72$

The values of the statistic $u(t_i)$ are then computed as $u(t_i) = [t_i - E(t_i)]/\sqrt{var(t_i)}$

Finally, the values of $u'(t_i)$ are similarly computed backward, starting from the end of the series with a trend and the intersection of these curves enables us to identify the beginning of trend in the series. The quantity $t_0$ is to be located approximately without any trends a time-series plot of the values $u(t_i)$ and $u'(t_i)$ shows curves that overlap several time. Spatial interpolation and mapping of the results have been done with the help of the geo-statistical wizard of ArcGIS software. Geo-statistics refers to statistical procedures for interpolating and describing spatially auto correlated random variables (Alijani 2007). Meteorological stations are few and sparsely located in mountainous areas of Iran. Hence, there is the lack of adequate data on temperature for these areas. Therefore, the Krigging model has been used in the present study which gives better

results (Alijani 2007). The Krigging model predicts the value of an unknown point ($u_0$) from its surrounding known points ($u_i$) using optimum weights: $Zu_0 = \sum \lambda_i Z\ vi$ I=1

### 2.2.2.1. *Mean minimum temperature in* Tehran stations

The ***Mehrabad*** station (figure2.2) is one of the leading stations for continuous recording of temperature in the province and even the whole of Iran. The statistical data available at the Mehrabad station has been from 1951 to 2011. The Mehrabad station chart does not indicate a process of significant increase or decrease in temperature. However, it shows a volatile and irregular fluctuation from about 1990 onwards.

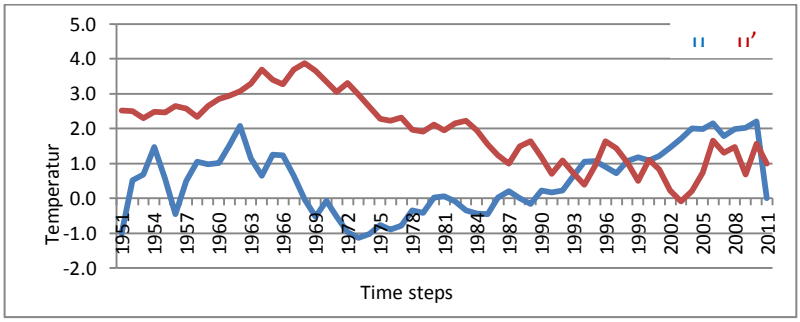


**Figure 2.2 Time series of minimum temperature in Mehrabad**

The ***Dushan-TaPPeh*** station (figure 2.3) is also one of the main and oldest stations of the city. This station holds data from 1972 to 2011. The time series show fluctuations in 1978 and 1990, indicating sudden changes through these years and no significant change can be seen and neither any trend.

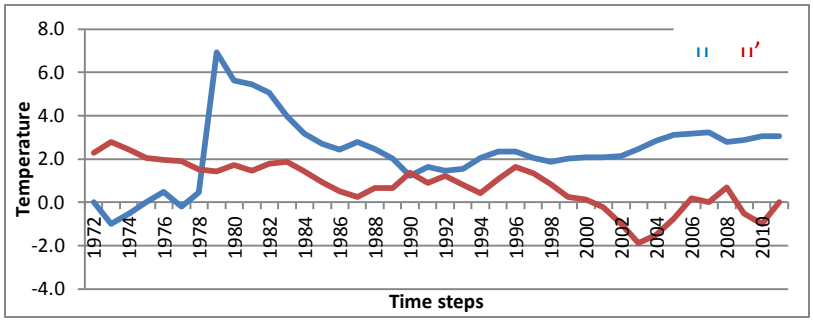


**Figure 2.3 Time series of minimum temperature in Doushan-Tapeh**

The statistical period data at the ***Shamiran*** station (figure 2.4) is from 1988 to 2011. It should be noted that the statistical period at this station is 23 years. Although this is a shorter period compared with the previous two stations and is less than the recommended 30 year period, however, shorter statistical period such as this can also demonstrate the temperature status at a station. Shamiran station is located at the extreme northern point in Tehran. No confluence of time series lines has taken place in the graph for this station, indicating that there has been no change or trend in temperature.

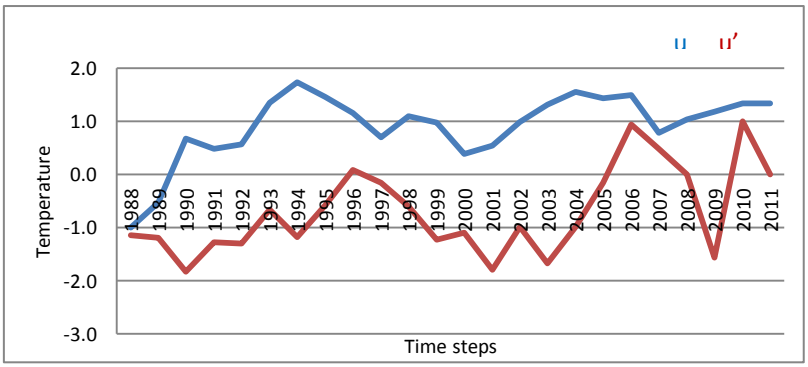


**Figure 2.4 Time series of minimum temperature in Shemiran**

The statistical period of ***Geophysics*** station (figure2.5) is from 1991 to 2011. As with the Shemiran station (figure 2.4), this station also holds over 20 years of recorded data. The station also shows fluctuations in the minimum temperature since 1993, but changes or trends based on time series of temperature cannot be seen.

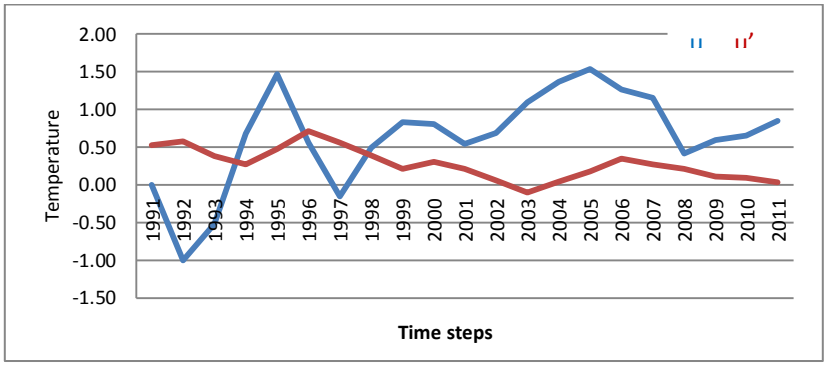


**Figure 2.5 Time series of minimum temperature in Geophysics**

The ***Chitgar*** station (figure 2.6) statistical period is from 1996 to 2011. This station recorded over 15 years of statistics in the west of Tehran. Chitgar station is located near the Chitgar forest Park. Out of the 5 stations studied, Chitgar is the only station showing a change of (-1°C) in the minimum temperature.

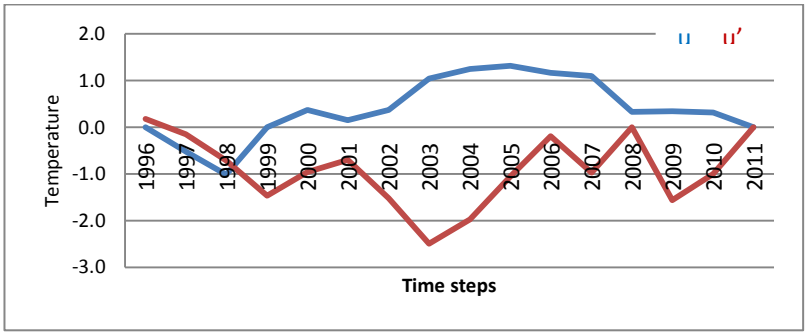


**Figure 2.6 Time series of minimum temperature in Chitgar**

### 2.2.2.2. Mean maximum temperature

The time series fluctuations of temperature can be seen from 1960 onwards in ***Mehrabad*** station (figure 2.7). During mid-statistical period coinciding with the 1980, it shows the highest level of fluctuations.

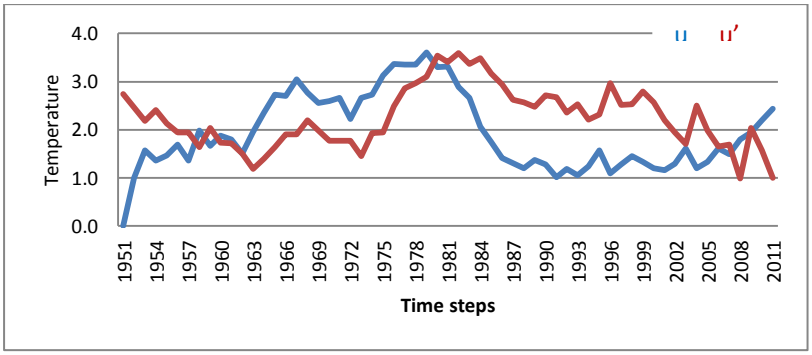


**Figure 2.7 Time series of maximum temperature in Mehrabad**

As can be seen at the ***Dushan-TaPPeh*** station (figure 2.18), some fluctuations in temperature is observed during the period of more than 40 years. Of course, this change is not interpreted as a temperature trend in the model.

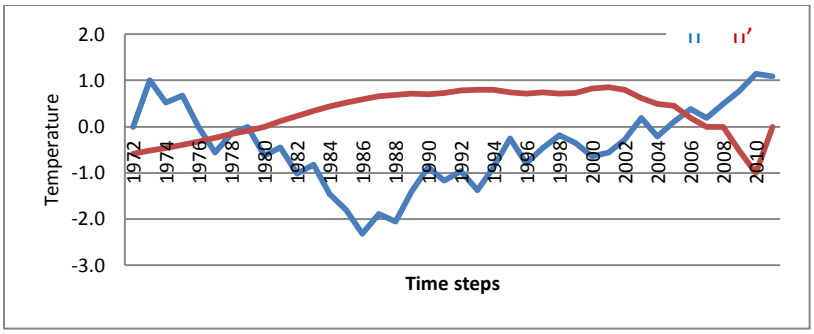


**Figure 2.8 Time series of maximum temperature in Doushan-Tapeh**

The ***Shemiran*** station (figure 2.9), with the statistical period data of more than 20 years, this station shows a change of 1.7°C increase in temperature in the northern Tehran.

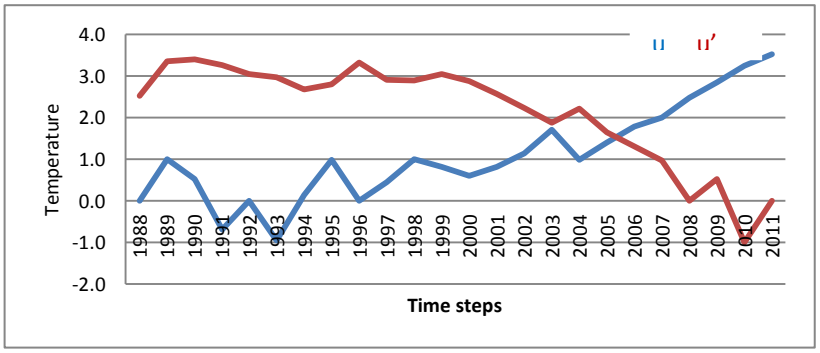


**Figure 2.9 Time series of maximum temperature in Shemiran**

As with the previous station, ***Geophysics*** station (figure 2.10), also with the statistical period data of more than 20 years, shows a change in increasing temperature.

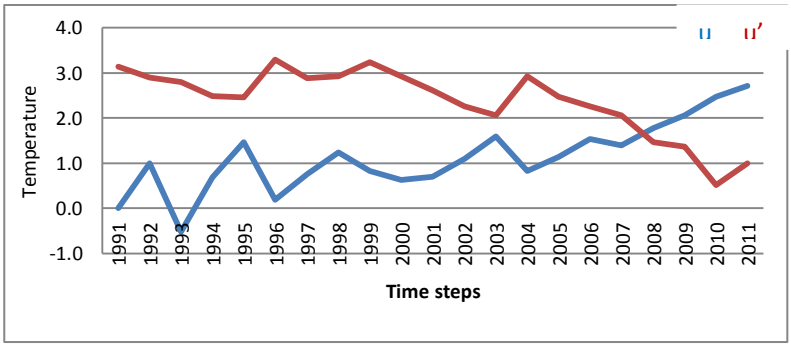


**Figure 2.10 Time series of maximum temperature in Geo physic**

As can be seen at the ***Chitgar*** station (figure 2.11), some fluctuations in temperature is observed during the period of 16 years. Of course, this change is not interpreted as a temperature trend in the model.

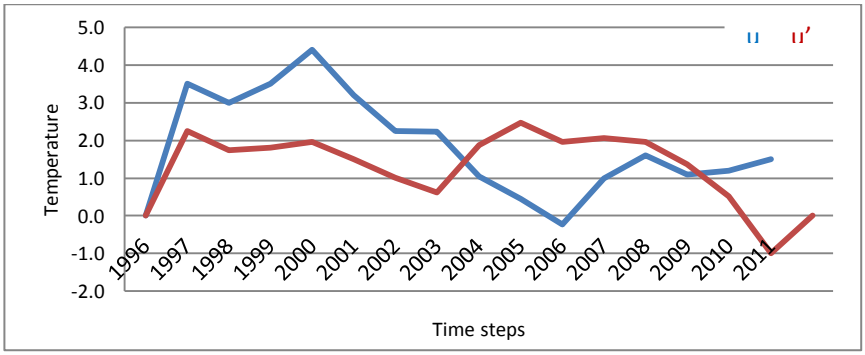


**Figure 2.11 Time series of maximum temperature in Chitgar**

Based on Kendall model, (u) and (u') in the diagrams provided show the time series. Lack of any confluence of two indicators is indicative of lack of any change in the time series Torkesh et al, (2002). The confluence of two graphs series1 (u) and series2 (u') indicate the point of change and trend. This is so, that if these lines intersect within the critical range of ±1.96 (u, u'), they mark the beginning of a sudden change in the datasets. However, periodical intersection of lines at this level denotes temperature fluctuation. In the case of critical intersect being outside of the time series it is indicative of a trend. With the confluence of lines above or below the standard number of 1.96, the test probability level is 95%. (Alijani, 1998).

## 2.3. Mean maximum and mean minimum monthly temperature

For the purpose of determining the best period to obtain the satellite images for and the assessment and analysis of the temperature and land cover changes, the averages of the lowest and highest monthly temperatures at 5 stations (figure 2.1) in the study area were calculated. The assessments of the average maximum and minimum temperature of all months of year show that at all stations the highest temperatures relate to July in summer and the lowest to January in winter. The results of these assessments are shown in the figures 2.2-2.6.

Use of the hottest and coldest months of year for the purpose of assessing and studying the fluctuations and changes in temperature has been favored by many researchers. For example,

Narisma et. al. (2002) in their research in Australia, used July and January to compare temperature and rainfall over 200 years.

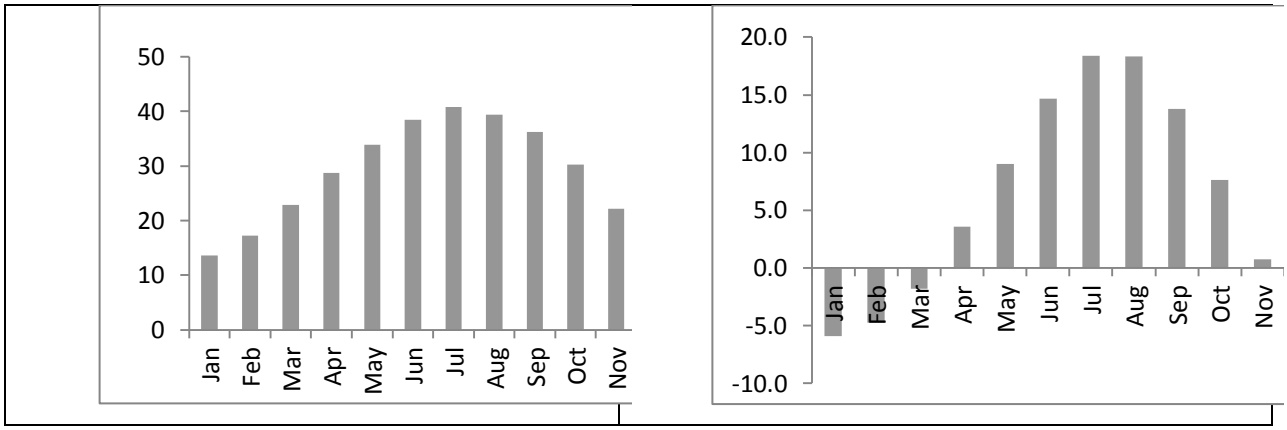


**Figure 2.12 Maximum and Minimum temperature in Mehrabad**

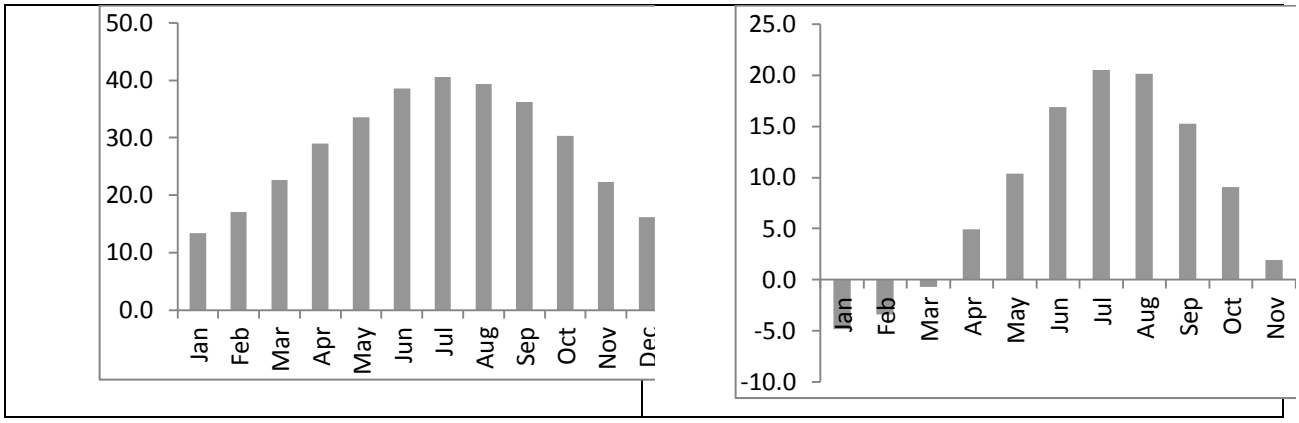


**Figure 2.13 Maximum and Minimum temperature in Doushan Tapeh**

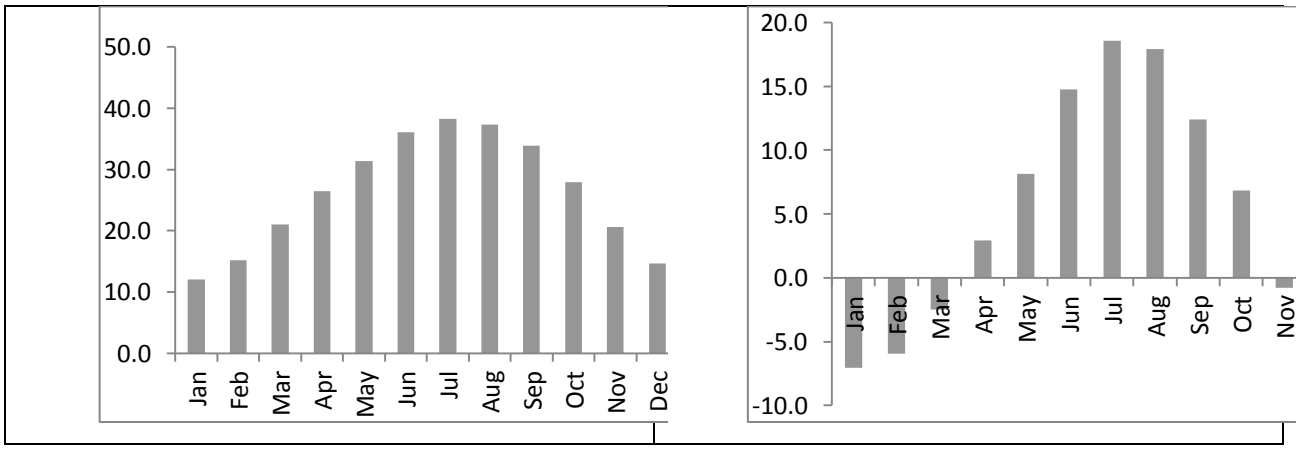


**Figure 2.14 Maximum and Minimum temperature in Shemiran**

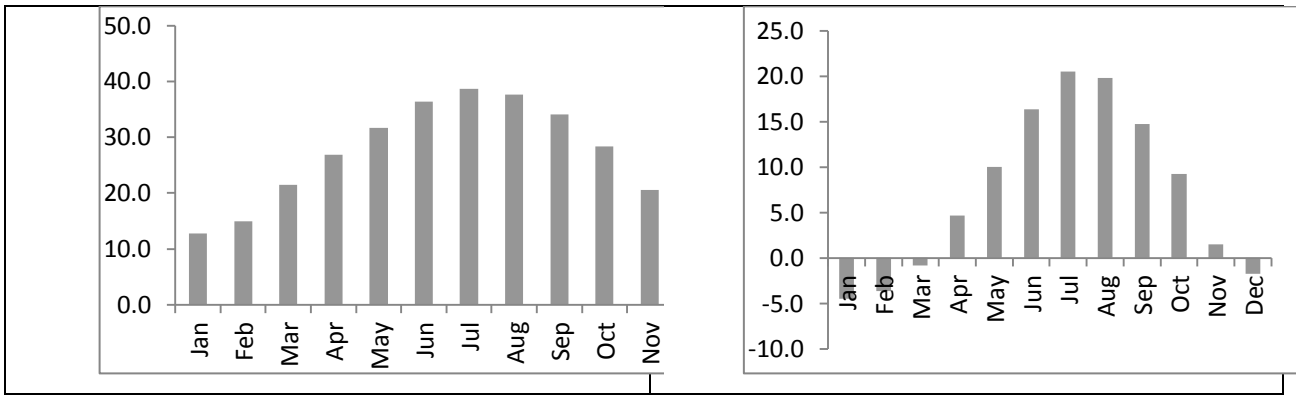


**Figure 2.15 Maximum and Minimum temperature in Geophysics**

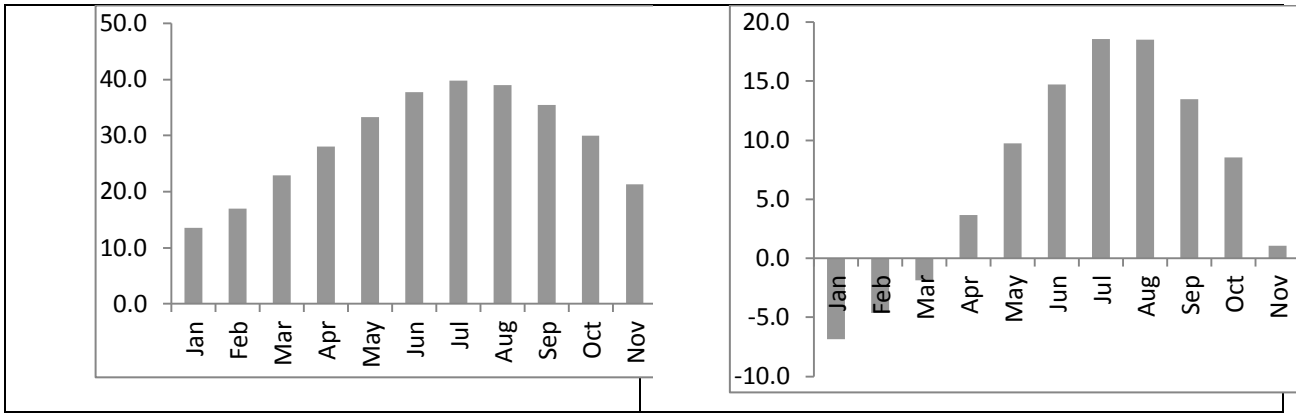


**Figure 2.16 Maximum and Minimum temperature in Chitgar**

The ***Mehrabad*** station (figure 2.12), shows the average maximum temperature of 41°C as the highest temperature for July and the average minimum temperature of -6°C, as the lowest monthly average temperature for January. The ***Dushan-Tapeh*** station (figure2.13), shows the highest temperature of about 41°C for July and the lowest temperature of -5°C for January and this is close to the temperature status of Mehrabad station. The ***Shemiran*** station (figure2.14) also shows average maximum and minimum monthly temperatures of 38°C in July and -7°C in January. The interesting point to note here is that, as this station is situated in the rural southern slopes of Elborz compared to the two earlier stations situated in the inner city area, it shows 3°C lower than the other two in the average maximum and 2°C lower in the average minimum temperature. The ***Geophysics*** station (figure 2.15), also has recorded the July temperature of 39°C and January temperature of -4.5°C as the maximum and minimum monthly temperatures.

The final station of ***Chitgar*** (figure2.16), as well as others has tabled the months of July and January temperatures as the hottest and coldest months of the year as 39°C and -7°C respectively.

In table 2.4 the mean and the standard deviation of temperatures have been shown. Mean temperature in figures 2.12 - 2.16 were analysed and the charts showed that during this statistical period there has been a normal distribution of temperature.

In all stations during the cold months the standard deviation shows higher figure compared to temperature during hot months. This (table 2.4) demonstrates the fact that the temperature fluctuations during the cold months of year are higher. However, during the hot months, Tehran particularly experiences a rather uniform temperature due to the dominance of subtropical high pressure Alijani et. al. (1997).

**Table 2.4 Maximum mean and STDEV temperature of Tehran stations (1951-2011)**

| Months | Mehrabad station | | Dushan tapeh stion | | Shemiran staion | | Geophsic staion | | Chitgar station | |
|---|---|---|---|---|---|---|---|---|---|---|
| | *Mean* | *STDVE* | *Mean* | *STDVE* | *Mean* | *STDVE* | *Mean* | *STDVE* | *Mean* | *STDVE* |
| **Jan** | 13.6 | 3.5 | 13.4 | 4.0 | 12.0 | 3.0 | 12.7 | 2.7 | 13.6 | 2.7 |
| **Feb** | 17.3 | 2.6 | 17.1 | 3.6 | 15.1 | 2.4 | 15.0 | 4.0 | 17.0 | 1.7 |
| **Mar** | 22.9 | 2.5 | 22.6 | 4.4 | 21.0 | 3.2 | 21.5 | 3.2 | 22.9 | 3.1 |
| **Apr** | 28.8 | 2.0 | 29.0 | 2.0 | 26.5 | 2.2 | 26.8 | 2.3 | 28.0 | 2.6 |
| **May** | 33.9 | 1.9 | 33.6 | 2.1 | 31.4 | 1.9 | 31.7 | 1.9 | 33.3 | 2.0 |
| **Jun** | 38.5 | 1.4 | 38.5 | 1.2 | 36.1 | 1.5 | 36.4 | 1.1 | 37.7 | 1.1 |
| **Jul** | 40.8 | 1.3 | 40.6 | 1.3 | 38.3 | 1.4 | 38.7 | 1.4 | 39.8 | 1.3 |
| **Aug** | 39.4 | 1.4 | 39.4 | 1.4 | 37.3 | 1.3 | 37.6 | 1.1 | 39.0 | 1.0 |
| **Sep** | 36.2 | 1.3 | 36.3 | 1.2 | 33.9 | 1.4 | 34.1 | 1.3 | 35.4 | 1.0 |
| **Oct** | 30.2 | 1.8 | 30.3 | 1.7 | 27.9 | 2.0 | 28.3 | 2.1 | 29.9 | 1.9 |
| **Nov** | 22.2 | 3.6 | 22.3 | 4.2 | 20.6 | 2.0 | 20.6 | 2.2 | 21.3 | 2.2 |
| **Dec** | 16.0 | 2.9 | 16.1 | 2.9 | 14.6 | 2.7 | 13.8 | 4.0 | 15.8 | 3.2 |

As can be seen in table 2.5 the standard deviation of minimum average temperature during cold months shows more than 3 degrees Celsius.

**Table 2.5 Minimum mean and STDEV temperature of Tehran stations (1951-2011)**

| Months | Mehrabad station | | Dushan tapeh stion | | Shemiran staion | | Geophsic staion | | Chitgar station | |
|---|---|---|---|---|---|---|---|---|---|---|
| | *Mean* | *STDVE* | *Mean* | *STDVE* | *Mean* | STDVE | *Mean* | *STDVE* | *Mean* | *STDVE* |
| **Jan** | -6.1 | 3.2 | -4.8 | 2.8 | -7.0 | 2.9 | -4.5 | 2.5 | -6.9 | 3.5 |
| **Feb** | -4.8 | 2.8 | -3.4 | 2.6 | -6.0 | 2.7 | -3.6 | 2.2 | -4.6 | 2.9 |
| **Mar** | -1.9 | 2.5 | -0.7 | 2.8 | -2.5 | 2.5 | -0.8 | 2.8 | -1.9 | 2.0 |
| **Apr** | 3.6 | 3.0 | 4.9 | 3.1 | 2.9 | 2.5 | 4.6 | 3.0 | 3.7 | 2.7 |
| **May** | 9.1 | 2.7 | 10.4 | 2.7 | 8.2 | 2.2 | 10.0 | 2.4 | 9.8 | 2.3 |
| **Jun** | 14.9 | 2.6 | 16.9 | 2.0 | 14.8 | 1.7 | 16.4 | 2.5 | 14.7 | 2.6 |
| **Jul** | 18.6 | 2.1 | 20.5 | 2.3 | 18.6 | 1.6 | 20.5 | 1.9 | 18.5 | 1.7 |
| **Aug** | 18.6 | 2.1 | 20.1 | 2.3 | 17.9 | 2.2 | 19.8 | 2.4 | 18.5 | 2.1 |
| **Sep** | 14.0 | 2.2 | 15.2 | 2.6 | 12.4 | 2.2 | 14.8 | 2.3 | 13.5 | 2.2 |
| **Oct** | 7.7 | 2.7 | 9.0 | 2.4 | 6.8 | 1.8 | 9.2 | 2.0 | 8.5 | 2.2 |
| **Nov** | 0.7 | 2.9 | 2.0 | 2.5 | -0.8 | 2.4 | 1.5 | 2.4 | 1.1 | 2.4 |
| **Dec** | -3.6 | 3.2 | -2.3 | 2.6 | -4.4 | 2.7 | -1.8 | 2.3 | -2.7 | 2.0 |

In fact, during the course of the period relating to this research fluctuation in temperature has been more during cold months of year. This could be due to the fact that various immigrating cold air masses affect Iran and specially Tehran during cold months. Alijani (1997).

## 2.4. Summery

There has been no confluence of lines in any of the stations graphs, above +1.96 or below -1.96, indicating that there has not been any increasing or decreasing temperature trend. Reviewing the mean maximum temperature, the Mehrabad station shows the highest occurrences of fluctuations of temperature during the past consecutive years. The Dushan-Tappeh and chitgar show some fluctuations during the period, while both, the Shemiran station in 2006 and the Geophysics station in 2008 show an increasing temperature change.

The analysis of the temperatures in 5 ground based stations in Tehran shows the fluctuating temperature increase in the mean minimum temperature at three stations of Mehrabad, Dushan-Tappeh and the Geophysics. The Shemiran station shows no confluence in the time series. Chitgar station is the only one showing decreasing temperature change amongst all other stations in Tehran. Based on the Mann-Kendal model no significant level of decrease or increase in the mean minimum/maximum temperatures can be seen in any of the stations.

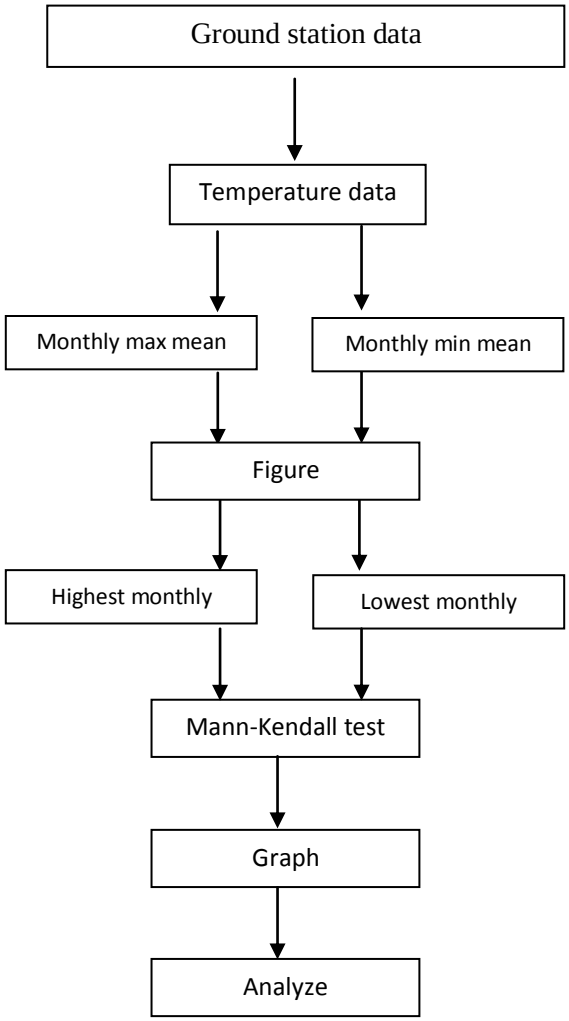


**Flow chart 1.1 Methodology of meteorological station**

## Excel view: maximum temperature in Mehrabad station, Mann-Kendall method

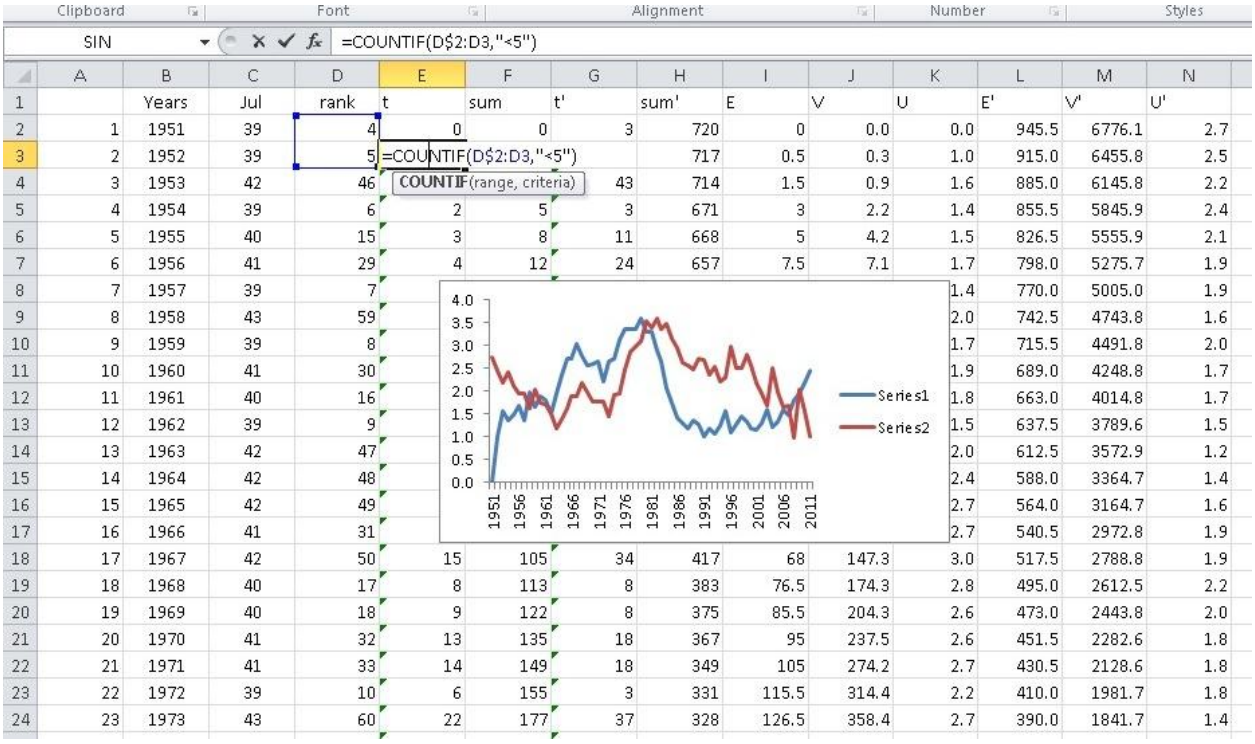


| | A | B | C | D | E | F | G | H | I | J | K | L | M | N |
|---|---|---|---|---|---|---|---|---|---|---|---|---|---|---|
| 1 | | Years | Jul | rank | t | sum | t' | sum' | E | V | U | E' | V' | U' |
| 2 | 1 | 1951 | 39 | 4 | 0 | 0 | 3 | 720 | 0 | 0.0 | 0.0 | 945.5 | 6776.1 | 2.7 |
| 3 | 2 | 1952 | 39 | 5 | =COUNTIF(D$2:D3,"<5") | | | 717 | 0.5 | 0.3 | 1.0 | 915.0 | 6455.8 | 2.5 |
| 4 | 3 | 1953 | 42 | 46 | | | 43 | 714 | 1.5 | 0.9 | 1.6 | 885.0 | 6145.8 | 2.2 |
| 5 | 4 | 1954 | 39 | 6 | 2 | 5 | 3 | 671 | 3 | 2.2 | 1.4 | 855.5 | 5845.9 | 2.4 |
| 6 | 5 | 1955 | 40 | 15 | 3 | 8 | 11 | 668 | 5 | 4.2 | 1.5 | 826.5 | 5555.9 | 2.1 |
| 7 | 6 | 1956 | 41 | 29 | 4 | 12 | 24 | 657 | 7.5 | 7.1 | 1.7 | 798.0 | 5275.7 | 1.9 |
| 8 | 7 | 1957 | 39 | 7 | | | | | | | 1.4 | 770.0 | 5005.0 | 1.9 |
| 9 | 8 | 1958 | 43 | 59 | | | | | | | 2.0 | 742.5 | 4743.8 | 1.6 |
| 10 | 9 | 1959 | 39 | 8 | | | | | | | 1.7 | 715.5 | 4491.8 | 2.0 |
| 11 | 10 | 1960 | 41 | 30 | | | | | | | 1.9 | 689.0 | 4248.8 | 1.7 |
| 12 | 11 | 1961 | 40 | 16 | | | | | | | 1.8 | 663.0 | 4014.8 | 1.7 |
| 13 | 12 | 1962 | 39 | 9 | | | | | | | 1.5 | 637.5 | 3789.6 | 1.5 |
| 14 | 13 | 1963 | 42 | 47 | | | | | | | 2.0 | 612.5 | 3572.9 | 1.2 |
| 15 | 14 | 1964 | 42 | 48 | | | | | | | 2.4 | 588.0 | 3364.7 | 1.4 |
| 16 | 15 | 1965 | 42 | 49 | | | | | | | 2.7 | 564.0 | 3164.7 | 1.6 |
| 17 | 16 | 1966 | 41 | 31 | | | | | | | 2.7 | 540.5 | 2972.8 | 1.9 |
| 18 | 17 | 1967 | 42 | 50 | 15 | 105 | 34 | 417 | 68 | 147.3 | 3.0 | 517.5 | 2788.8 | 1.9 |
| 19 | 18 | 1968 | 40 | 17 | 8 | 113 | 8 | 383 | 76.5 | 174.3 | 2.8 | 495.0 | 2612.5 | 2.2 |
| 20 | 19 | 1969 | 40 | 18 | 9 | 122 | 8 | 375 | 85.5 | 204.3 | 2.6 | 473.0 | 2443.8 | 2.0 |
| 21 | 20 | 1970 | 41 | 32 | 13 | 135 | 18 | 367 | 95 | 237.5 | 2.6 | 451.5 | 2282.6 | 1.8 |
| 22 | 21 | 1971 | 41 | 33 | 14 | 149 | 18 | 349 | 105 | 274.2 | 2.7 | 430.5 | 2128.6 | 1.8 |
| 23 | 22 | 1972 | 39 | 10 | 6 | 155 | 3 | 331 | 115.5 | 314.4 | 2.2 | 410.0 | 1981.7 | 1.8 |
| 24 | 23 | 1973 | 43 | 60 | 22 | 177 | 37 | 328 | 126.5 | 358.4 | 2.7 | 390.0 | 1841.7 | 1.4 |

## Reference


1. Alijani, B., M. Kaviani 1998, The principles of climatology. Payam-e Noor publisher, Tehran.

2. Alijani1, B., J. O'Brien, B. Yarnal3 2007, spatial analysis of precipitation intensity and concentration in Iran, Theoretical and APPlied Climatology. Vol. 94, PP.107–124

3. Bandyopadhyay. A; A. Bhadra; N. S. Raghuwanshi; and R. Singh 2011. Temporal Trends in Estimates of Reference Evapotranspiration over India, Journal of Hydrologic Engineering, Vol 14.

4. Haan, C.T. 1977, *Statistical Methods in Hydrology*. The Iowa State University Press, Ames.

5. Kendall, M. G. 1955. Rank Correlation Methods. Griffin, London.

6. Mann, H. B. 1945, Nonparametric tests against trend. Econometrica, Vol.13, PP.245-259.

7. Mishra, N.; D. Khare; R.Shukla and K. Kumar, 2014, Trend Analysis of Air Temperature Time Series by Mann Kendall Test - A Case Study of Upper Ganga Canal Command (1901-2002) , British Journal of APPlied Science & Technology, Vol. 28, PP. 4066-4082.

8. Modarres, R. and Silva, V. 2007. Rainfall trends in arid & semi-arid regions of Iran. Journal of Arid Environments, Vol. 70, PP.344–355.

9. Narisma G. T and A. J. Pitman 2002. ,The Impact of 200 Years of Land Cover Change on the Australian Near-Surface Climate, Jornal of, hydrometeorology, vol 4, PP 424-437.

10. Onoz, B., & Bayazit, M. 2003. The power of statistical tests for trend detection. Turkish Journal of Engineering Environmental Science, Vol.27, PP.247-251.

11. Widyasamratri, 2013, A comparison of air temperature and land surface temperature to detect urbanization effect in Jakarta, Indonesia, Atmosphere & Oceanography & Climate change, University of Yamanashi, Japan.

# Chapter 3

**Land cover classification and change detection**

## 3.1. Introduction

Change in the type of land cover is a process that has occurred due to human activities in different areas of the Earth over time. Although natural factors (Earthquakes, volcanic eruption, erosion etc.) are also effective in the process of land cover change, their impact is very limited compared to the effects of human activities. Recent analyses suggest that 83% of the Earth's land surface has been affected by human settlement and activities, leaving only 17% in wilderness (WCS and CIESIN 2002). Environmental scientists are interested in examining land cover changes and assessing the impact on other environmental factors (Amiri, et al 2009) and (Weng, 2001). For these assessments the classification of land cover and the detection of changes during different periods of time is one of the subjects that are studied.

Change detection is the process of identifying differences in the state of an object or a phenomenon by observing it at different times (Singh, 1989). . The time (period during which change has taken place) and accuracy of change detection on the Earth's surface is important for understanding the relationships and interactions between human and his environment and can provide guidance for the management and use of Earth's resources such as available water body and various types of land. To put it simply, it helps us to be aware of are degree of freedom and the limits within which human can menuver in their activities related to land use without exceeding them overuse. Identification and awareness of changes and their causes over various time periods is essential in order to prevent and control any further damage and destruction. This knowledge and awareness has become possible with availability and use of existing tools such as satellite imagery. The biggest changes in land cover occurs in cities, so studying these changes can be useful for managing city resources.

Also in the case of Tehran, the study of this city via satellite images for the purpose of determining changes over time has indeed drawn the interest of researchers and city management. Tehran is a key centre for manufacturing, housing, transportation and distribution

in the country of Iran. Accelerated urban development and the lack of proper planning have made a significant impact on land cover changes. Population density and the unique geographical location of Tehran (see below and also the study area section in chapter one, page 19) from one side and the land cover changes from another give hand to hand to make Tehran one of the most vulnerable cities in Iran, in terms environment. Tehran is situated in a basin shaped territory surrounded in the north by the southern slopes of the Alborz heights and in the south by the sub-desert plains of Kavir (Figure 3.17). An extensive study of land cover change over the past decades and its impact on the climate and environmental factors of the city of Tehran can help to identify the environmental threats it is facing, so that a solution can be thought of to control them. One of the objectives of this thesis has therefore been to study the land cover of Tehran, using the 1980 (MSS), 1990, 2000, 2009 and 2014 Landsat images for the month of July of these years. These satellite images which are freely available to users will be downloaded from the (USGS) website and will be prepared using the ArcGIS and the Erdas softwares prior to classification. The images for the month of July, as well as being selected as the images for the hottest month of year, are also used for the classification and analysis of land cover changes. The reason for this is that during this month all land cover types are in their original state (i.e. they do not have seasonal specific forms such as, frost, waterlog or autumn falls), and the sky over Tehran is clearer with the least or no cloud or fog and therefore the produced images are of the desired clarity and quality.

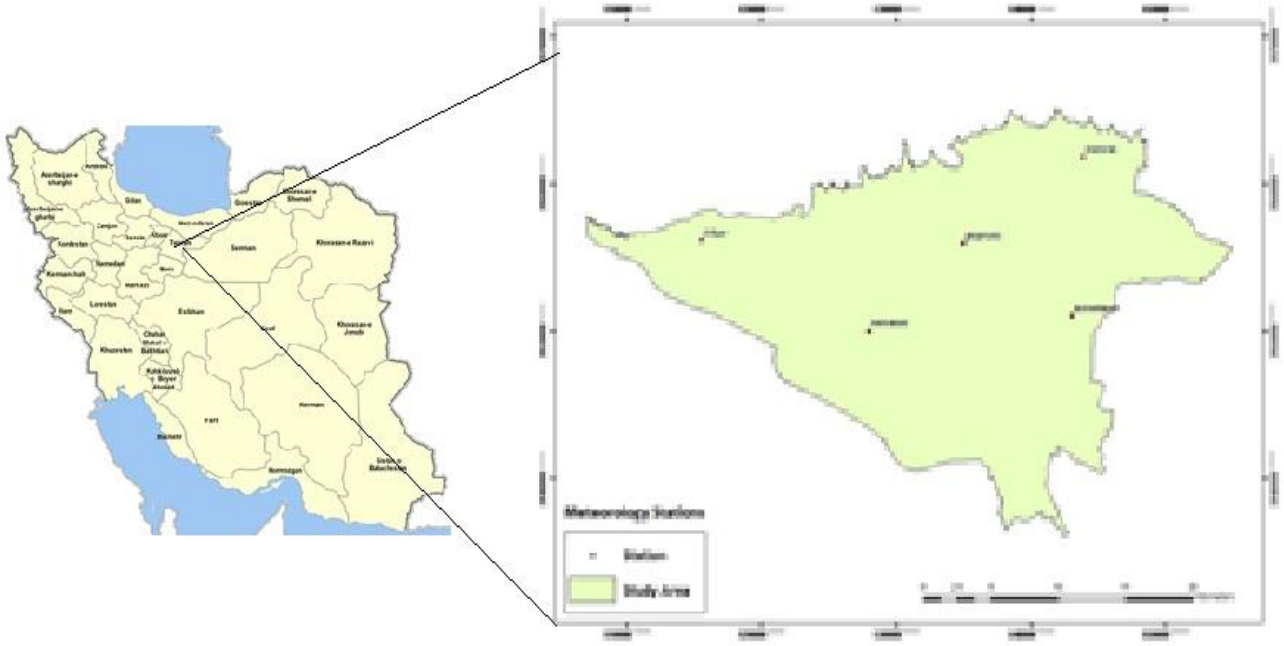

**Figure 3.17 city of Tehran position**

In this chapter the selection of a suitable method of classification of satellite images will be discussed together with the evaluation of overall accuracy of classification with random sampling method. The extent of land cover change from 1990 to 2014 will also be assessed by the Recode method (page 53), which is one of the detection methods in the Erdas software.

## 3.2. Classification of Satellite images

To classify the land cover, images of July months with no cloud or fog in Tehran, images from 1990 to 2014 were used. The time intervals of the selected images are 10 yearly to allow the comparison and review of the changes more reliably. After examining satellite images of Tehran at the USGS site, every effort was made to ascertain the images selected were suitable in terms of quality( no clouds and fog).

The first step for classification of land cover is the process of stacking the layers by combining the appropriate bands and this will be done using the Erdas software. Also, in order to achieve a better classification result a combination of all bands will be used except the thermal band of Landsat images.

### 3.2.1. Land cover classification method

There are two known methods for classifying land cover; supervised classification and unsupervised Classification. Out of the two methods, supervised classification method is considered a more acceptable method by researchers. Since choosing of pixels in each class is done knowledgably and therefore of high accuracy and there is a greater variety in the available algorithms geared towards supervised classification. The primary difference between classification algorithms is the way in which they determine how an individual pixel is assigned to a land cover category (Horning, 2004). In this study, supervised signature extraction with the maximum likelihood algorithm was employed to classify the land cover images. For the purpose of determining a true classification, a total of more than 50 training sites in each image were chosen to ensure all land cover classes are adequately represented in the training statistics.

Having studied many research papers about land cover classification methods it was concluded that most researchers have used the supervised classification method, including, (weng, 2001), (Falahatkar et.al, 2011), (Alavipanah, 2003) and also (Amiri et. al, 2009). After classifying the images using the selected classification method, four classes of land cover were identified in the study area including Barren land, built-up, vegetation (being an urban area vegetation is of green space types such as grass and does not include forest or agricultural type), and water body and their land cover figures were drawn as shown in (Figures 3.18-3.21). Ultimately, the important step was then to assess the accuracy of classification and also the corresponding coefficient of correlation between the raster image and the classified image.

### 3.2.2. Accuracy assessment of Land cover classification

Having classified the satellite images, the next step was to assess the accuracy of these classifications. In other words, an appropriate method was used to confirm what percentage of the classified image pixels realistically belong to the correct class or what percentage of the pixels in a class are unrelated and have been placed in the wrong class**.**

The accuracy of all classified images were checked with stratified random sampling method by which 100 samples were selected from each land cover. Then the randomly selected land cover type on the reference image (un-classified raster image) were compared with the land

cover type on the classified images. Stratification is the process of dividing members of a population into homogeneous subgroups before sampling. Every element in the population must be assigned to only one stratum and no population element can be excluded. This improves the representativeness of the sample by reducing sampling error (Table 3.6).

Goncalves et al (2007) compared four comparative sampling methods and calculated the Kappa coefficient of each. The stratified sampling method showed the highest Kapa coefficient. The resulting table completed in this way in the Erdas contains the codes from the raster image with the codes from the classified image against them and the differences were noted. These differences mean that a pixel was wrongly interpreted and placed in an inappropriate class. Finally, the result of accuracy assessment were calculated by using random sampling method and the percentages of accuracy were tabulated as in table 3.6. Also, the Kappa coefficient was applied to measure the correlation level between the raster image and the classified images and this process together with results were calculated using the Erdas software.

### 3.2.3. Kappa coefficient

The Kappa coefficient is used when the aim is to measure the degree of agreement between two observers. This coefficient is only used for variables that have both the same comparison factors as well as equal number of categories. The Kappa coefficient value which is also known as the Cohen's Kappa, always fluctuates between 0 and 1. The higher the value and being closer to 1 is the indication of higher reliability of agreement between the two observers. However, when the value is closer to 0 then we witness the least agreement between them. The Kapa coefficient is a discrete multivariate technique used in accuracy assessment (Congalton, 1988).

The assessment of classified images against the reference image (un-classified raster image) showed a correlation of over 0.7 between them. The result of this assessment of the images was produced in the Erdas in the form of a final report. It should be noted that Kappa coefficient of 0.7 and higher is considered as the acceptable agreement (Table.3.6). A research paper (virera et al, 2005), titled "Understanding Inter-observer Agreement, the Kappa Statistic", and stated the Kappa agreement level as below.

< 0 –less than chance agreement,

0.01–0.20 Slight agreement,

0.21– 0.40 Fair agreement

0.41–0.60 Moderate agreement,

0.61–0.80 Substantial agreement,

0.81–0.99 almost perfect agreement.

The table below shows the results of Kappa coefficient for our supervised classification. The values shown for various classes have been between 0.75 and 0.85 which according to Kappa coefficient offer a substantial agreement.

Based on this table, derived from the Erdas, the accuracy of classifications were between 88.7% as the lowest for 2014 and 92.4% for 2009. Also their correlation on the basis of Kappa coefficient was between 0.75 and 0.85 relating to the years between 1990 and 2014. Overall, the results obtained, show that the completed classifications of land cover images hold a high level of accuracy and correlation.

**Table 3.6 Accuracy assessment and kappa coefficient**

| year | Accuracy assessment | Kappa coefficient |
|---|---|---|
| 1990 | 89.1% | 0.82 |
| 2000 | 88.8% | 0.77 |
| 2009 | 92.4% | 0.80 |
| 2014 | 88.7% | 0.75 |

Following the above steps and the result of classification produced the land cover maps for each period as shown in figures (3.18-3.21) and discussed separately.

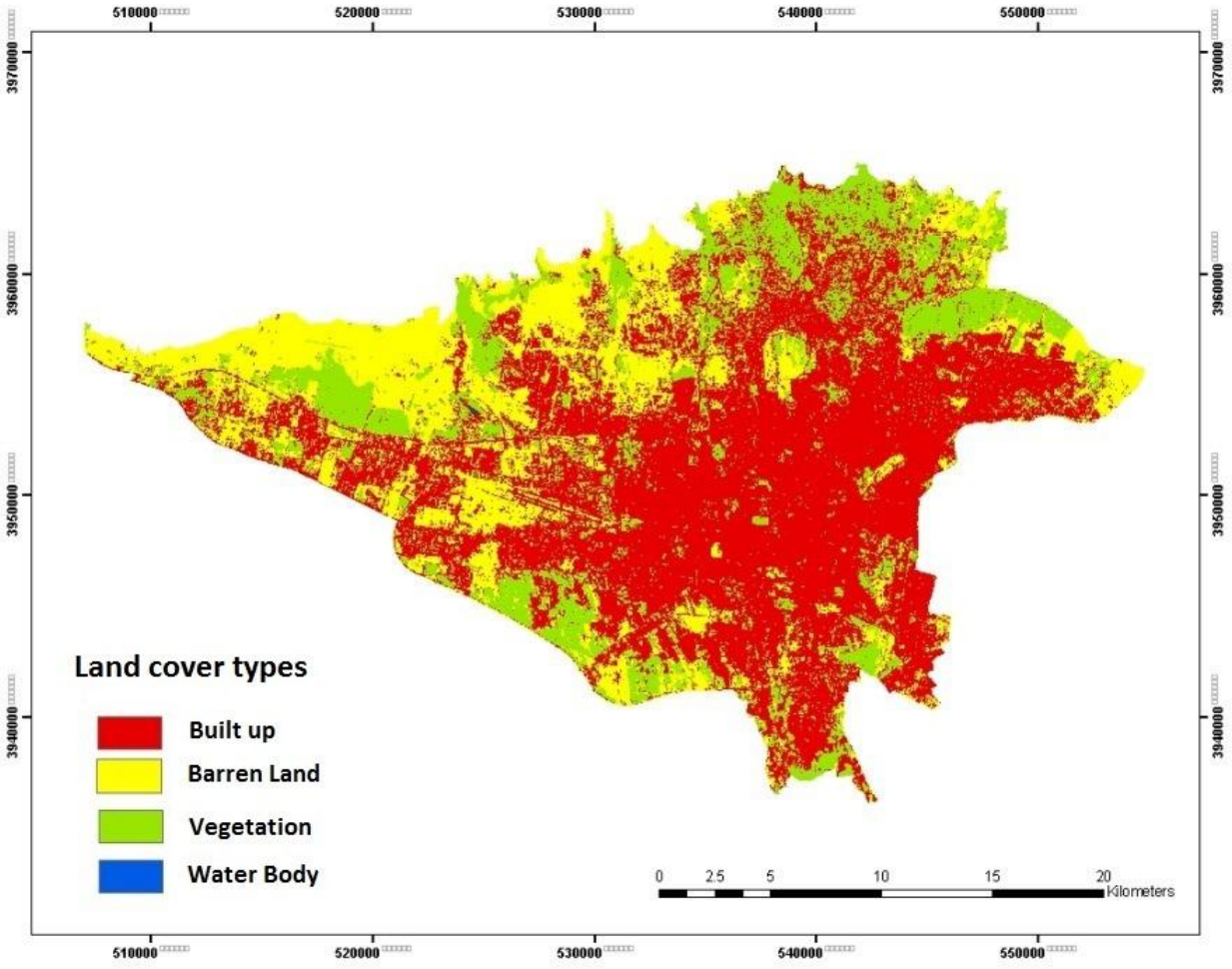


**Figure 3.18 Tehran city land cover types in July 1990**

Figure 3.18 show the percentage of each type of land cover in 1990 including built up 52.4%. Barren land 25.9% and vegetation of 21.5% of the total area. Tehran is very low in surface water body which in this period it was 0.03%, that is a very small percentage of the total land area.(table 3.7).

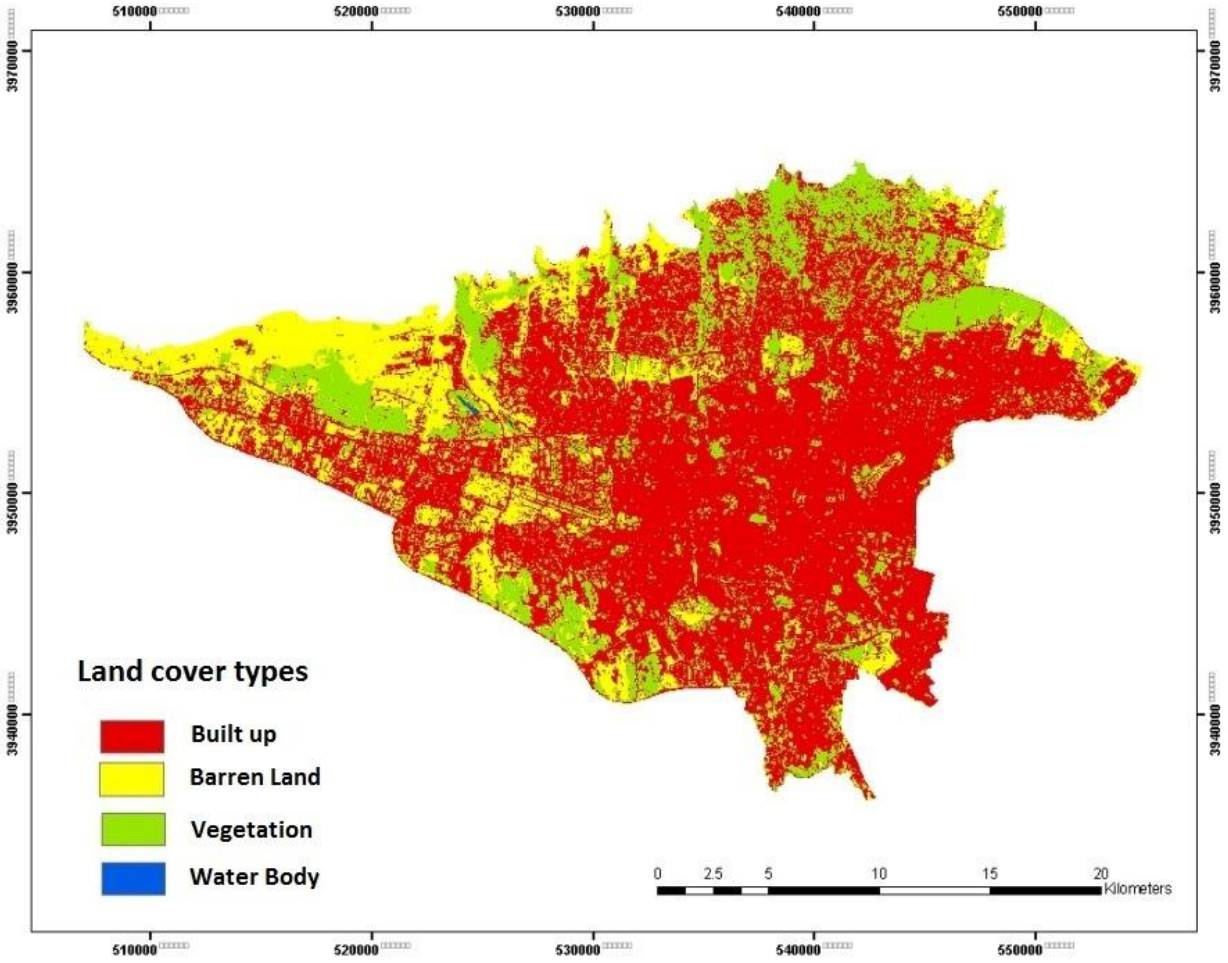


**Figure 3.19 Tehran city land cover types in July 2000**

Barren and vegetation land cover change to built-up in year 2000 can be seen in figure 3.19. Although the speed of these changes have been slower compared with the previous period (figure 3.18), however the magnitude of this change in the north is clearly prominent. A noticeable size of land space of the north has undergone construction and build-up. So much so that it amounts to 60.7% of the land area, making this a growth of 8%. The level of land cover changes according to table 3.7 includes built-up area of 60.7% of the total land area in Tehran, barren land 19.3% and vegetation has covered 19.8% of the total land. Water body includes the lowest of all and that is 0.03%.

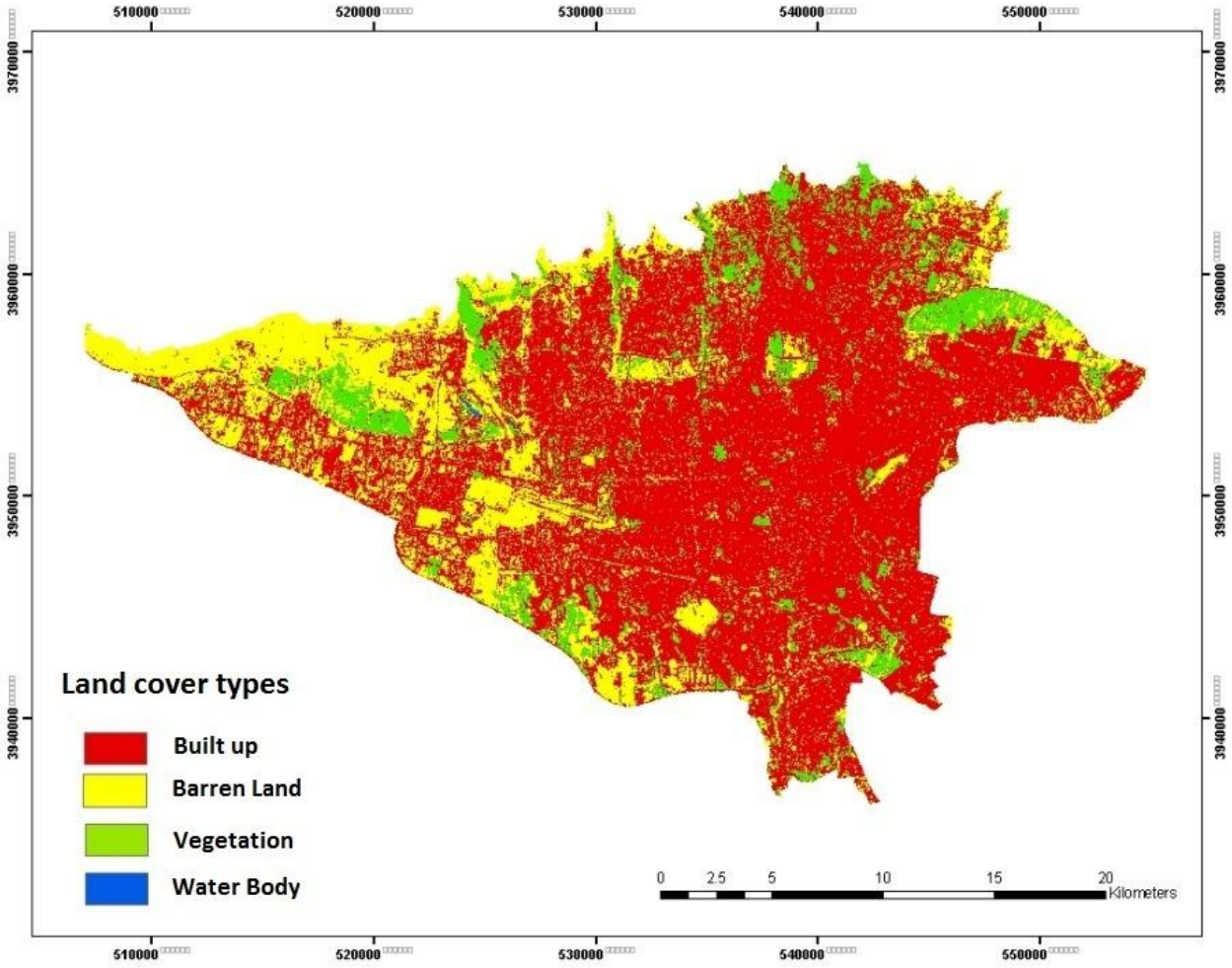


**Figure 3.20 Tehran city land cover types in July 2009**

In 2009 (figure 3.20), the destruction of vegetation and its consequent reduction of 8% compared with the previous period makes it the biggest change that has taken place. Along with this extreme reduction in vegetation cover, barren land and built-up have each increased by about 4%. In the northeast of Tehran the biggest destruction of vegetation has been towards conversion to built-up and in other areas and mostly in the south this has been toward change to barren land. Most destruction of vegetation has taken place in this year, as with 7% compared to previous 10 years; it has taken 11.6% share to itself. Barren land shows 4.5% increase in relation to the previous 10 years and includes 23.9% of the land in Tehran. Built-up area also has taken 64.3%.

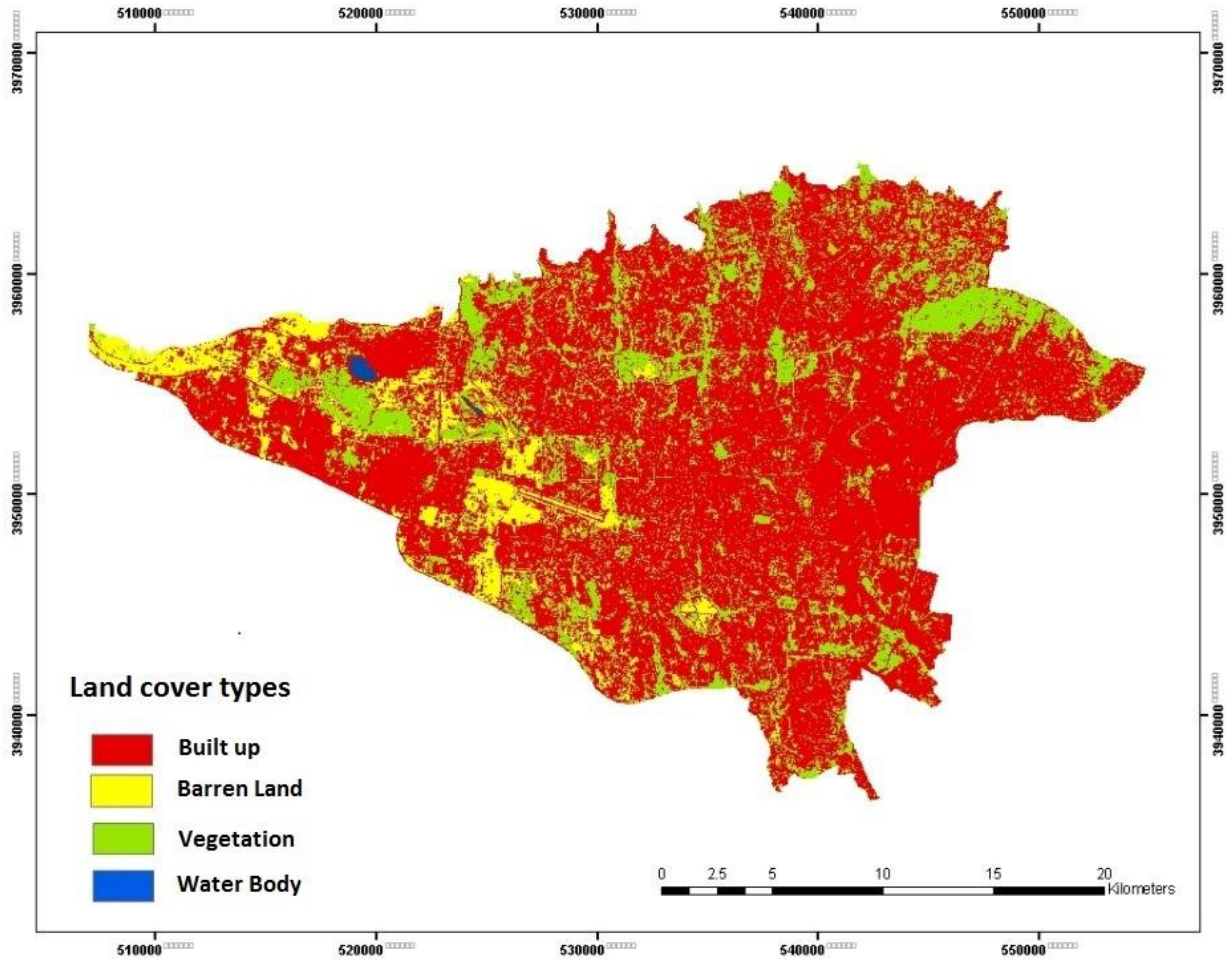


**Figure 3.21 Tehran city land cover type in July 2014**

In this year, vegetation land cover area has reached 19.8%. That of barren land reached 10.8% and as with the previous 3 periods, built-up area has continued to increase to reach 68.95% in this year. Water body also has reached its highest increase of its land cover in 2014 (figure 3.21) shows a significant difference compared to the 25 year before that, from 1990 to 2009. It seems that after 2009 the municipal risk managers have understood the crisis and have tried to take control of urban land cover status. As it is obvious from the (figure 3.21), the creation of green spaces has drawn some attention as compared to the last 5 years and the area of vegetation has increased by 7% in 2009 from 11.6% reaching 19.8% in 2014. Barren lands of 23.9% in 2009 reached 10% in 2014 which is actually devoted to vegetation. The most important change in land cover which can be seen in (figure 3.21) is the water body of the Chitgar artificial

lake in western Tehran that has increased the water body of 0.03% in the last 30 years to 17% in this year. Also the expansion of urban land covers of 4% in 2009 shows that the buildup on barren lands has increased. For the final image relating to July 2014, the overall classification accuracy is 88.7% and the kappa coefficient shows a value of 0.75. As can be seen in the table 3.5 of 2014, 68% of urban land is dedicated to built-up land drawn from the highest point of the southern slopes of Elborz in the north and the lands leading to semi-desert plains in southern Tehran. These two factors (the slopes of Elborz and the semi desert area), which in the 1980s and before were deterrents to the spread of urban buildup, seem to have disappeared and the area has become fully occupied. In 2014, only a small part of the West remains as barren land accounting for 10.8% of the area (table 3.7), part of which of course is the Mehrabad airport runways. Although in this year vegetation land cover has increased by19.8% (table 3.7) compared to 2009, however this has only helped the situation to return to its previous state of year 2000.

## 3.3. Comparison of land covers types during 1990 -2014

Land cover changes in Tehran during the 1990, 2000, 2009 and 2014 have been analyzed and the results are shown as the percentage change table based on supervised classification comparison in the table of 3.7. The percentage of each land cover listed separately for different years to help better analyze the figures.

**Table 3.7 Land covers change (in percent and hector) 1990-2014**

| year | Built up | Barren land | vegetation | Water body |
|---|---|---|---|---|
| 1990 | 52.4% | 25.9% | 21.5% | 0.03% |
| 2000 | 60.7% | 19.3% | 19.8% | 0.03% |
| 2009 | 64.3% | 23.9% | 11.6% | 0.03% |
| 2014 | 68.9% | 10.8% | 19.8% | 0.17% |

The above results show built-up area expansion has greatly increased through the 1990-2014 period to about than twice the previous 25 years to that. The majority of this 16.5% expansion has taken place during the period of 1990 to 2014 (table 3.7). During the 3 periods after this, the expansion of built-up area has remained between 4%-8% during each period. The bulk of barren and vegetation land cover area from 1990 to 2000 (table 3.7) has had a

continuously reducing trend. The land cover type comparison table shows a relationship between the reduction in these areas and the increase of built-up area. As the table shows, barren lands have had greater reduction compared with that of vegetation. From 1990 to 1990, built-up area shows 8% increase, barren land 6%, while vegetation shows 2% decrease.

In 2009 compared with previous to that, there has been an increase in barren land area. On the same year vegetation shows a considerable reduction, which indicates destruction of vegetation and its conversion to barren lands. The opposite of this situation has taken place in 2014(table 3.7) and there has been a 13% reduction in barren lands, 8% increase in vegetation, while built-up area has only increased by 4%, explaining the situation with barren land reduction. It seems that after the destruction of vegetation in 2009 (3.7) the situation has been noticed and actions have taken place to remedy it by creating this vegetation area.

All together, the total share of water body in Tehran is very minimal and with the construction of an artificial lake in the west of Tehran in 2012, the water body surface area has also increased in 2014, compared to previous periods.

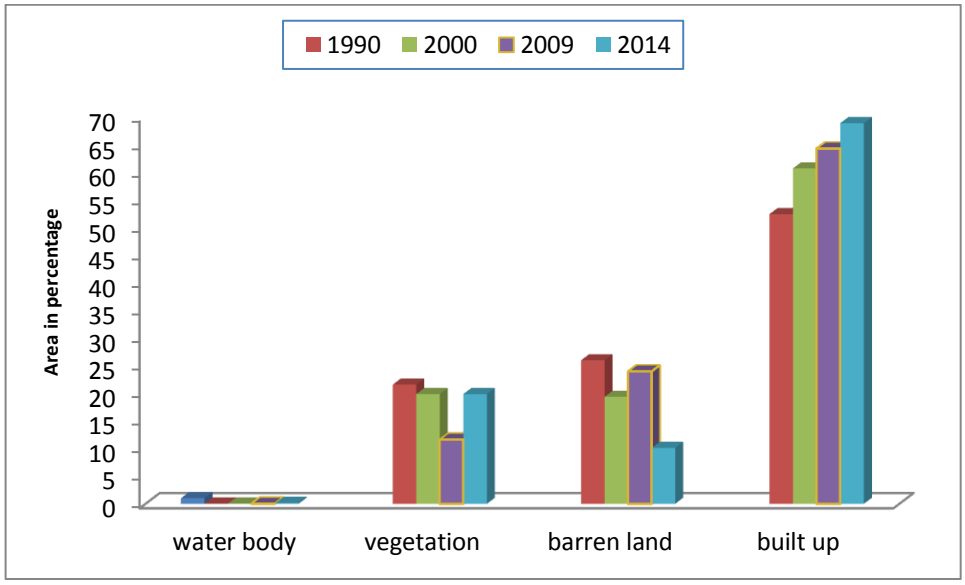


**Figure 3.22 change in land cover composition from 1980 to 2014**

## 3.4. Change detection of land cover

To determine land cover changes in Tehran, the Erdas software was used with the Recode method over the three consecutive periods of 1990-2000, 2000-2009 and 2009-2014.

In this method, the land cover of interest is separated from the rest of the classified land covers using the recode option in the Erdas and is assigned a code (of for example 1 for built-up) and all other land cover types are given a code of zero. This step is repeated in turn for all other land cover types in separate images until all land cover types are coded. Then, these are compared with the classified image of the next period and the output of this comparison shows the changes in each land cover type since the previous period. (Figures from 3.23 to 3.31 are for detection through recode method).

For example, if the first land cover of interest is vegetation, this will be recoded and masked in the image of 1990 and compared with image of 2000. This will produce an image according to the difference in the value of each land cover between the images of 1990 and 2000 and will thus show what percentage of the vegetation has changed to any other land cover.

This process was repeated in turn for each of the four classified land covers for every one of the three periods to show the changes in each decade. The classified Land cover (figures3.19-3.21) and their corresponding graph (Figure 3.22) represent the fact that majority of land cover in Tehran have been converted from vegetation and barren lands to built-up area. Now, the investigation of these changes in vegetation and barren lands during the four decades and the extent of change and conversion of these to any other type will be followed and explained.

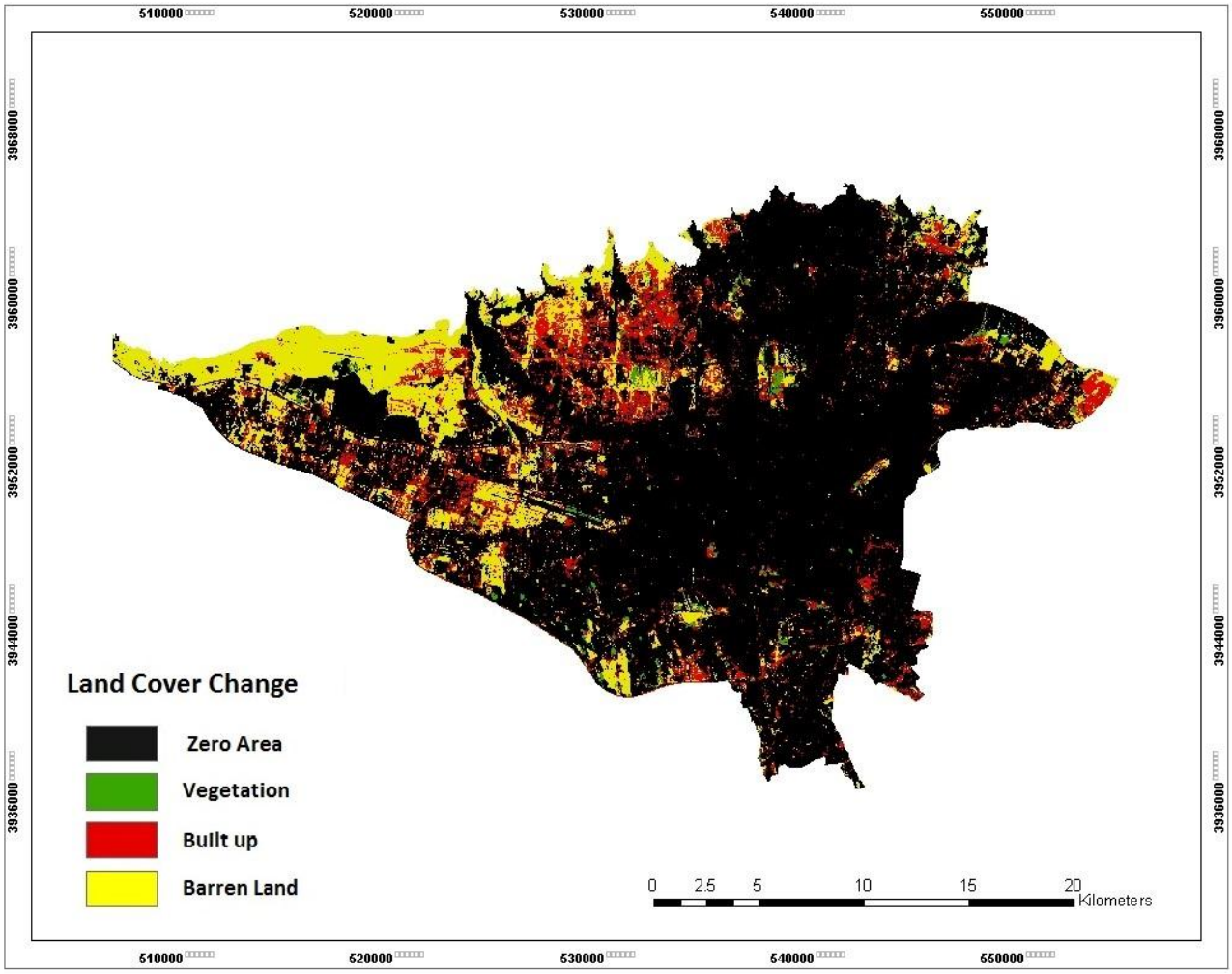


**Figure 3.23 barren land changes 1990-2000**

Between 1990 and 2000 figure 3.23, the process of reducing the level of barren land continued to exist. As seen in figure 3.23 most of the changes, as with the previous decade, have been the barren land conversion to built-up that can clearly be seen in red in the northern half. In this period part of barren lands have been converted to built-up area (table 3.6), a major part of which has been in the north and towards the slopes of southern Alborz. Also, as we see on the figure 3.23, the green which indicates change of barren land to vegetation is very little and only marked in the form of tiny dots.

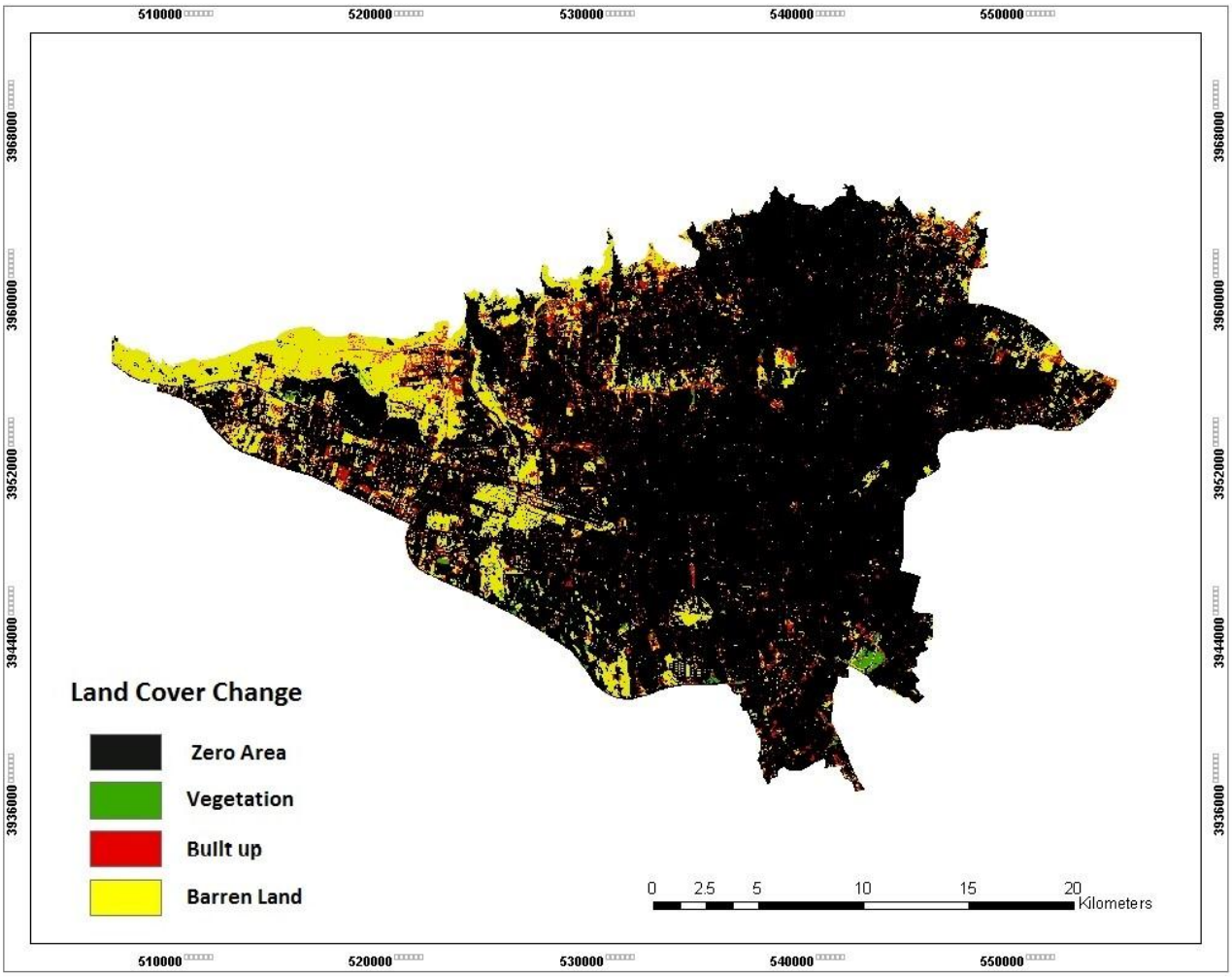


**Figure 3.24 barren land changes 2000-2009**

It seems that during the years between 2000- 2009 figure 3.24 the process of barren land change has slowed down, compared to the previous two decades (figure 3.23 and 3.24). As shown, very small scattered barren land changes have taken place in the northern half which can be seen as built-up. Changes to vegetation, as with previous decade has been very little and only in the southern area of the figure a small vegetation cover can be seen.

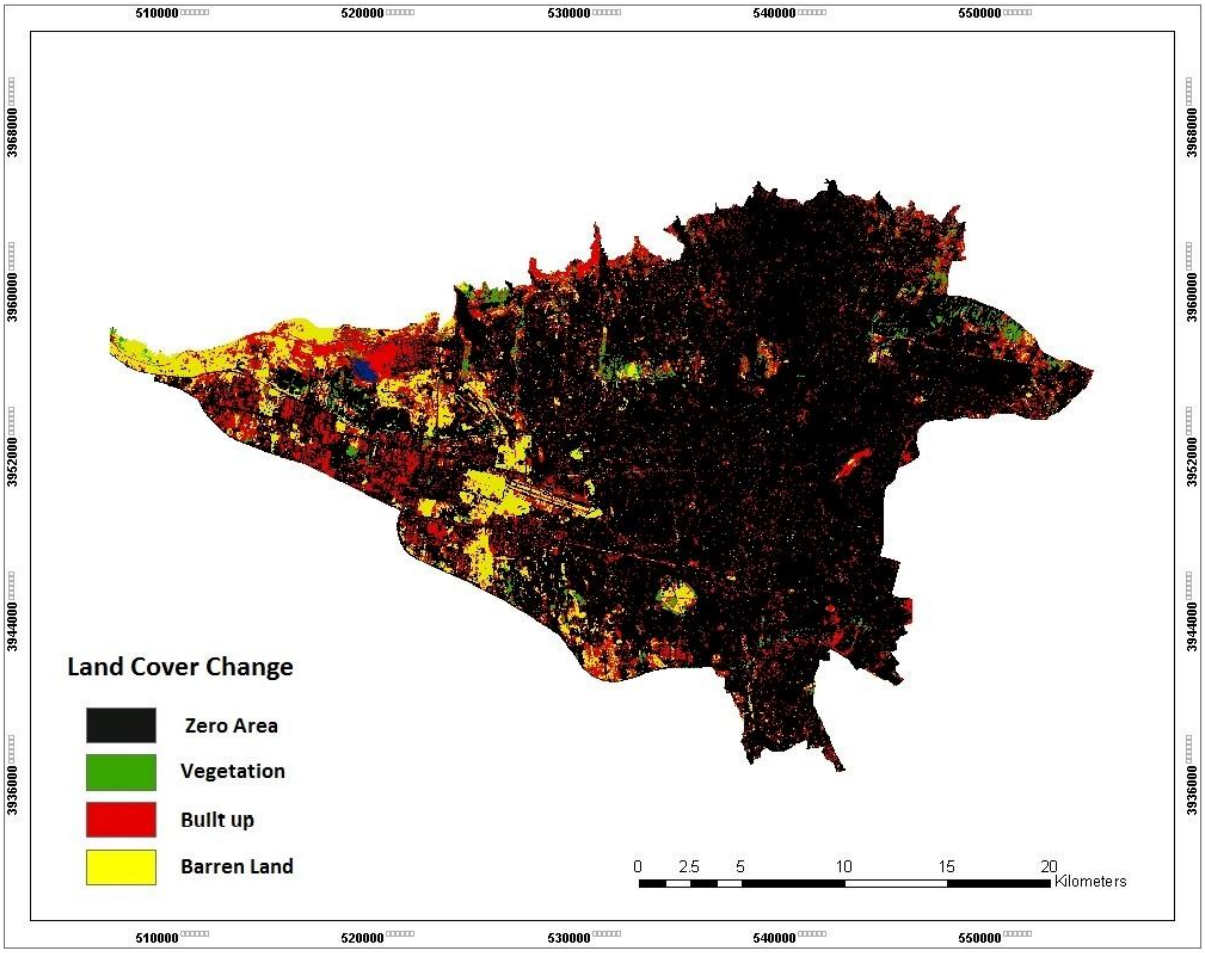


**Figure 3.25 barren land changes 2009-2014**

Figure 3.25 which relates to the years between 2009 and 2014, suggests that barren land cover change has accelerated compared to the previous period of 2000-2009 (figure3.24). Again, these changes, which signify an intense change in the North and West, have been from barren lands to built-up. However, as can be seen, part of these barren lands, especially in the East where the forest park of Sorkhe-Hesar is located, has changed to vegetation covers which are indicated as scattered green spots in figure 3.24. It seems that during the period of 2009-2014, more attention has been paid to revitalizing barren lands and turning them into vegetation. A unique feature of land cover change figure 3.25 of this period in Tehran is the construction and appearance of Cheetgar artificial lake. This however small but significant area can be seen in blue and has taken a tiny share of the vast land area of Tehran for itself. Generally, the share of

water cover in Tehran has always been very little. From 1990 until 2009 there had not been any visible change in water body. Therefore in land cover change detection of water cover including this lake which did not exist on the previous decade's figures has not been included. To the west of this lake where the Cheetgar forest park is located, land cover change of barren land to vegetation can be seen. As can be seen from the figures 3.22 to 3.25 a major part of the barren land during the 25 years between 1990 and 2014 shows perceptible change and the majority of this were urbanized. Apart from small regions around west of Tehran, no barren land is visible in other parts of the city.

As can be seen in the figure 3.24 a major part of the change in barren land has been in the direction of conversion to built-up and only a small part has changed to vegetation. As it is visible in the figure 3.21, this change from barren land to built-up during the previous10 year period accounts for more than half of barren lands. The extent of this change has been more severe in the south than other areas. So it seems the spread and expansion of the built-up cover has preferred the flatlands and desert like area of the south rather than the hilly and mountainous area of north of Tehran. The share of vegetation cover in these land cover type change has been very little and ironically majority of this can been seen in the south, where the expansion of built-up land can be seen most.

Apart from the Cheetgar artificial lake shown in figure 3.25, there is no significant water cover in Tehran. The lake was constructed between 2009- 2014 and that is why it is not seen in previous years land cover figures. Therefore, in analyzing land covers it will not be investigated as a separate class. In the image below, the 4 steps of barren land assessment has been demonstrated in a single view from the Erdas and the process of changes on this land cover type has been shown. The changes on vegetation cover of the city of Tehran during the decades of 1990-2000, 2000-2009 and 2009-2014 are assessed in continuation of this chapter.

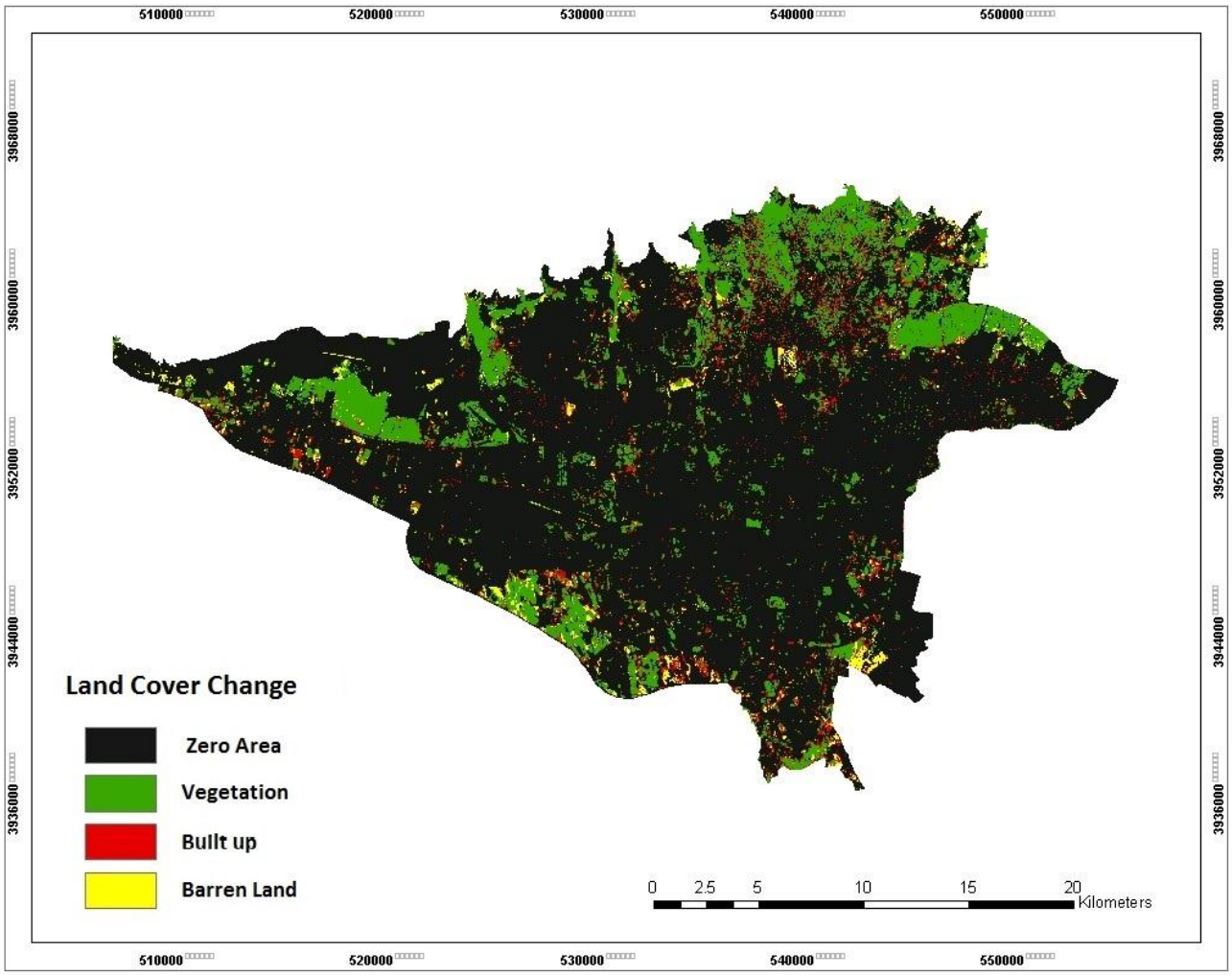


**Figure 3.26 vegetation changes 1990-2000**

In figure 3.26, changes of vegetation cover during the period of 1990-2000 can be seen to have taken place with a slow pace of conversion of these lands to built-up areas. In the north and south of this figure, a gradual expansion of built area towards the vegetated land can be seen, indicated in red.

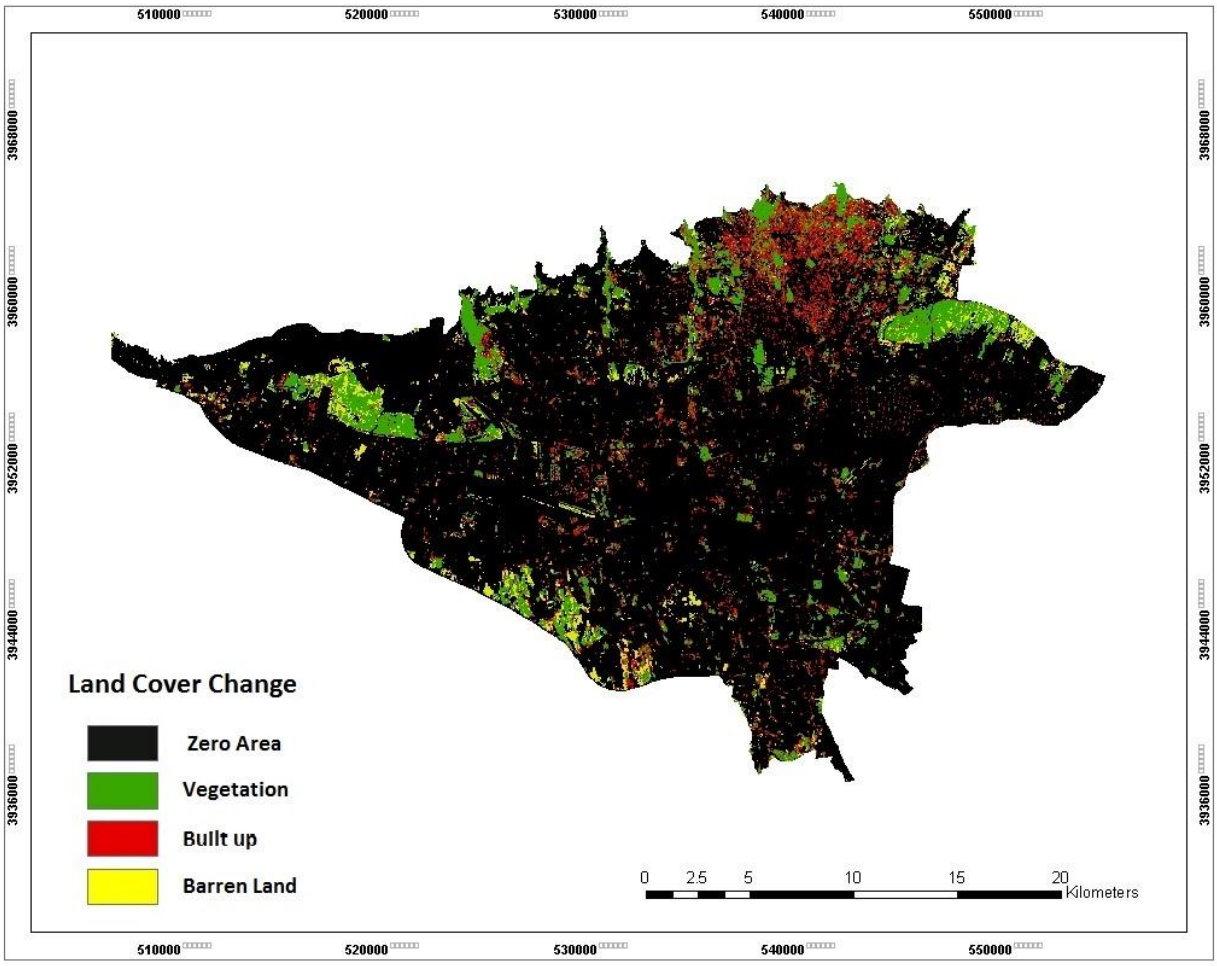


**Figure 3.27 vegetation changes 2000-2009**

Between 2000 and 2009 extreme changes have taken place on vegetation cover figure 3.27. So much so, that on the figure especially in the north, conversion of vegetated land to built-up area is very noticeable. The destruction of vegetation cover across the city, shown in red and yellow colours visualizes the fact that this devastation had been unprecedented compared to the previous two decades. It can be said that almost half of the vegetation cover of the city of Tehran was lost during this decade.

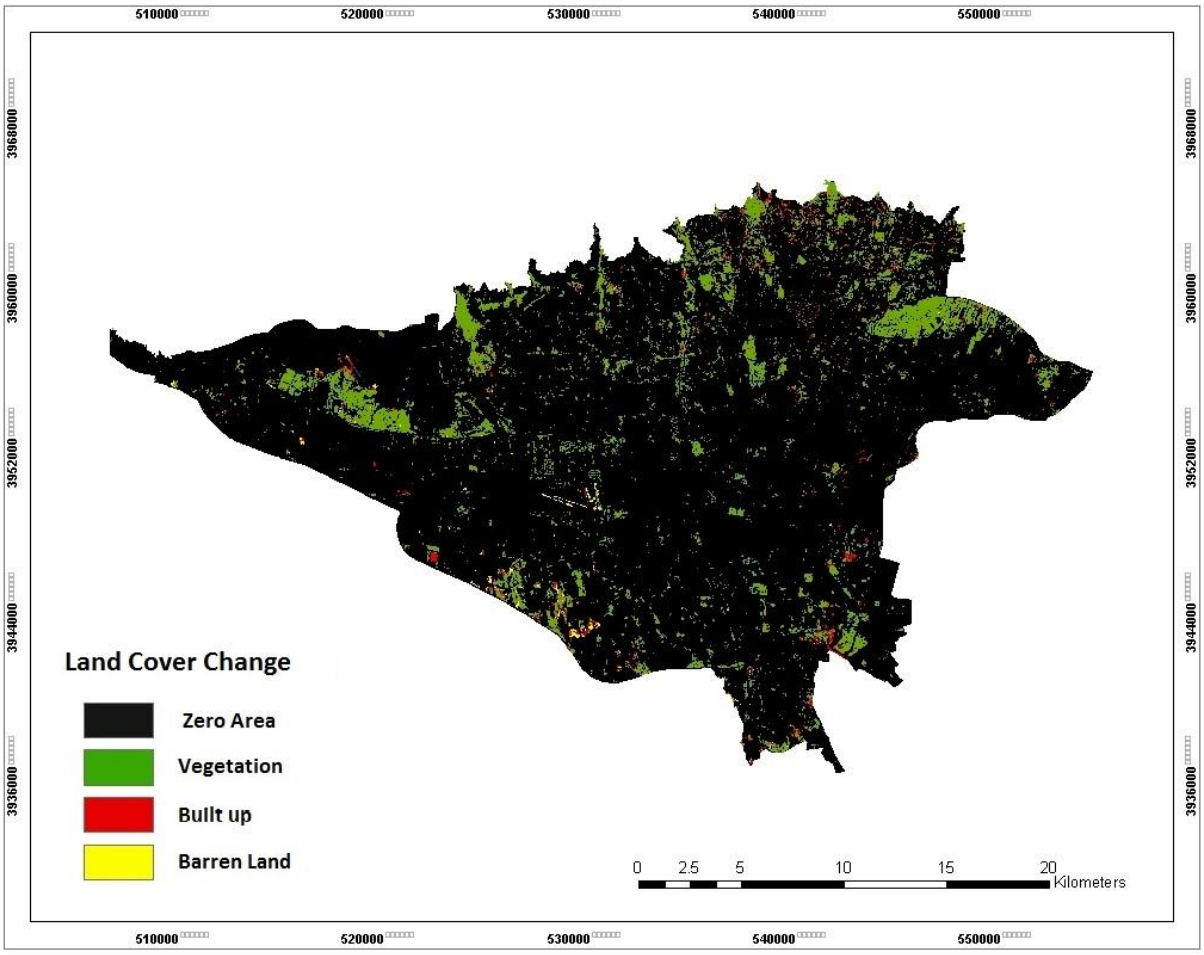


**Figure 3.28 vegetation changes 2009-2014**

According to this figure from 2009 (figure 3.27) to 2014 (figure 3.28) the destruction trend of vegetation cover was halted. There are of course a few small and limited number of red spot on this figure which are negligible. As a whole, the vegetation cover of the city of Tehran during the 25 years between 1990 and 2014 shows a huge reduction which was mostly caused by conversion of these lands to increased built up and urbanization expansion in this mega city. Following on from here, land cover changes in relation to built-up cover will be discussed. It should be noted that built-up land cover includes all types of human constructed buildings such as residential buildings, industrial centers and highways.

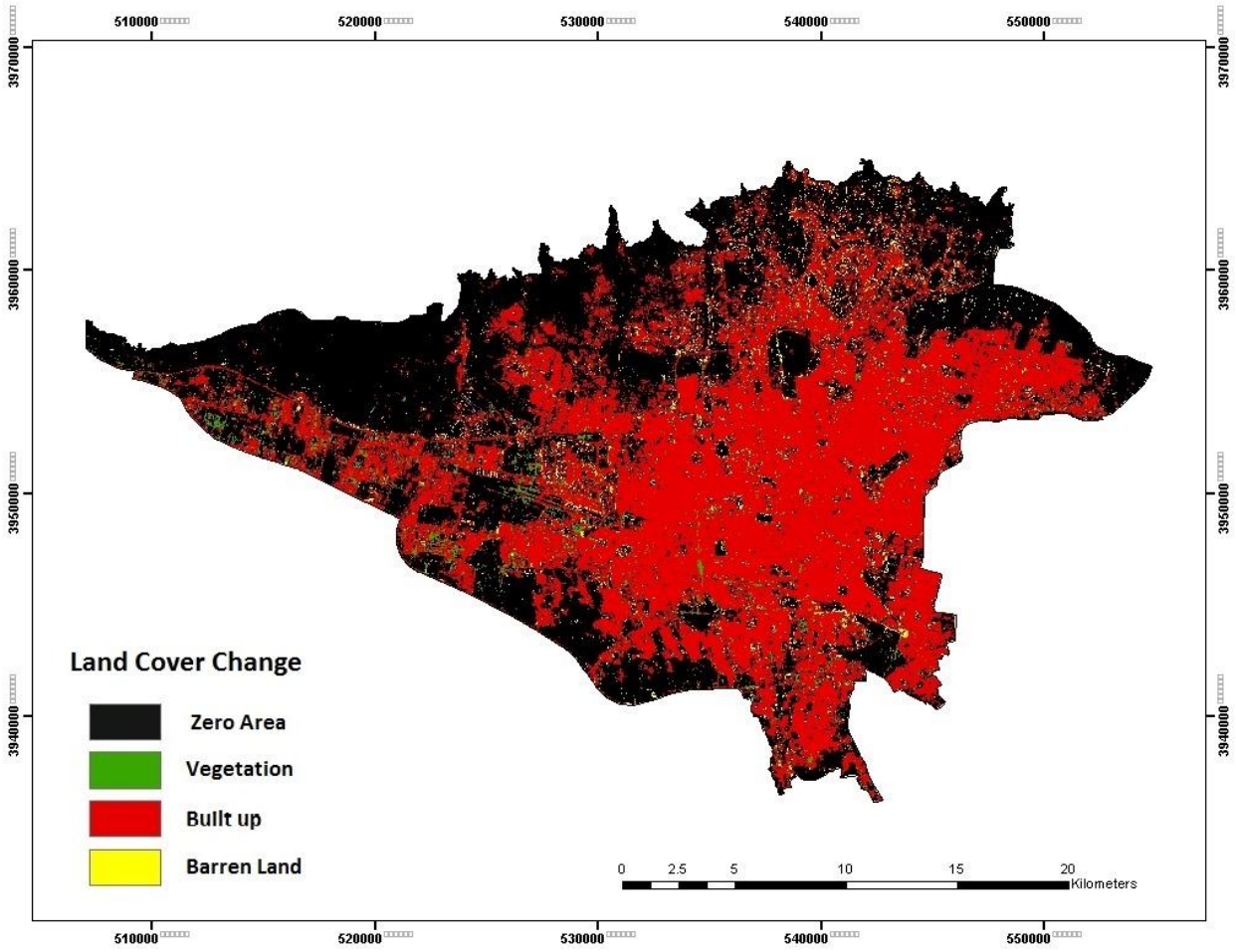


**Figure 3.29 built up changes 1990-2000**

During the period of 1990-2000 (figure 3.29), a major part of the land in Tehran has been converted to built-up, which compared with the previous period (figure 3.28) has very much increased. The expansion of the built-up area has mostly been towards the south and almost all of the land area of the southern half has been built on and this shows that the expansion of urbanization in Tehran and the physical dimension of the city has particularly been in the southern direction with flat lands. The proportion of expansion of built-up area in the north has been smaller than that of the south. Parts of the built-up area have been converted to vegetation and water body, most of which has been due to demolition of limited amount of eroded old buildings or the city renovations.

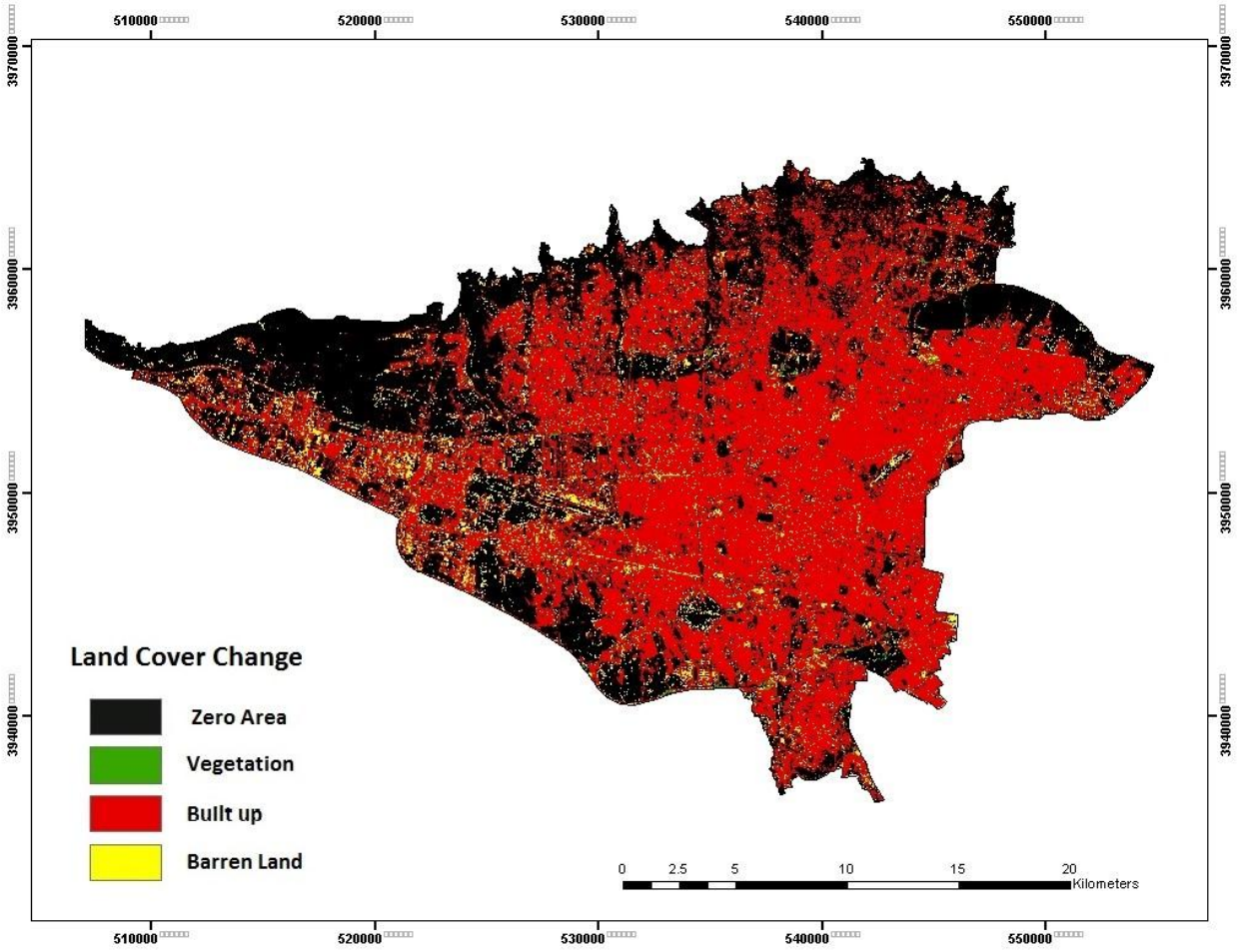


**Figure 3.30 built up changes 2000-2009**

As shown in figure 3.304, most of the city area has been filled with built-up cover. This cover with an area of 39445.47 which has enclosed the city area from north to south is almost twice as much as the built-up area in previous period (Figure 3.29). In this period part of the built-up area has been converted to barren land and some part of it to vegetation. These barren lands are mostly in the western half and the southwest of Tehran and have been due to demolition of the old buildings, vast highway constructions as well as park lawns in Tehran in this period.

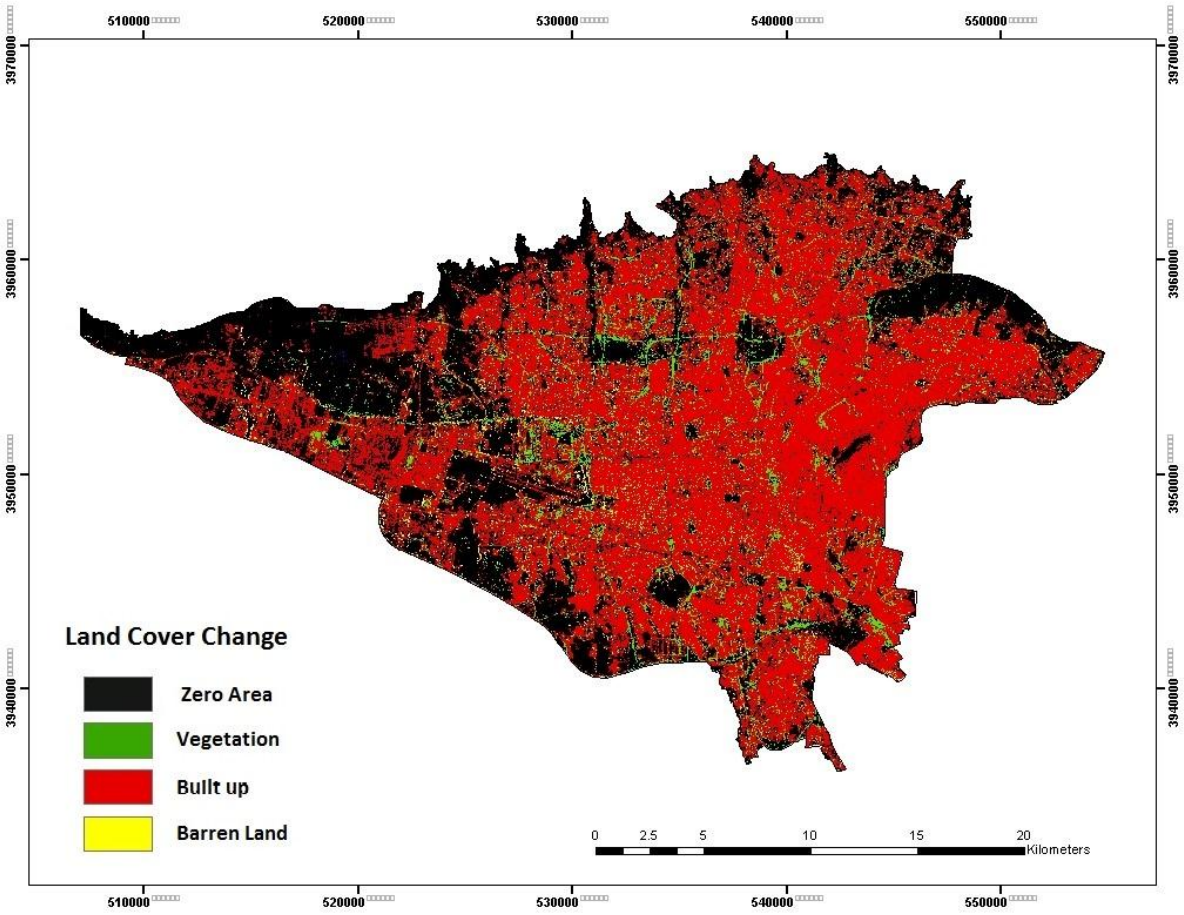


**Figure 3. 31 built-up changes 2009-2014**

In the period of 2009-2014 (figure 3.31), the level of building and construction in Tehran reached it's highest in the 25 years. In this period a substantial part of the land which had been barren in figure 3.34, was converted to vegetation and show the green belts across the city. During the 25 year period the city of Tehran has very much been developed and all sorts of constructions have taken place in almost all parts of the city. These building constructions which in the beginning were carried out by the migrants of villages and small cities without planning permissions around the city borders gradually have turned into city suburbia around Tehran.

Eventually with the intervention of the government and particularly the city council of Tehran, efforts were made to control these constructions by various means and much increased control was gained over construction of buildings. Nevertheless, the expansion of the city of Tehran and the conversion of barren land and even vegetation to built-up was unavoidable. At

present there are strict regulation in place for any type of construction due to the limiting factors of this city. In recent years the idea of beautifying and construction of green spaces across the city has greatly drawn the attention of the city managers and the biggest confirmation of this has been the construction of large parks and the artificial lake of Chitgar.

Here, the result of the steps followed so far have helped to produce matrix tables summarizing the analysis of land cover changes in each period, these matrix tables are discussed below. In matrix table 3.8, highlighted values denote no change. That is to say any area in 1990 has still remained the same in 2000. In 1990, the total area of barren land was 32,410.31 hectares, which has reached an area of 11859.43 hectares in 2000 and 28988.64 hectares of it were allocated to the built-up.

**Table 3.8 Land cover change matrix (in hectare) 1990-2000**

| | | **land cover 1990** | | | | |
|---|---|---|---|---|---|---|
| **land cover 2000** | | Water Body | Vegetation | Barren Land | Built Up | Grand Total |
| | Water Body | 7.81 | 0.03 | 1.12 | 12.46 | **21.42** |
| | Vegetation | 0.01 | 9158.67 | 1130.63 | 1870.07 | **12159.38** |
| | Barren Land | 0.06 | 2637.15 | 5625.97 | 28988.64 | **37251.83** |
| | Built Up | 0 | 1297.82 | 9022.47 | 1539.14 | **11859.43** |
| | Grand Total | **7.89** | **13093.68** | **15780.18** | **32410.31** | **61292.05** |

The above table shows that for example in 1990 the total barren land was 32410.31 hectares and since then until year 2000 12.46 hectares changed into water body, 1870.07 hectares to vegetation, 28988.64 hectares to built-up. Only 1539.14 hectares of the total from 1990 still remained as barren land. Comparing the total of built-up cover from 1990 until 2000 shows the land cover area has increased over two folds from 15780.18 hectares to 37251.83 hectares. The total Vegetation cover area of 13093.98 hectares has decreased to 12159.38 hectares. The above analysis clarify that the highly perceptible amount of reduction in the barren land area together with the reduction in the vegetation cover can be traced to the intense increase in the built-up land cover area.

**Table 3.9 Land cover change matrix (in hectare) 2000-2009**

| land cover 2009 | Land cover 2000 | | | | |
|---|---|---|---|---|---|
| | water body | vegetation | barren land | built up | Grand Total |
| water body | 19.26 | 1.26 | 2.07 | 0.81 | **23.4** |
| vegetation | 0 | 6138.99 | 505.35 | 520.65 | **7164.99** |
| barren land | 0.09 | 4024.98 | 32700.6 | 2719.8 | **39445.47** |
| built up | 2.07 | 2003.85 | 4062.87 | 8643.33 | **14712.12** |
| Grand Total | **21.42** | **12169.08** | **37270.89** | **11884.59** | **61345.98** |

Comparison of barren lands in 2000 and 2009 indicated an increase in the area of this land from 11884.59 to 14712.12 hectares. (Matrix table 3.9). In this period, the total built-up area has also increased. On the other hand, vegetation has decreased sharply in this period from 12169,08 in 2000 to 7164,47, which is close to the destruction of about half of the vegetation cover in this period. Of the total vegetation cover in this period 2003.85 hectares to barren land and 4024.98 has change to built-up.

**Table 3.10 Land cover change matrix (in hectare) 2009-2014**

| land cover 2014 | Land cover 2009 | | | | |
|---|---|---|---|---|---|
| | water body | vegetation | barren land | built up | Grand Total |
| water body | 16.56 | 5.76 | 2.43 | 82.89 | **107.64** |
| vegetation | 0.18 | 6187.77 | 4311.72 | 1659.6 | **12159.27** |
| barren land | 6.48 | 816.21 | 33719.85 | 8350.83 | **42893.37** |
| built up | 0.18 | 155.25 | 1411.47 | 4618.8 | **6185.7** |
| Grand Total | **23.4** | **7164.99** | **39445.47** | **14712.12** | **61345.98** |

During the 2009-2014 period, land cover (Matrix Table 3.10) differs significantly from the previous period (matrix 3.9). In this period, barren land has fallen sharply from 14712.12 hectares in 2009 to 6185.7 hectares in 2014. In contrast to vegetation and water body, a significant increase in levels is observed. Vegetation cover has become 12159.27 hectares and water body has 107.64 hectares of land in 2014. During this period, the increase in built-up area from 39,445.47 hectares has reached 42893.37 hectares and as in the previous two years, the increasing trend is continued.

## 3.5. Summery

The Comparison of images and the analysis of land cover changes over 25 years suggests that in Tehran, the same as any other major city in the world, the change trend of land cover has commonly been the conversion of vegetation and barren land into built-up areas.

Built-up area takes the biggest share of Tehran's land cover. The expansion of built-up area has followed a regularly increasing trend from 19**90** to 2014. Vegetation and barren lands have both experienced reduction and increase over different periods. Also, water body has continually had the lowest share of land cover, being explanatory of the fact that Tehran has a lack of access to shallow waters.

Altogether, the analyses of land cover changes from 1990 to 2014 indicate that these changes have been extensive and a major part of these have been in the direction of change to built-up land from all other types of land covers. In other words, the expansion of urbanization in Tehran has destroyed and sacrificed the vegetation and barren lands in the area. Without a doubt, these extensive changes in the land cover of the area have not been without consequence and impact on the temperature, energy bill and the microclimate of the city. Having determined the changes in land cover types, temperature and the effect of land cover change on temperature will be discussed in the following chapters.

## Reference

1. Alavi Panah, S. K.Ch B Komaki, A Goorabi and H R Matinfar, 2007. Characterizing Land Cover Types and Surface Condition of Yardang Region in Lut Desert ( Iran ) Based upon Landsat Satellite Images, World Applied Sciences Journal 2, vol. 3, pp. 212-228.

2. Amiri, R., Qihao Weng and A. Alimohammadi, 2009. Spatial temporal dynamics of land surface temperature in relation to fractional vegetation cover and land use/cover in the Tabriz urban area, Iran, Remote Sensing of Environment, Vol 14, pp 2606- 2617.

3. Congalton, R.G, 1991, A Review of Assessing the Accuracy of Classifications of Remotely Sensed Data, Remote sensing environment, vol.37, pp.35-46.

4. Falahatkar. S., Seyed Mohsen Hosseini and Ali Reza Soffiania, 2011, Indian Journal of Science and Technology, vol. 4, pp. 0974- 6846.

5. Gonçalves, R.P., C. Assis, O. Vieira, 2007, Comparison of sampling methods to classification of remotely sensed images, IV Simpósio Internacional de Agricultura de Precisão, 23 a 25 de outubro de 2007, Viçosa-MG.

6. Horning,N., 2004, Land cover classification methods, Center for Biodiversity and Conservation, American Museum of Natural History.

7. Kwesabal, D.A, A. Andesikuteb Yakubu, L.A.Nathaniel, J. D. Nyomo and K.Magaji, 2014, Determination of change matrix among the landuse/landcover types in Jalingo metropolis, Nigeria, International Journal of Innovation and Applied Studies, vol.8, pp. 213-224.

8. Singh, A., 1989, Review article digital change detection techniques using remotely-sensed data, International Journal of Remote Sensing, vol, 10, pp. 989-1003.

9. virera , j., MD. Joanne, M. Garrett, 2005, Understanding Inter-observer Agreement: The Kappa Statistic, Family Medicine, pp.360.

10. Weng, Q.2001. Effect of development of cities on the Earth temperature in the Zhujiang detta in China. INT. J. Remote sensing, 10, 1999-2014.

# Chapter 4

**Analysis of Land Surface Temperature**

## 4.1. Introduction

Land surface temperature (LST) is an important parameter in the Earth's system and the processes in the atmosphere. Knowledge of the LST plays an important role in a wide variety of scientific studies such as global change, ecology and hydrology. Xiaolei (2014).

Amongst all climate determining factors, temperature is particularly considered the most important and effective factor controlling all the others. (Alijani, 1998). A change in temperature is relatively more apparent and its consequence on life is so much more effective than any other factor which can influence human life in many ways. In environmental studies temperature has therefore drawn the attention of researchers, environmentalists and city councils as the most influential climatic factor.

Land cover change, Life style (urban) and predominant activities in populated centers such as cities, altogether have serious effects on the temperature and microclimate of populated areas and in the long term can change temperature pattern. Obviously, the type of activity in urban area is far different than that in other areas such as villages and country sides and so changes in land cover in different regions depends on the type of activity and hence land use in each region. The main activities of people in villages are farming and agriculture, rather than manufacturing and construction. The type of land occupied in these rejoins is forestry and vegetation and not for factories and highways and construction and land cover changes take place accordingly. City Temperature changes in long or even short term can dominate and limit urban design and developments. Thus, management and planners are keen to determine the cause and the level of possible changes to devise a solution to the resulting consequences.

Due to the complexity of surface temperature, ground measurement over extensive areas on Earth is not practical. However, with the development of remote sensing, it has been possible to measure the land surface (LST) over the entire globe with sufficiently high temporal

resolution. Use of satellite measurement in environmental studies has been favored by researchers for many reasons, some of which are outlined here.

With regards to high capability of satellite measurement in gathering the electromagnetic spectrum reflection of the Earth's phenomenon such as infrared spectrum the possibility of assessing the LST exists on various regions including city areas. (Alavipanah, 2007). Retrieval of temperature data using satellite has many advantages over gathering ground data. The limit in the possible number of synoptic stations across cities (dependant on the availability of resources, suitable points, the funds and the size of the area, etc.) is a disadvantage that has been overcome with the use of satellites which offer the capacity of capturing data from the surface over a wide area.

## 4.2. Data and methodology

In this chapter the land surface temperatures of Tehran from 1990 to 2015 have been analyzed using the Landsat thermal bands of 5, 7 and 8. To analyse the temperature, the Landsat thermal band images for July of the years of 1990, 2000, 2009 and 2014 have been used as the images for the hottest month and those for January of the years 1991, 2001, 2010 and 2015 as the coldest month in Iran.

The necessary preparation processes of the thermal band of the images prior to analysis are explained later in this chapter. Also, it should be noted that the reason for January and July as the coldest and hottest month of year not being in the same Georgian calendar year is that this is different than the Persian calendar of Iran. For example the July of 1990 and January of 1991 are the summer and winter of the same Persian calendar year and the selected satellite image are in the order of seasons which can never fall in the same Georgian calendar year to begin with.

Prior to calculating the land surface temperature the thermal band of all images must first be prepared. For this purpose, band 6 of Landsat 5 and 7 and band 10 of Landsat 8 OLI images were chosen to be calculated. The images of Landsat 8 contain two thermal bands of 10 and 11. In this research only the images of thermal band 10 for 2014 and 2015 of Landsat 8 will be used. The reason for this is the important USGS (Jan. 6, 2014) notice on the NASA Landsat science (http://Landsat.gsfc.nasa.gov) website.

> "**Important TIRS calibration notice from USGS, Jan. 6, 2014**: "Due to the larger calibration uncertainty associated with TIRS band 11, it is recommended that users refrain from relying on band 11 data in quantitative analysis of the TIRS data, such as the use of split window techniques for atmospheric correction and retrieval of surface temperature values.".

Also, "for the LST retrieval, possessing only one thermal band is an important limitation that does not allow applying a split-window method", (Sobrino et al, 1996). On this basis and as well as various other issues explained later, the single channel method was chosen for the LST retrieval. To calculate the LST, an appropriate method must be selected, depending on the type of satellite for the imagery as the source of data (e.g. MODIS, Aster, LandSat), the number of used thermal bands (one or more) available, the natural geographical characteristics of the area under study (e.g. weather, number of land cover types) and finally the availability of the data such the land surface emissivity (LSE) prior to processing the LST is also important.

All of the above have been considered in this research including the fact that the LSEs for the study area land cover types are not known and must be calculated. Therefore, the most appropriate method for this research the LST was obtained by following the NDVI based emissivity method. Sobrino, Raissouni, and Li (2001), using the ArcGIS software.

### 4.2.1. Thermal band processing for the LST retrieval.

Having accessed the satellite images, steps must be taken to calibrate the required band of these images to be able to use their data. These steps are followed as described in the Landsat users' handbook available at NASA website. For this study the thermal bands of Landsat 5, 7 and 8 were used with the following steps for image calibration and correction.

#### 4.2.1.1. *Conversion of the Digital Number (DN) to Spectral Radiance (L)*

The Landsat (or other data source) images are generally delivered as images with raw digital number (DN) values. As no spectral index can be applied to this raw data therefore the

data have to be prepared for analysis by converting the DN values into reflective values. These are calculated using the below formula (USGS 2001).

Lλ= *gain* DN +offset or*

$$L\lambda = ((LMAX\lambda - LMIN\lambda)/(QCALMAX-QCALMIN)) * (QCAL-QCALMIN) + LMIN\lambda \quad (1)$$

Where,

The QCALMIN, QCALMAX and QCAL are the Digital Number

The LMINλ and LMAXλ are the spectral radiances for thermal band at digital numbers

***4.2.1.2. Brightness temperature conversion***

The Landsat images thermal band data can be converted from spectral radiance temperature using the equation (2), by (NASA, 2008). The required values for this are obtained from the header file of the images.

$$T_B = \frac{K_2}{\ln\left(\frac{K_1}{L\lambda} + 1\right)} - 273.15 \quad (2)$$

Where,

T = Effective at-satellite temperature in Kelvin

K1 = Calibration constant 1 (watts/meter squared*ster*µm) (666.09)

K2 = Calibration 2 (Kelvin) (1282.71)

Lλ = Spectral radiance (watts/meter squared*ster*µm)

**Table 4.11 Landsat image Thermal Band Calibration Constants**

| Landsat | Constant 1- K1<br>watts/(meter squared * ster * µm) | Constant 2 - K2<br>Kelvin |
|---|---|---|
| Landsat 5 | 607.76 | 1260.56 |
| Landsat 7 | 666.09 | 1282.71 |
| Landsat8 | 774.119(b10) | 1321.0789 |

In processing the Landsat images for the LST retrieval the steps taken have been followed as shown in the flow chart and outlined here.

- Conversion of the Digital Number (DN) to Spectral Radiance (L)
- Conversion of brightness temperature
- Calculation of the NDVI
- Calculation of proportion of vegetation
- Calculation of the emissivity
- Calculation of the LST

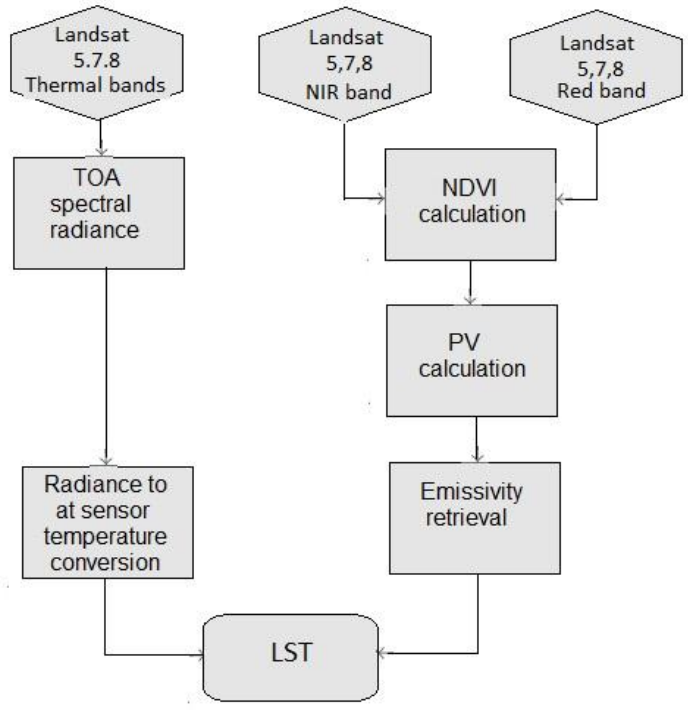


**LST retrieval flow chart**

Having completed these steps in order to obtain the (LST), the normalized difference vegetation index (NDVI) is then calculated to take into account the effect of Emissivity on the LST. Also, with regards to the fact that the NDVI value is used in the emissivity calculation formula, therefore, first the NDVI is calculate and then the emissivity.

### 4.2.2. Normalized Difference Vegetation Index (NDVI)

Land surface emissivity is best and easy to obtain from Normalized Difference Vegetation Index (NDVI), Sobrino and Raissouni (2000), Valor and Caselles (1996), and Van de Griend and Owe (1993). Some of the phenomena and effects, such as ground vegetation vary over time due to natural causes or human causes which affect the conditions and performance of the environment. Therefore, detection, visualization, prediction and evaluation of such changes in an environment are very important. Today, the production of an accurate land cover map is considered one of the important tools in planning and development. For the purpose of monitoring and assessment of field vegetation, access to up to date data is usually difficult and limited. Features such as the provision of a broad and integrated vision of a region, repeatability, convenience, and accuracy are what make the use of such data and information over any other method when it comes to the analysis of the vegetation cover and change control. Accordingly, many researchers consider the use of remote sensing technique as the most appropriate method to investigate vegetation cover and data evaluation. In fact, the prevailing view in the field of research and vegetation monitoring is using remote sensing vegetation indices.

These indices are mathematical combination of multiple bands of digital satellite images which make use of significant difference in the blue, red, green and near-infrared vegetation reflectance wavelengths. They use simple mathematical operations like addition, subtraction or other linear combinations to change the value of each pixel in different bands into a numerical index. Several decades have passed since the first application of vegetation indices for different purposes and are still being widely used. Among the variety of vegetation indices, NDVI is one of the global vegetation indices which is used for the preparation of permanent vegetation location and time information. The index is based on the fact that the chlorophyll in the plants can absorb red light, and the mesophyll layer of leaf reflects the near-infrared light. NDVI is the most commonly used vegetation index for monitoring vegetation globally. Mathematically NDVI is calculated using the below formula (Carlson and Ripley 1997) and (Sobrino et al 2008):

$$NDVI = \frac{R_{NIR} - R_{red}}{R_{NIR} + R_{red}} \quad (3)$$

The significance of NDVI value from -1 to 1 in interpretation of NDVI images in remote sensing is the visible light in 0.4 to 0.7 micron range that is absorbed with great intensity by the chlorophyll in plant cells to perform photosynthesis activity. In contrast, the near-infrared wavelengths of 0.7 to 1.1 micron are strongly reflected by the leaf cells, because the absorption of these wavelengths by a sharp rise in temperature can cause the destruction of plant tissues. Because of this difference in absorption and reflection, plants in the range of the visible spectrum appear dark and in the range of near infrared appear brightly colored. Water body seems to be more willing to absorb near infrared rather than the visible light range and therefore in this range they appear bright. Barren land and other complications, such as buildings absorb all wavelengths of visible and near-infrared range equally and reflect the same range so both can be seen with the NDVI values ranging between -1 to +1. The water levels of the index tend to have a negative -1 values, barren lands tend to show zero and vegetation tend to have a value of +1. In this study vegetation cover map has been prepared based on the table below which shows the minimum and the maximum values of NDVI calculated using the ArcGIS software. These results are used to calculate the Pv and the emissivity.

**Table 4.12 NDVI maximum and minimum 1990-2015**

| Year | Month | Minimum NDVI | Maximum NDVI |
|---|---|---|---|
| 1990 | July | -0.245 | 0.608 |
| 1991 | January | -0.35 | 0.424 |
| 2000 | July | -0.55 | 0.509 |
| 2001 | January | -0.317 | 0.388 |
| 2009 | July | -0.271 | 0.606 |
| 2010 | January | -0.364 | 0.364 |
| 2014 | July | -0.142 | 0.565 |
| 2015 | January | -0.161 | 0.417 |

The above table shows that the maximum NDVI is higher in July months than those for January. This is clearly due to the fact that vegetation cover in July is denser and in January being winter, vegetation is thinner.

### 4.2.3. Emissivity

The emissivity or the rate at which emission takes place on the Earth's surface has an effect on its temperature level dependent on the surface cover material type. It is necessary to calculate the emissivity of a surface using suitable methods, as its precision will have an immense effect on the reality of the surface temperature.

In this section first the emissivity of proportion vegetation is calculated. (Sobrino, 2004). Proportion vegetation is calculated using the below formula:

$$P_v = \left[ \frac{NDVI - NDVI_{min}}{NDVI_{max} - NDVI_{min}} \right]^2 \qquad (4)$$

$$E = 0.004Pv + 0.986 \qquad (5)$$

Where,

E is emissivity

0.004 is the standard deviation of the NDVI value of 0.986 and (constants)

PV is the proportion of vegetation.

Having calculated the PV using the ArcGIS software, the emissivity is calculated using this formula which has been used by a number of researchers in their work to calculate emissivity.

**Table 4.13 Maximum and Minimum Emissivity (1990-2015)**

| Year | Minimum Emissivity | Maximum Emissivity |
|---|---|---|
| 1990 | 0.986 | 0.996 |
| 1991 | 0.986 | 0.989 |
| 2000 | 0.986 | 0.99 |
| 2001 | 0.986 | 0.988 |
| 2009 | 0.986 | 0.989 |
| 2010 | 0.986 | 0.989 |
| 2014 | 0.986 | 0.99 |
| 2015 | 0.986 | 0.99 |

Suresh et al, (2016) in land surface temperature studies in Devikulam Taluk used this formula to calculate the emissivity. Also Sobrino, (2004) used this formula in the paper, "Land surface temperature retrieval from Landsat TM 5". Also another researcher who used this formula in their studies to calculate emissivity (in Singapore) was Ping Chen et al, (2006).

## 4.3. Land Surface Temperature calculation

With the provision of the required parameters to obtain the LST, the below formula Artis & Carnahan, (1982) is used for the calculation using the ArcGIS software.

$$T_s = \frac{T_B}{1 + (\lambda \times T_B / \rho) \ln \varepsilon} \qquad (6)$$

Where, λ is the wavelength of emitted radiance for which the peak response and the average of the limiting wavelengths (λ = 11.5 μm)

$T_B$ = Temperature thermal band (Centigrade)

ρ = h x c/σ (1.438 x 10-2 mK),

σ = Stefan Boltzmann's constant (5.67 x 10-8 Wm-2K-4 = 1.38 x 10-23 J/K),

h = Planck's constant (6.626 x 10-34 Jsec),

c = velocity of light (2.998 x 108 m/sec),

and ε = spectral emissivity

The LST of all images for months of January and July were calculated using the above formula. As the calculated temperature for each image is also visible in the LST (figures 4.32 to 4.35 for January and 4.36 to 39 for July) they have different ranges from each other. This can pose a problem when it comes to the temperature range comparison of each image. Therefore, to avoid this, these temperatures must be standardized and have the same unit.

## 4.4. Normalized Land Surface Temperature

As mentioned above, the calculated temperature changes have different ranges. Therefore, the direct comparison of the outright data of derived temperatures is not comparable. Therefore, using a statistical method, the surface temperature data should first be standardized. Using two parameters of minimum and maximum temperatures of each image, the land surface temperature of all images were normalized. So, all images found a uniform distribution and their temperature distribution became between 0 and 1(Mo & al 2011). The term below was used for normalizing the images.

$N= (T-T_{max}) / (T_{max} -T_{min})$ were, (7)

N= normalized temperature of image

T= the LST of image

$T_{max}$ = the maximum LST of image

$T_{min}$ = the maximum LST of image

Normalized images were divided into 5 temperature classes (table 4.14) using their average and rate curvature Xu et al, (2011). This classification is shown in the form of spectrum including 5 color spectrums from minimum to maximum temperatures between 0-1. Usually the rising temperature change from one class to another is gentle and with the gradual change of colors the appearance of this change in temperature is better visualized.

**Table 4.14 Classification of surface temperature on five categories**

| Range | Category |
|---|---|
| $T <= T_{mean}$ -1.5 std | very low temperature (class1) |
| $T_{mean}$ -1.5 std < T < $T_{mean}$ - std | low temperature (class2) |
| $T_{mean}$ -1.5 std < T <= $T_{mean}$ + std | middle temperature (class3) |
| $T_{mean}$ +1.5 std < T <= $T_{mean}$ + 1.5 std | high temperature(class4) |
| T > $T_{mean}$ + 1.5 std | very high temperature(class5) |

In the Table 4.15 where,

T= land surface temperature,

$T_{mean}$= mean of surface temperature

And, STD= standard deviation of surface temperature

In the proceeding, the standardized temperature figures of January during 4 consecutive periods will be demonstrated in order to provide a better comparability of temperature change (Figure 4.32 to 4.35). Land surface temperature figures during this month has been explained later in this chapter (Figure 4.40 to 4.43) and this has been applied to the month of July in the same manner. The standardized figures have been compared to analyze the temperature change in this month during the 3 observed periods (figure 4.36 to 4.39) and then the land surface temperature figures and the situation of their temperature distribution has been explained. (Figure 4.44 to 4.47).

## 4.4.1. Normalized temperature in January

Continuing in this chapter, the standardized temperature figures of January are shown to allow the comparison of temperature changes during the last 25 years. However, the explanation of temperature changes are on the basis of land surface temperature figures as the aim is to analyze the surface temperature, which is only possible with the actual values.

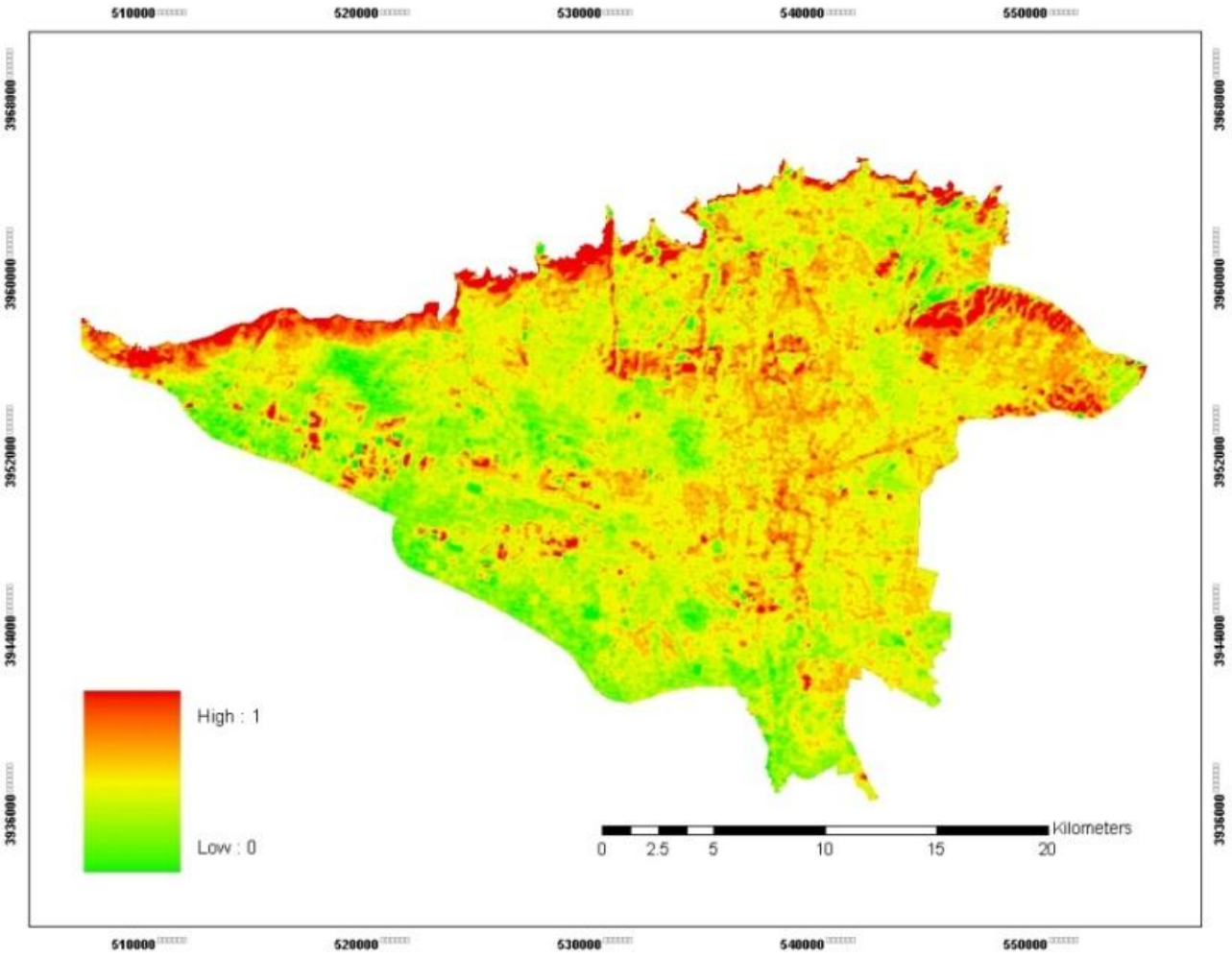


**Figure 4.32 the normalized LST in January 1991**

The highest temperature can be seen in the north and northeast and central parts, while the lowest temperature can be seen in the west and south western areas (figure 4.32). The average and high temperatures can be seen over the central area coinciding with the built-up area towards south and also on the western axis. The lowest temperature can be seen in the southern half and southwestern barren lands due to the nature of their sub-desert area.

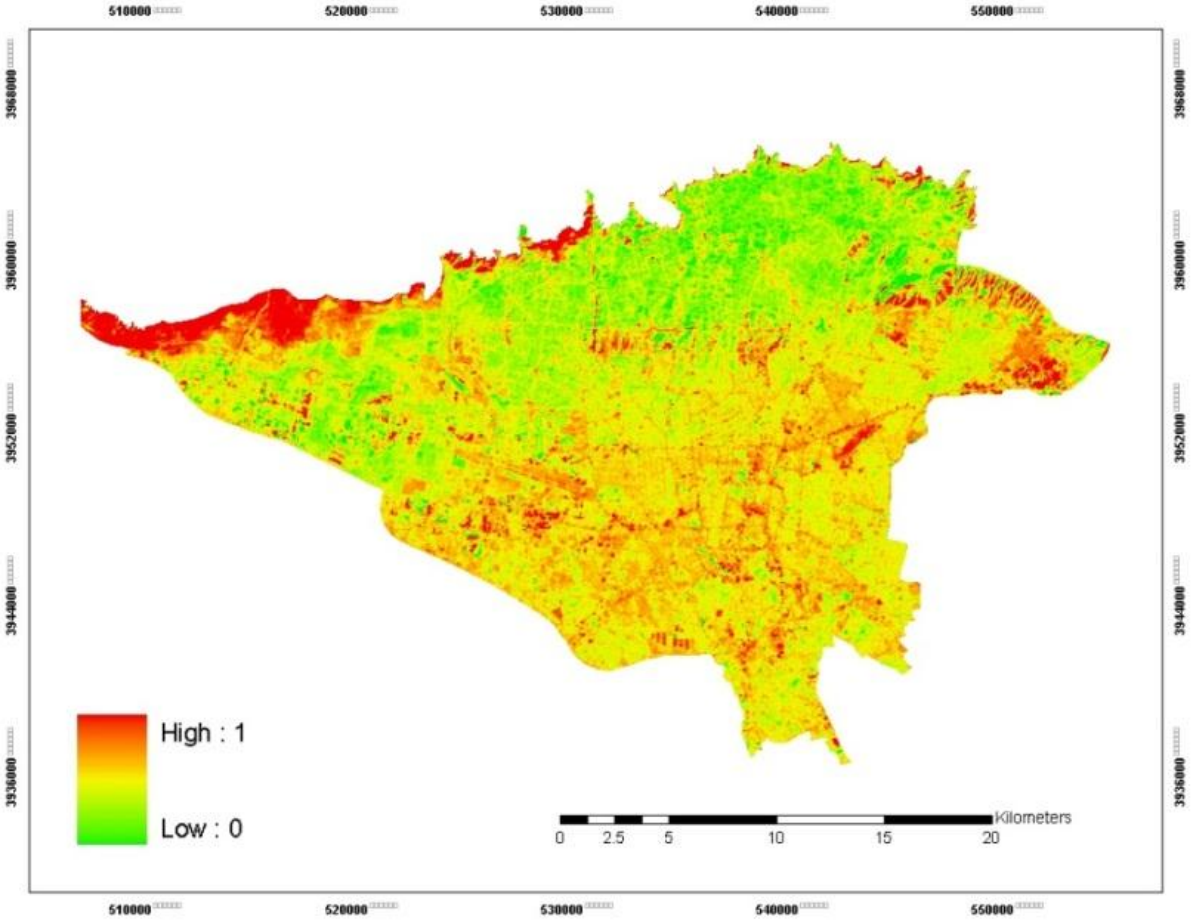


**Figure 4.33 the normalized LST in January 2001**

In figure 4.33, northwest, north and parts of southern half show the highest temperature. The south shows middle temperature and the northeast shows the lowest. With the expansion of built-up towards the south the average and high temperatures have fallen over this area. The lowest temperature can be seen in the northeastern area of Tehran with the highest altitude and the highest temperature in the northwest which is part of the barren lands.

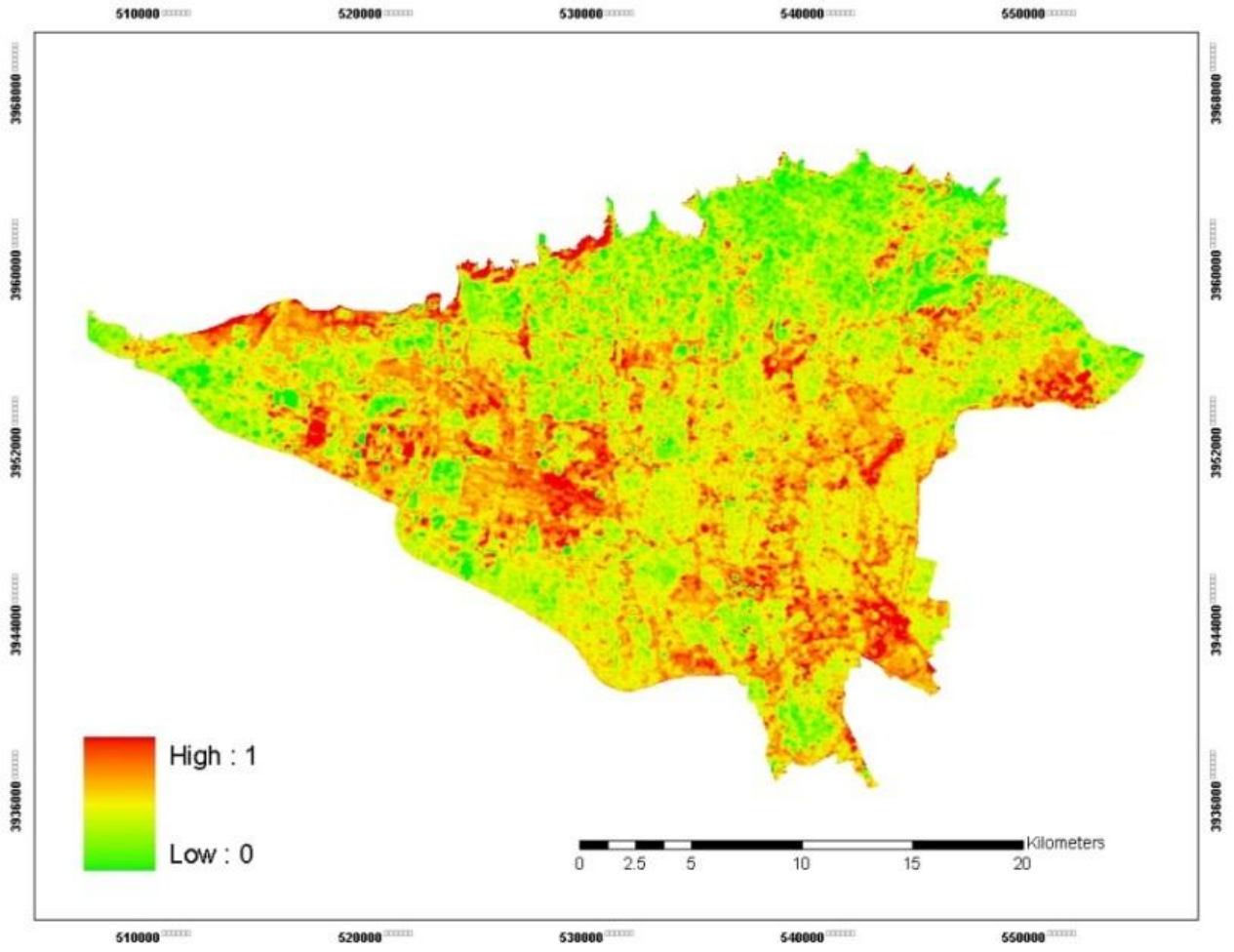


**Figure 4.34 the normalized LST in January 2010**

In figure 4.34 highest and lowest temperature patterns in the study area is almost similar to the situations in 2001, figure 4.33. The lowest temperature can be seen in the northeast and the southern region shows a middle temperature up to very high. High and average temperatures can be seen over the built-up area extending from north to the southern half and the west. With the highest temperature falling over the west, the temperature model is in a changing state in parallel with the expansion of this industrial pole towards the western area. Vegetation cover and parts of the barren land show the lowest temperature.

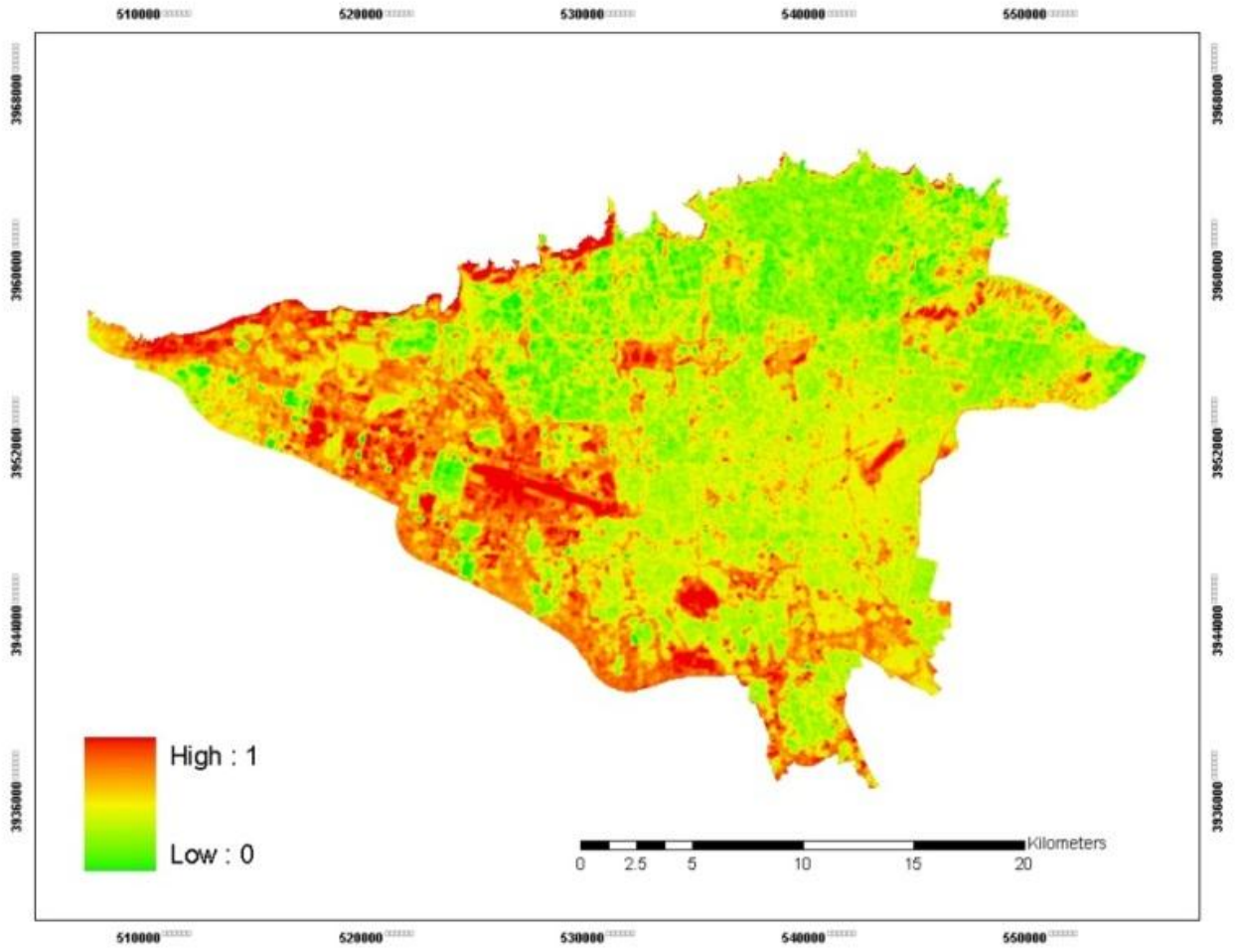


**Figure 4.35 the normalized LST in January 2015**

The highest temperature can be seen in the western half (where is considered the industrial center of Tehran). The northeastern region shows the lowest temperature as in the previous three decades. Scattered parts with middle temperature can also be seen. The comparison of temperature in January as the coldest month in the study area over 4 consecutive periods, shows that in 1991, 2001 and 2010 (figure 4.32-4.35) the highest and also the middle temperature patterns have been in specific regions of the study area. Only in 1991 the western region shows the lowest temperature and this in 2001 and 2010 is in northeastern region. In 2015 the highest temperature has intensified in the western part. Also the coldest temperature has been in the northeast, same as in previous two periods. In fact, from 1991 to 2015, a gradual change is identified in the temperature pattern of the city of Tehran.

## 4.4.2. Normalized temperature in July

Here, the normalized temperature of July is discussed as the hottest month in the study area.

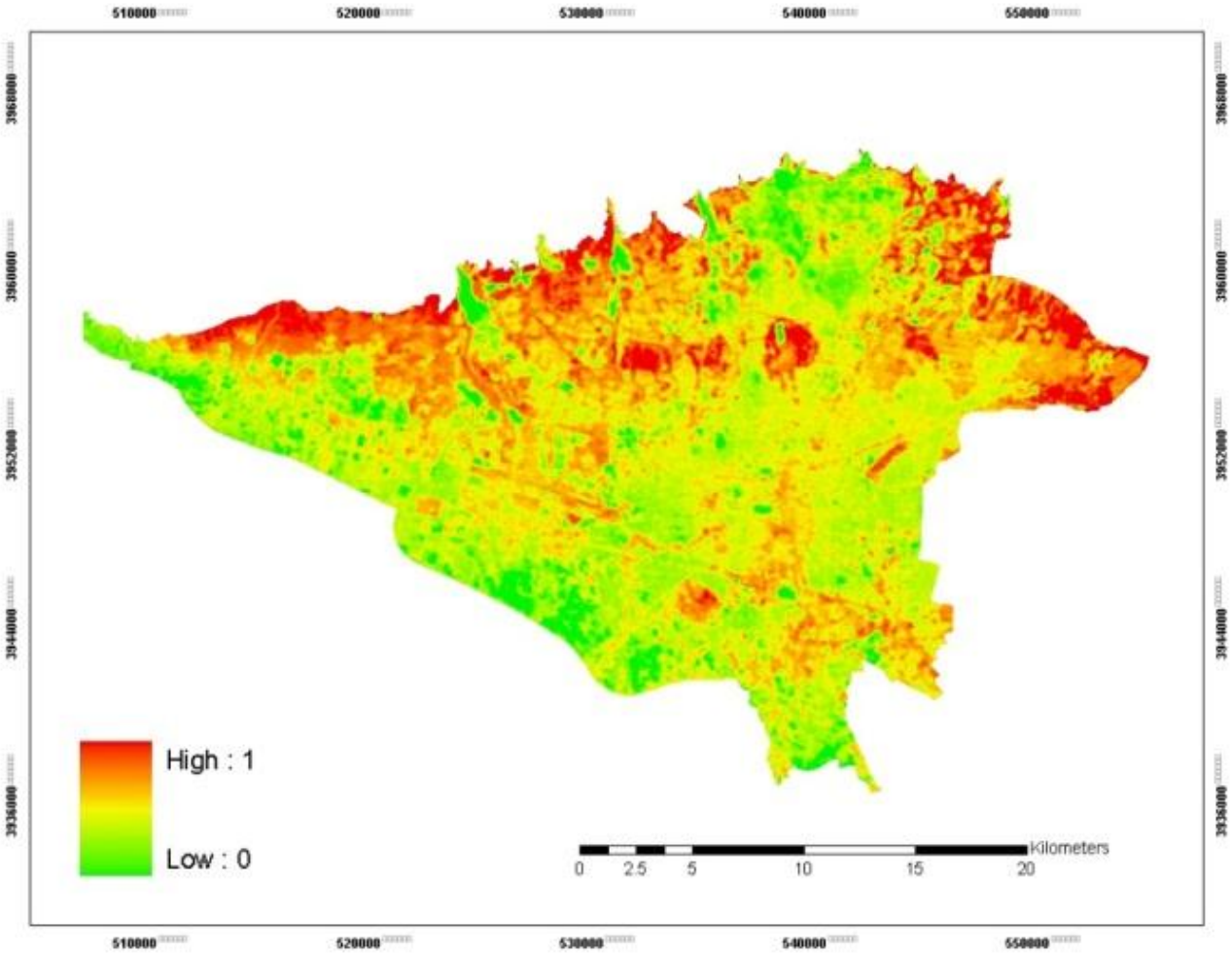


**Figure 4.36 the normalized LST in July1990**

The eastern region and also northern half show the highest temperature, except part of northeast. However, in the southern and western areas the temperature is from very low to high. The highest and lowest temperature patterns are similar to the pattern of (figure 4.32) of 1991. Barren lands and built-up area show average and high temperatures respectively and vegetation cover shows the lowest temperature.

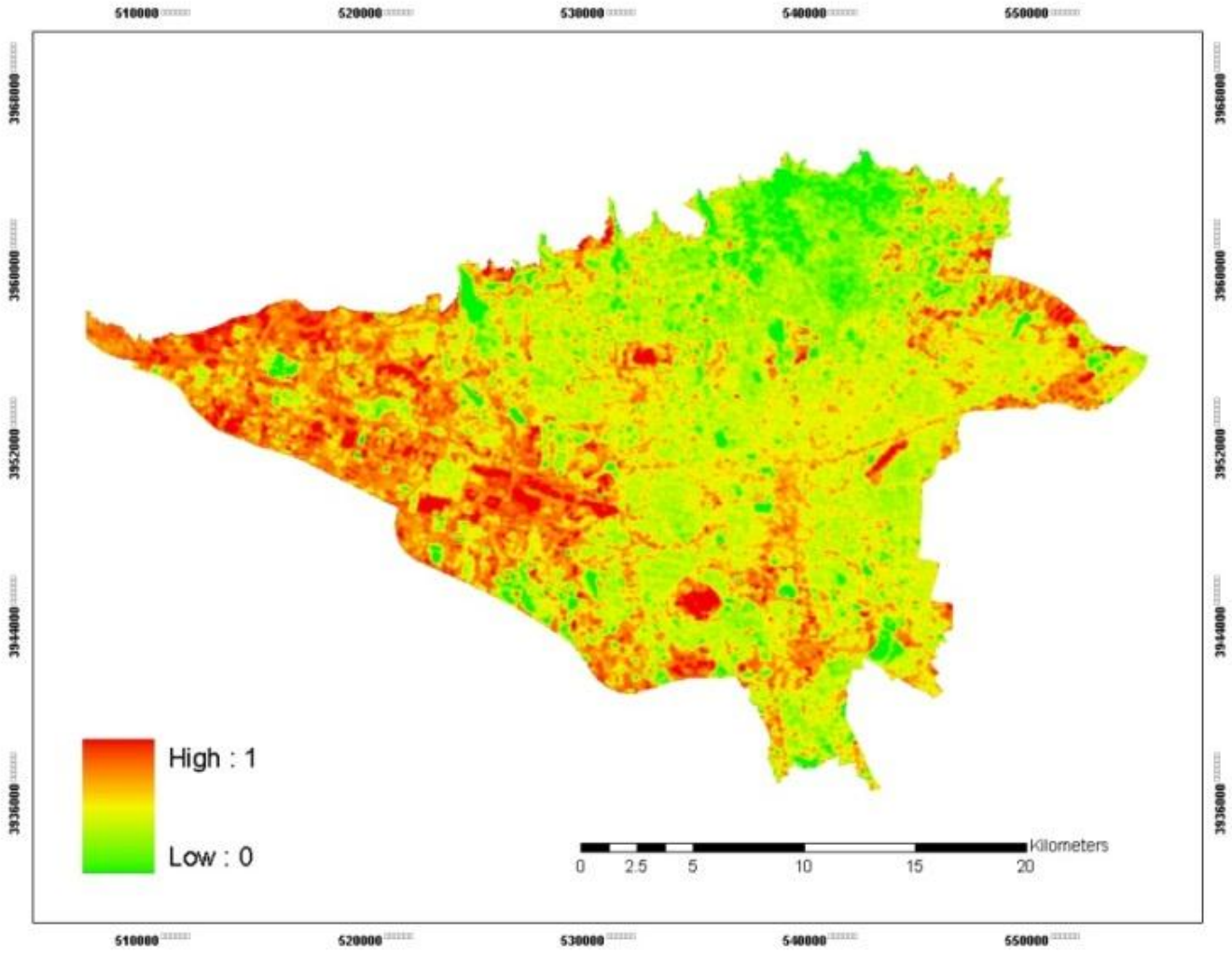


**Figure 4.37 the normalized LST in July 2000**

In figure 4.37 the highest and lowest temperature pattern has changed. Highest temperature is in the western half and scattered parts in the east and south. Lowest temperature as in all previous periods is intensified in the northeast. High and middle temperatures can be seen in the central and southern regions. Highest temperature is over barren lands, the airport and also the western industrial area. Vegetation cover shows the lowest temperature and built-up areas in the center show average to high temperatures.

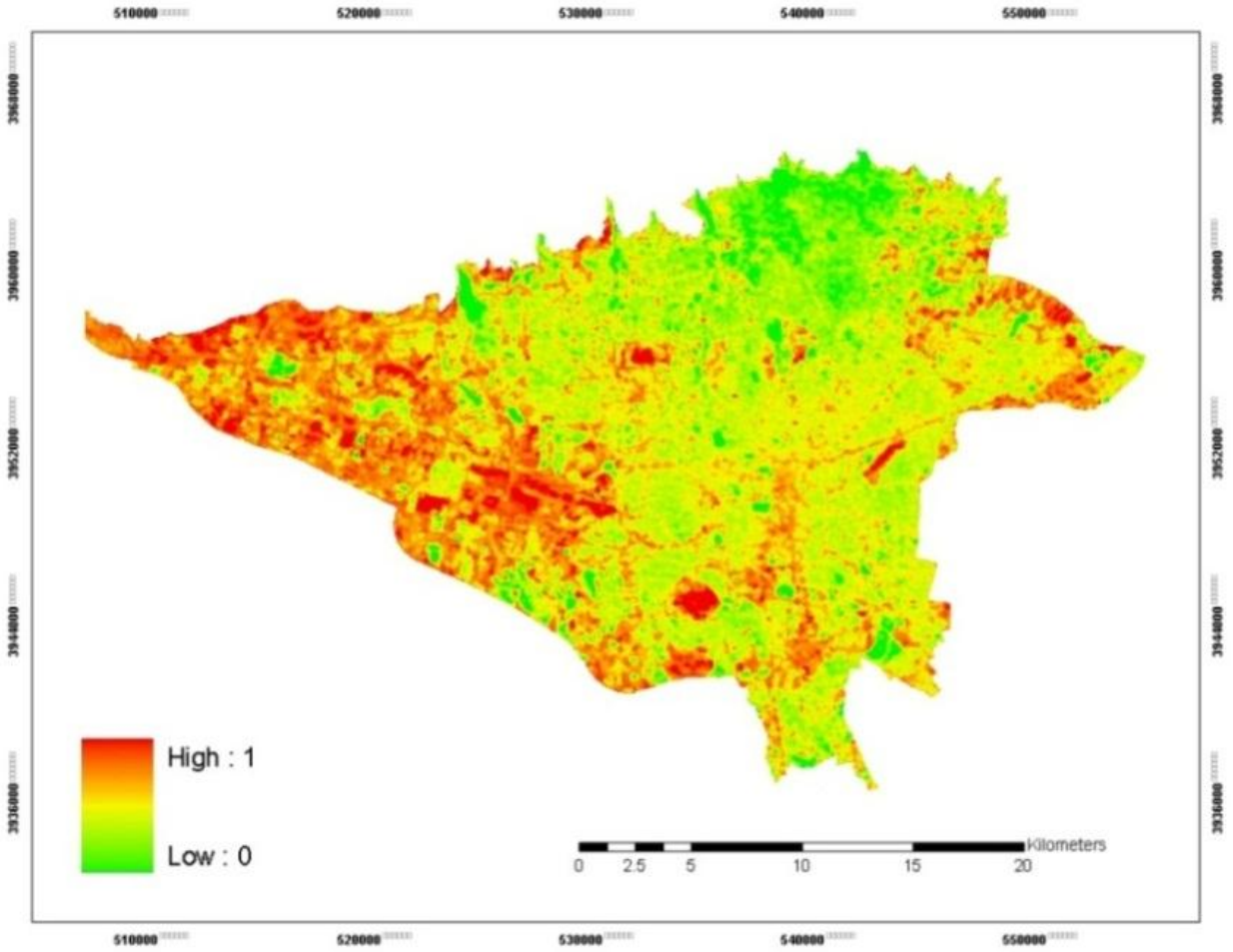


**Figure 4.38- The normalized LST in July 2009**

In figure 4.38 of year 2009, the temperature model is similar to that of figure 4.37. Highest temperature is in the west and the lowest temperature in the north, having the highest altitude in Tehran and small parts of south and east. Middle temperature is in central parts. The highest and lowest temperature pattern in this period is the same as the previous two periods.

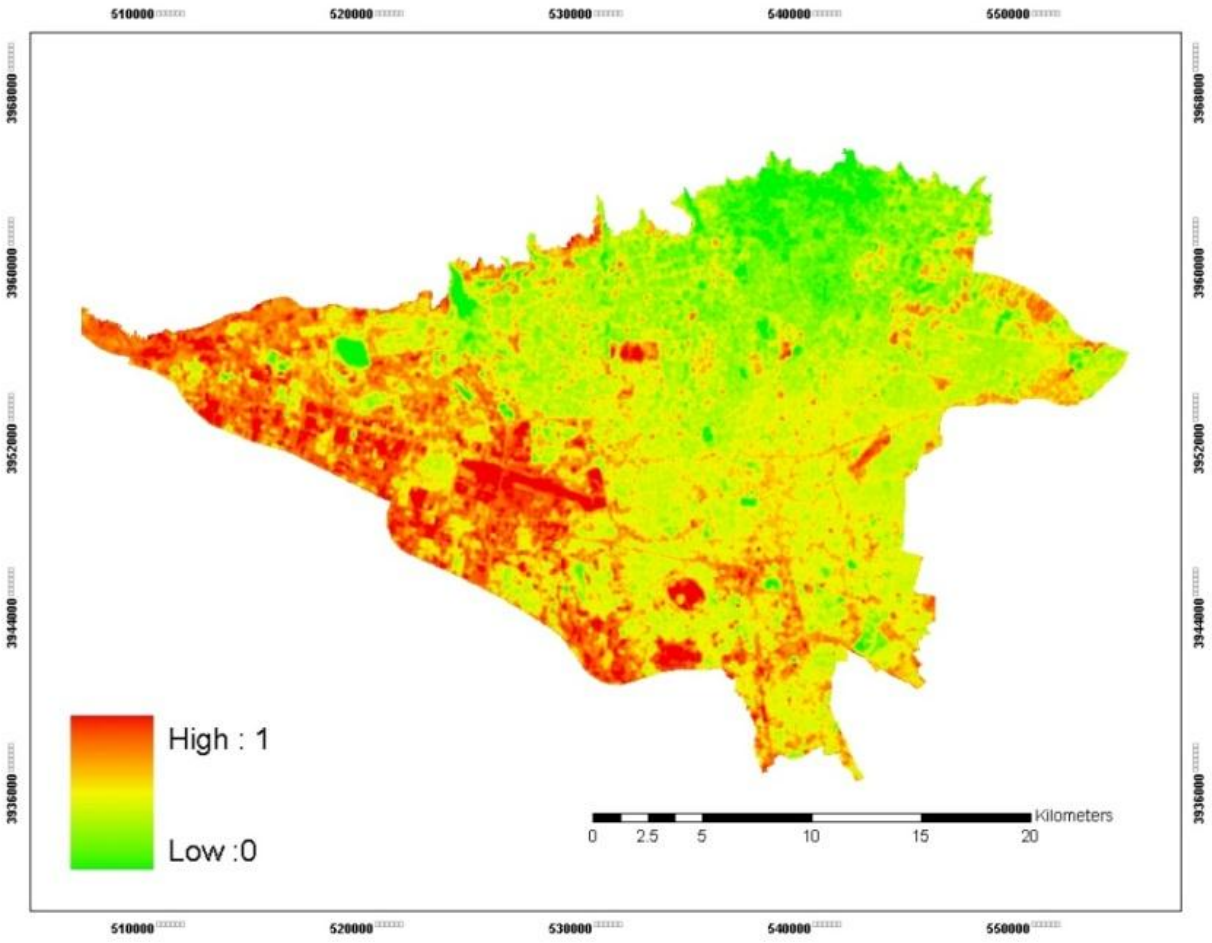


**Figure 4.39 the normalized LST in July 2014**

In figure 4.39, the maximum temperature is in the western half. The minimum temperature as with previous periods is again in the north east and the middle temperature is in the central parts. The highest temperature has fallen over the western area with the largest space of barren lands, airport and industrial centers. The northern heights and the area with vegetation cover show the lowest temperature and the built-up shows average temperature.

The assessment of the temperature in the years between 1990 and 2015 (figure 4.32 to 4.39) shows that the highest and lowest temperature pattern in 1990 figure3.40 is almost similar to 1991, figure 4.32. The highest temperature can be seen in the north of study area and the lowest in parts of west, and the central parts show middle temperature. In the years of 2000, 2009 (figures 4.37, 4.38) and 2014, the minimum and maximum temperature pattern has changed,

compared to that of 1990 figure 4.36. In this year highest temperature is in the west and the lowest in northeast. The central parts show the middle temperature.

## 4.5. Land surface temperature in January

Here, the land surface temperature of Tehran in January of 1991, 2001, 2010 and 2015 figures 4.40 to 4.43 are analyzed.

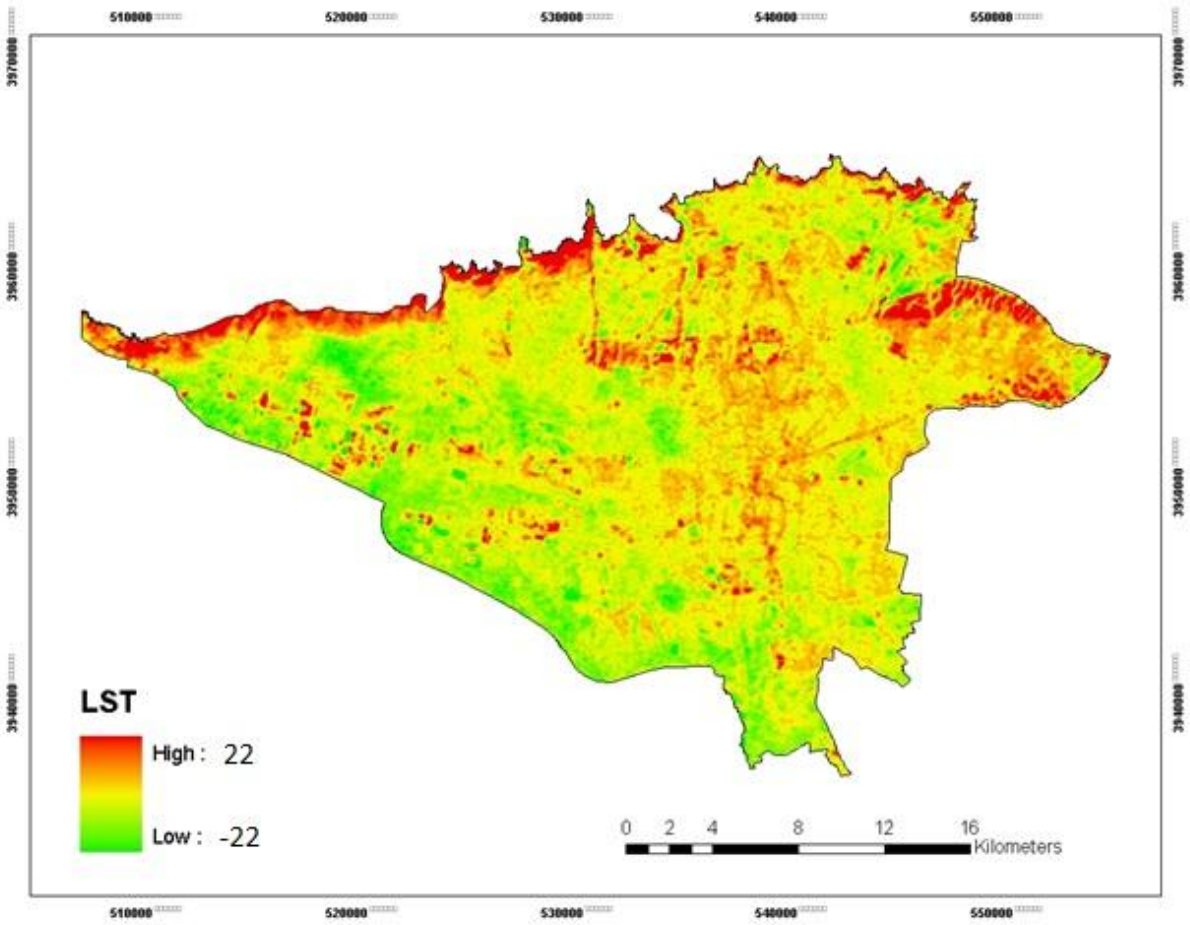


**Figure 4.40 the LST in January 1991**

As can been seen, January being the coldest month of winter in Iran. Most areas on this map show colors of yellow, orange and red denoting temperatures closer to maximum. The central and northern half of the map as well as the southern areas show the lowest temperatures.

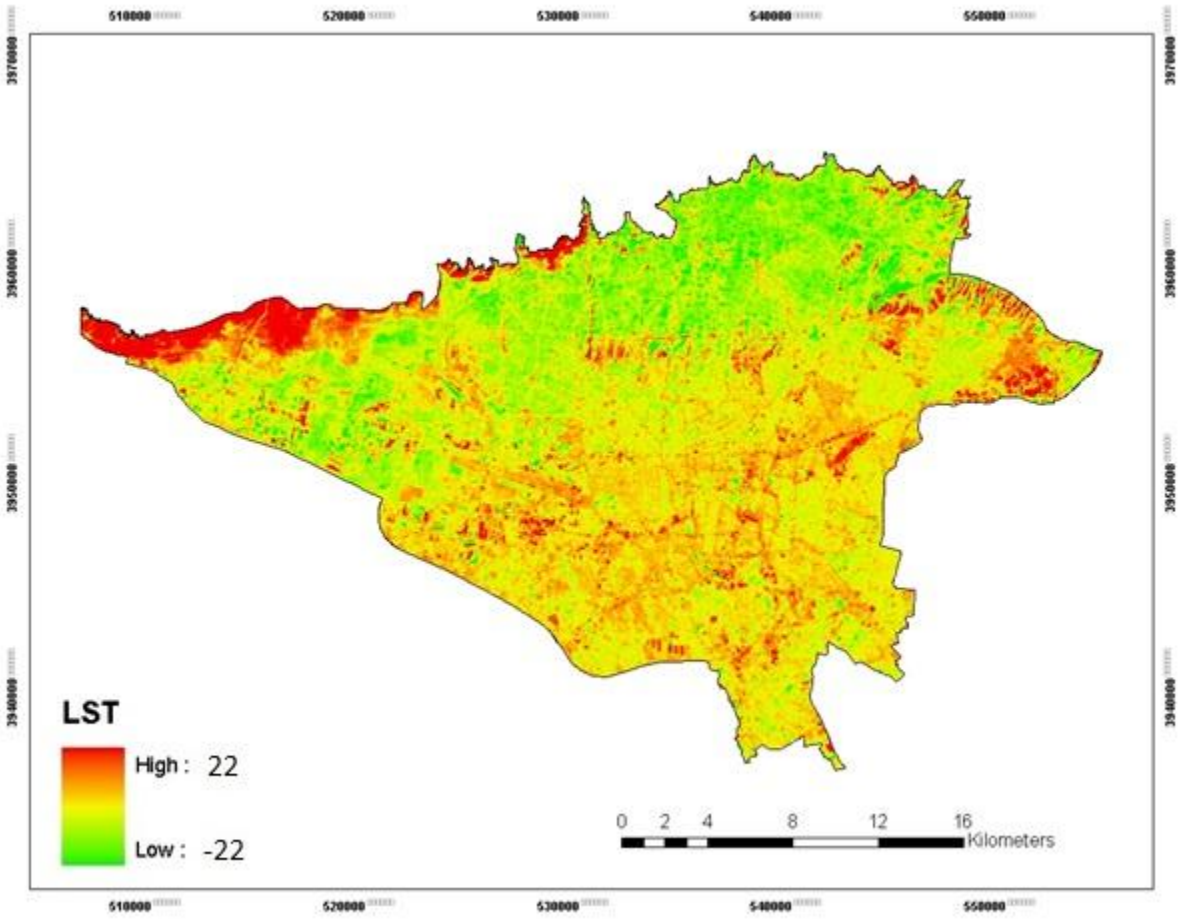


**Figure 4.41 the LST in January 2001**

This year, the temperature increase has spread from the center of the map in all directions. However, compared to 1991 (figure4.40) this temperature increase in the southern half is clearly visible. The striking point to note is that the maximum temperature is increased from -18 C° in 1991 to -16 C° in 2001 and also the minimum temperatures in 2001 shows a 2 C° increase.

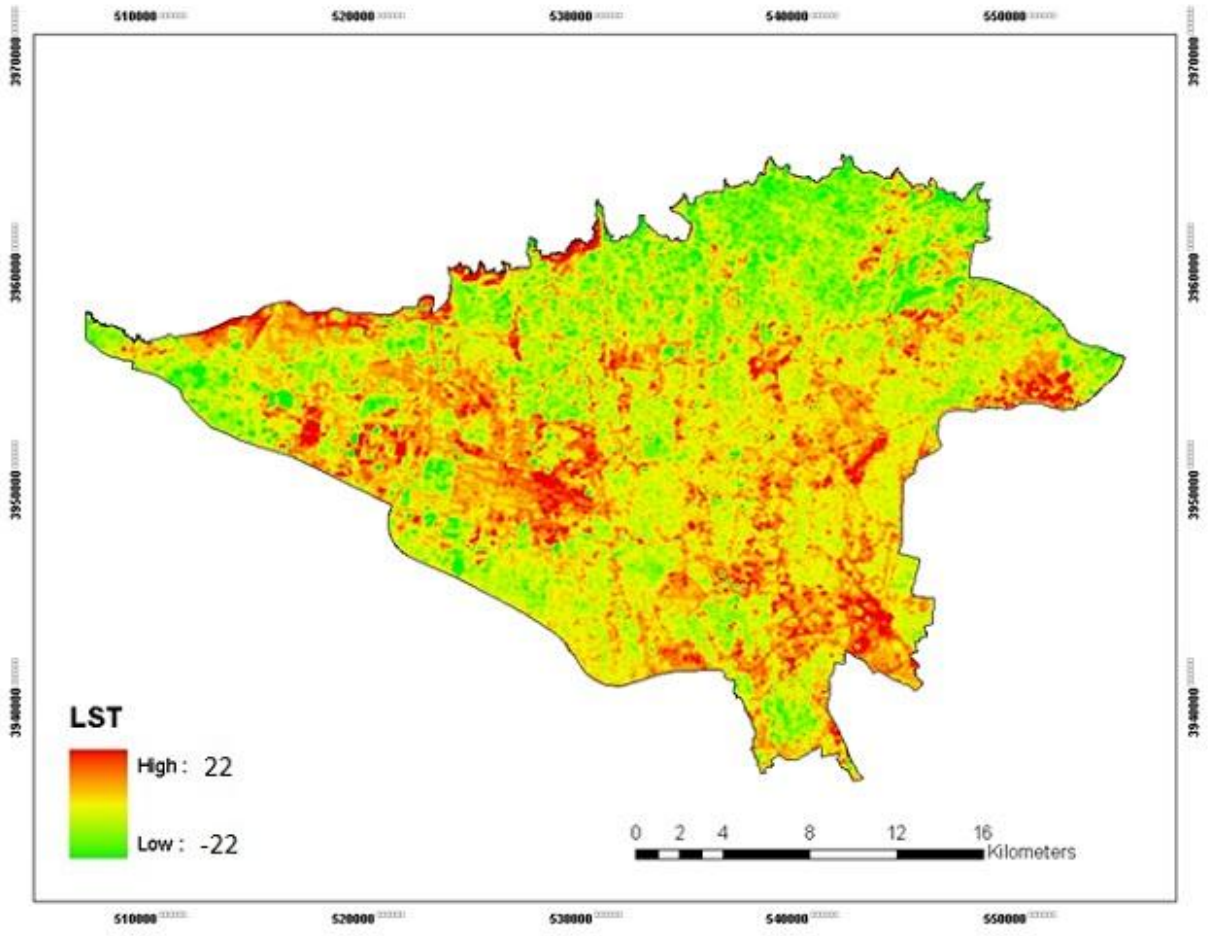


**Figure 4.42 the LST in January 2010**

Figure 4.42 shows the maximum temperature has been over 11C° and minimum temperature under -19C°. The temperature distribution model during this year has almost followed that of 2001 (figure 4.41) with the only difference being the increase in the overall area showing maximum temperature.

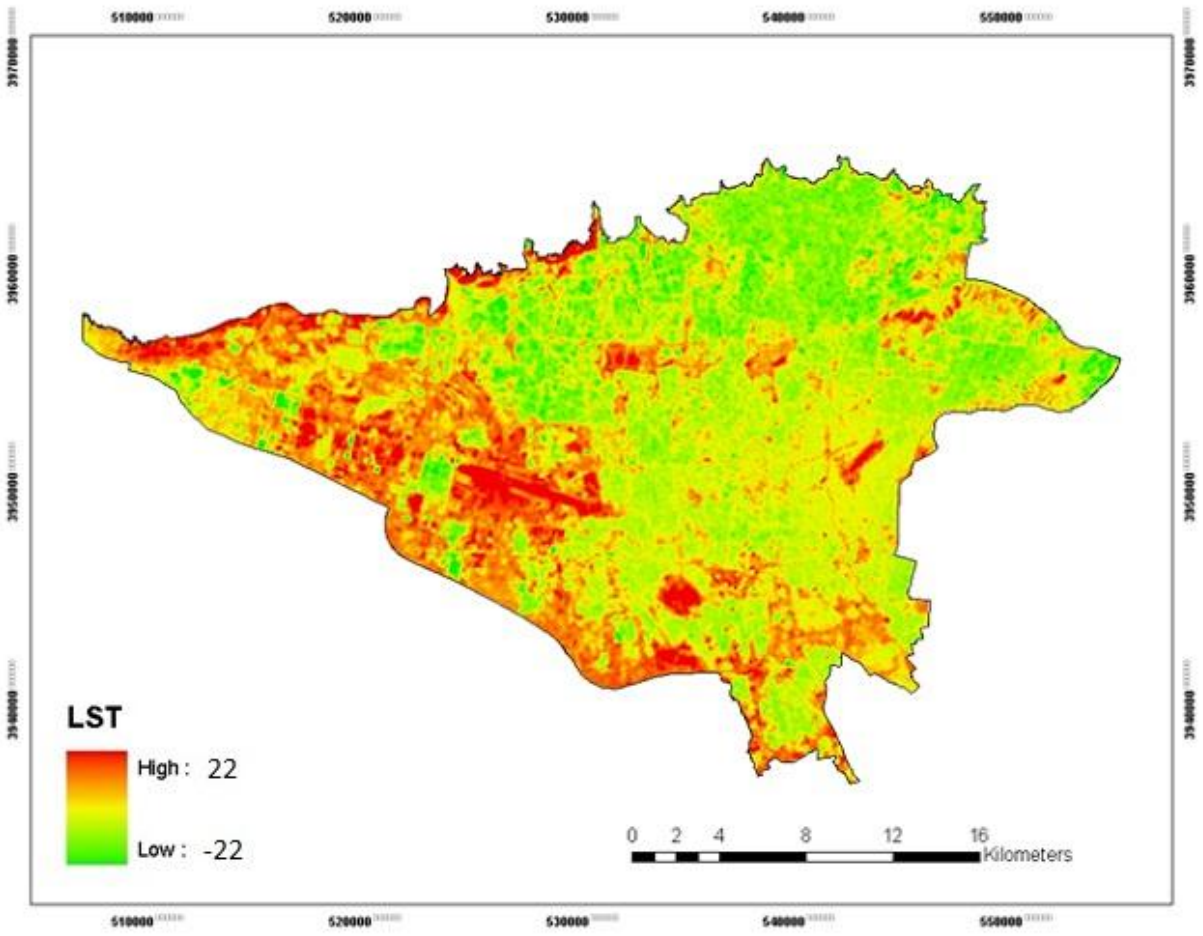


**Figure 4.43 the LST in January 2015**

Figure 4.43 shows the distribution of temperature for 2015. During this year a locational change in the maximum temperature is noticed which is more concentrated in the west, where the highest concentration of industrialization has taken place during recent years. The Mehrabad airport shows the highest temperature. Of course this has been the case in previous decades of 1991, 2001 and 2010 (figures 4.40 to 4.43). Mehrabad in the west has shown the highest temperature. Study of the figure 4.40 and 4.41 shows the distribution of temperature during the first two decades has been similar. However, in the last two decades and particularly in 2015 figure 4.43, distribution of maximum temperature shows a significantly noticeable change in temperature model

## 4.6. Land surface temperature in July.

Here, we analyze the land surface temperature figures 4.44 to 4.47 of July during the years of 1990, 2000, 2009 and 2014.

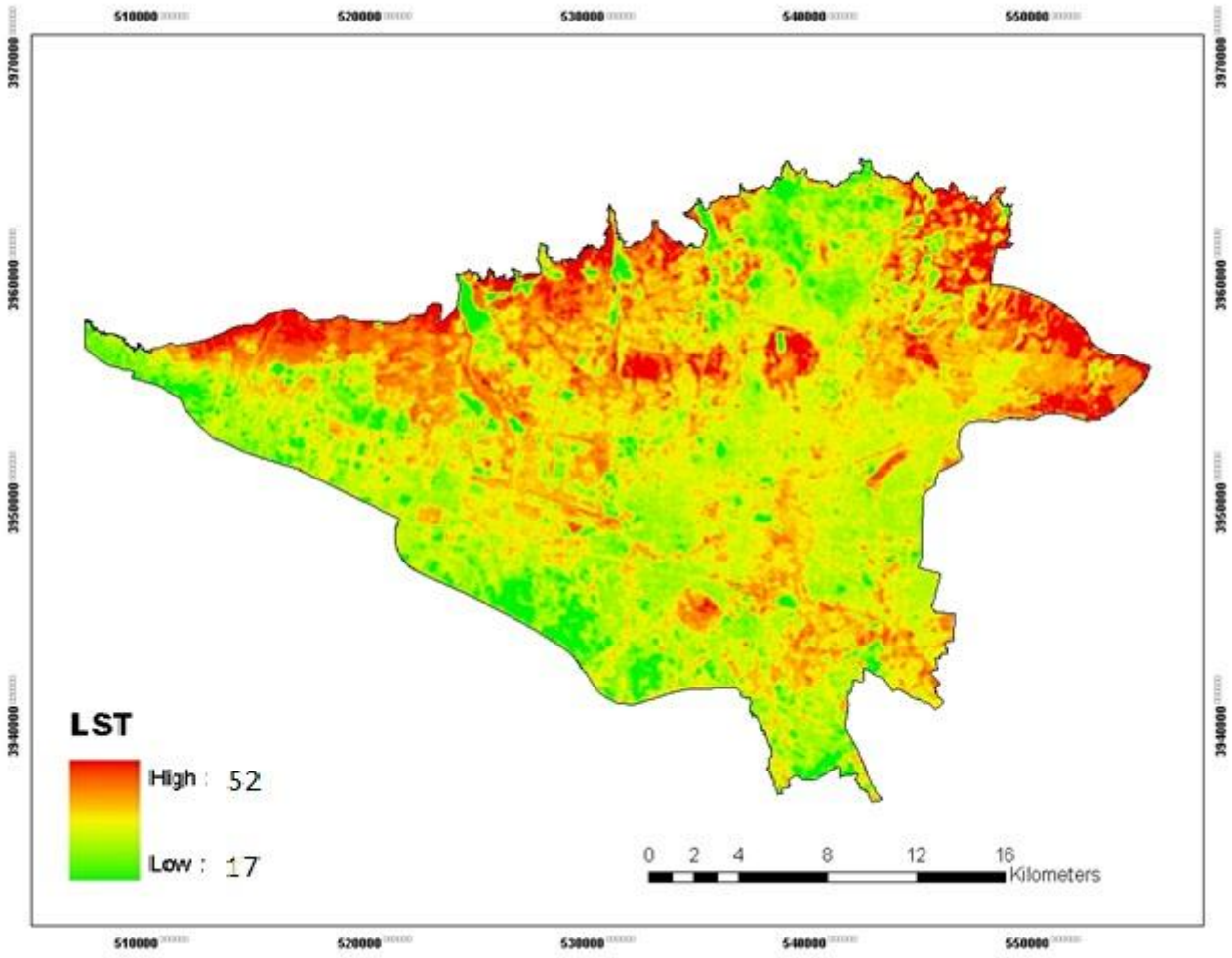


**Figure 4.44 the LST in July 1990**

Figure 4.44 shows the maximum temperature of 46.9 C° and minimum of 17 C°. This maximum temperature is visible in the northern half where mainly is barren land. The central region shows a high temperature and there is a reduction in temperature going towards the west and south.

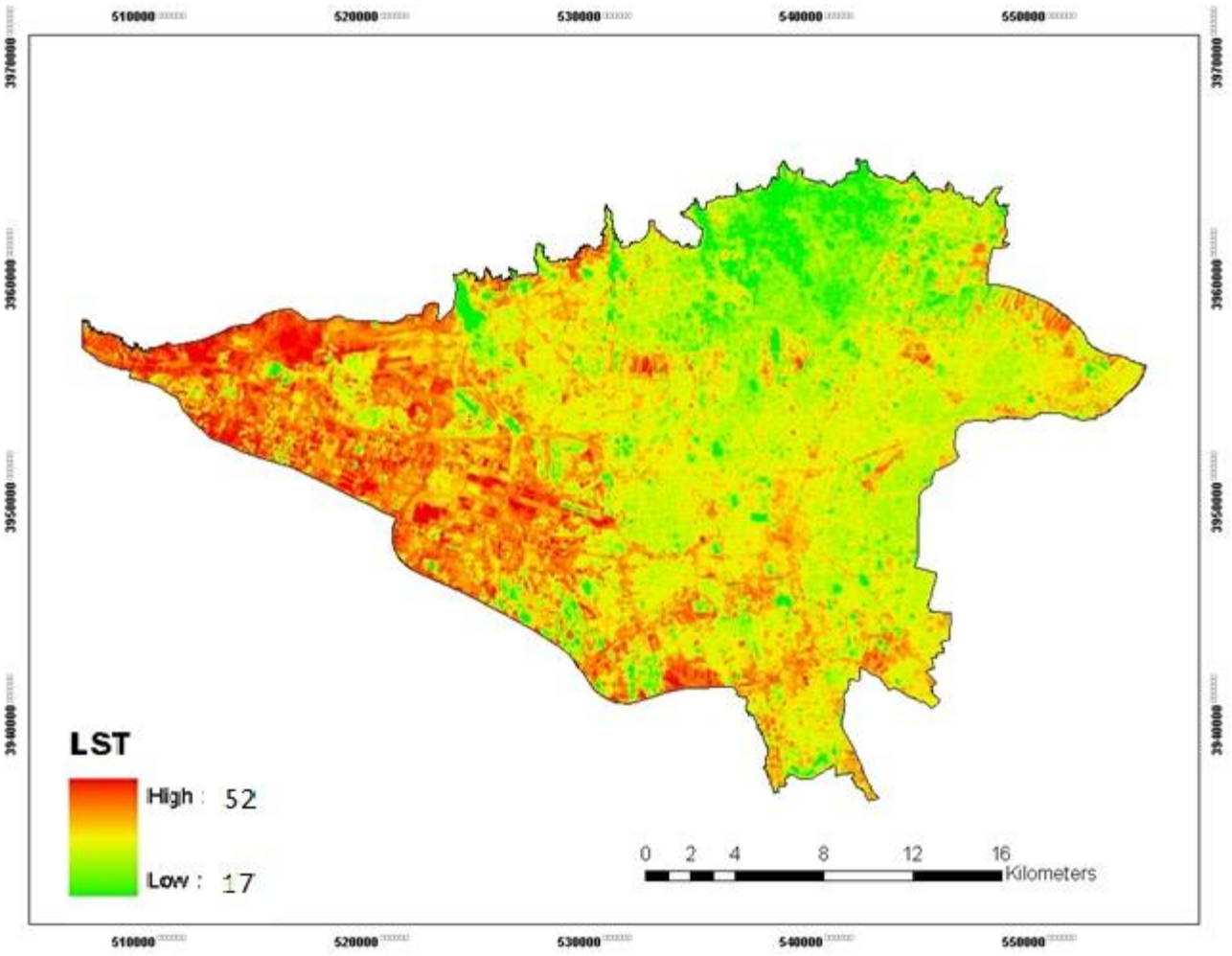


**Figure 4.45 the LST in July 2000**

In figure 4.45 the minimum temperature of 20 C° and maximum of 49 C° have been observed over the western half. Both of the minimum and maximum temperatures in year 2000 show a temperature increase of 3 C° compared with the year 1990 (figure 4.44). The comparison of the figures show that the maximum temperature distribution has moved from the northern half in 1990 to the west of Tehran in year 2000 (figure 4.45).

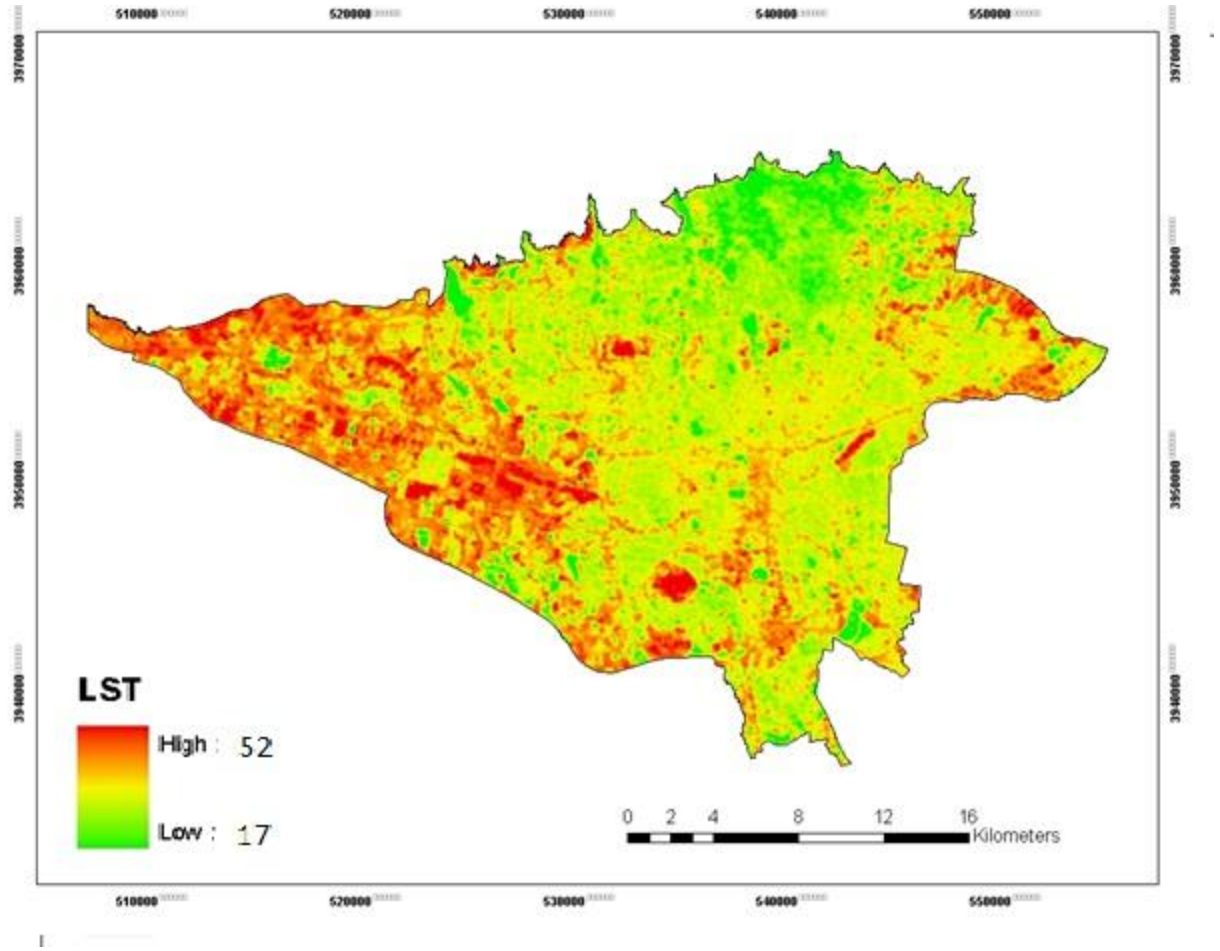


**Figure 4.46 the LST in July 2009**

Figure 4.46 demonstrates the temperature distribution in 2009. It shows a maximum temperature in the west and part of central region similar to year 2000 (figure 4.45). The interesting point to note here is the temperature distribution in figure 4.45 of year 2000 and in figure 4.46 of year 2009 being almost identical. The maximum and minimum temperatures in this year compared with year 2000 figure 4.45 have increased by 3 C° and 6 C° respectively. As mentioned earlier, this temperature increase of over 3 C° has also been noticed during the period between 1990 (figure 4.40) and 2000 (figure 4.45).

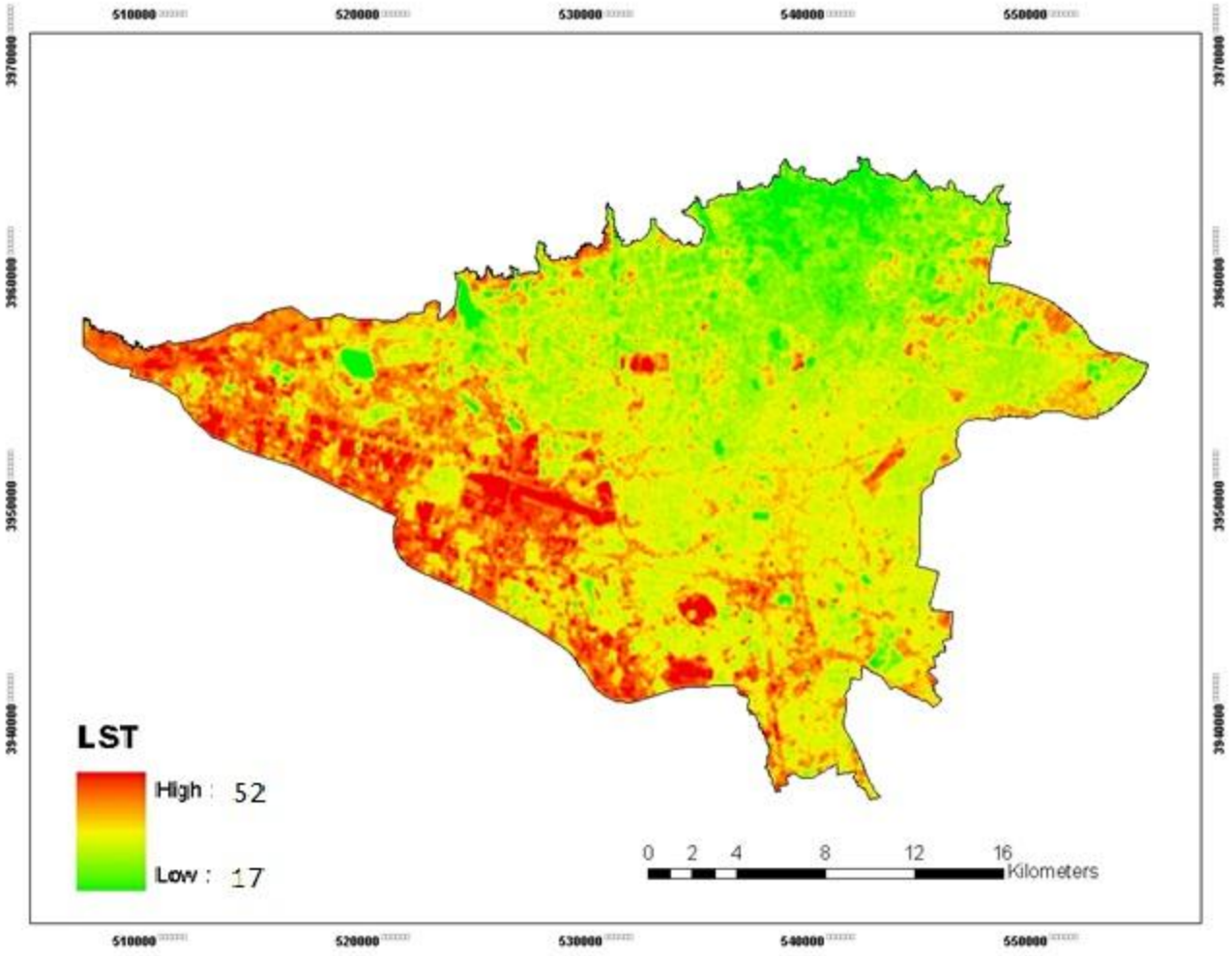


**Figure 4.47 the LST in July 2014**

Figure 4.47 of July 2014 also similar to the previous decades witnesses the domination of maximum temperature in the western half of Tehran. An interesting point here is the site of artificial Lake of Cheetgar beside the Cheetgar Park as the most important water body constructed in recent years which did not exist in the figure 4.46 of 2009 and prior to that. As can be seen in this figure, the minimum temperature is 26C° and the maximum temperature is 46C°. In this year compared to the previous 2 periods, both minimum and the maximum temperatures show a drop.

## 4.7. Summery

Landsat 5, 7 and 8 were used to calculate the surface temperature of the thermal band. Given the different conditions, including the number of bands used, and the various relative conditions of the study area, the single-channel algorithm was selected. In order to obtain the emissivity, the NDVI index was first calculated in the ArcGIS, then the PV was calculated. With regards to the type of land covers in the city including vegetation, water body, built-up and barren lands, the NDVI method was used to calculate the emissivity. According to the research literature available, this method has been used in the past in numerous studies in urban areas, the references for which are given in the relevant section in this chapter. Normalization was used to determine the range of each temperature class, and based on this, 5 temperature categories were determined and shown in spectral form. (Given that the air temperature is calculated based on the land surface temperature, the normalization is used to determine the number of air temperature classes).

The maximum surface temperature pattern in January 1991 (Fig. 4.40) and 2001 (figure 4.41) as well as July 1990 (figure4.44) are similar to each other, so that in all years these maximum temperatures can be seen in the north, central area and also in the western part of the study area. However, the maximum temperature distribution pattern of the July 2000, 2009 and 2014 and also January 2010 and 2015 has changed. This changed has taken place in the western half of the study area. During the years of studied period the minimum temperature has been in the north eastern part of the study area.

**Reference**


1. Alavi Panah, S. K.Ch B Komaki, A Goorabi and H R Matinfar, 2007. Characterizing Land Cover Types and Surface Condition of Yardang Region in Lut Desert ( Iran ) Based upon Landsat Satellite Images, World APPlied Sciences Journal 2, VOL. 3, PP. 212-228.

2. Alijani, B., M. Kaviani 1998. The principles of climatology. Payam-e Noor publisher, Tehran.

3. Artis, D. A., & Carnahan, W. H. (1982). Survey of emissivity variability in thermography of urban areas. Remote Sensing of Environment, Vol.12, PP.313– 329.

4. Chen, X. L., Zhao, H. M., Li, P.X & Yin, Z.Y. 2006. Remote sensing image–based analysis of the relationship between urban heat island and urban use/cover changes. Remote sensing of Environment, VOL 104, PP. 133-146.

5. Dash, P. Land surface temperature and emissivity estimation from passive sensor data: theory and practice-current trends, International Journal of Remote Sensing, VOL. 23, PP.2563-2594.

6. Friedl, M.A., 2002, Forward and inverse modelling of land surface energy balance using surface temperature measurements. Remote Sensing of Environment, VOL.79, PP.344-354.

7. Mo X., C. Cheng., F. Zhai., H. Li. (2011). Study on temporal and spatial variation of the urban heat island based on Landsat TM/ETM+ in central city and Binhai New Area of Tianjin, Multimedia Technology (ICMT), 2011 International Conference on. 26-28 July 2011, PP. 4616-4622.

8. Oguz. H, 2017, Automated land surface temperature retrieval from Landsat 8 satellite imagery: a case study of diyarbakir – turkey, Turkish journal of forest science.

9. QIN, Z., KARNIELI, A., and BERLINER, P., 2001, A mono-window algorithm for etrieving

Land surface temperature from Landsat TM data and its aPPlication to the Israel-Egypt border region. International Journal of Remote Sensing, VOL.22, PP.3719–3746.

10. Schmugge, T., Hook, S.J., and Coll, C, 1998, Recovering surface temperature and emissivity from thermal infrared multispectral data.Remote Sensing of Environment, Vol.65, PP.121- 131.

11. Sobrino.J.A., C.Jiménez-Muñoz and L.Paolini, 2004, Land surface temperature retrieval from Landsat TM 5, Remote Sensing of Environment, VOL 90, VOL 4, PP. 434-440.

12. Sobrino.J.A., Raissouni, and Li, 2001, "A Comparative Study of Land Surface Emissivity Retrieval from NOAA Data, Remote Sensing of Environment, Vol. 75, PP. 256–266

13. Sobrino. J. A, J. C. Jime´Nez-Mun˜ Oz, J. El-Kharraz, M. Go´ Mez, M. Romaguera and G. So` Ria, 2004, Single-channel and two-channel methods for land surface temperature retrieval from DAIS data and its aPPlication to the Barrax site , International Journal Remote Sensing, VOL. 25, NO. 1, PP. 215–230.

14. Suresh. S, Ajay Suresh. V, Mani. K, 2016, Estimation of land surface temperature of high range mountain landscape of devikulam taluk using Landsat 8 data, International Journal of Research in Engineering and Technology, eISSN. 2319-1163, pISSN. 2321-7308.

15. Xu H., Y. Chen., S. Dan., W. Qiu. (2011). Spatial and temporal analysis of urban heat island effect in Chengdu city by remote sensing. Geo informatics, 2011 19th international conference on, shanghai, 24-26 June 2011, PP. 1-5.

16. Xiaolei Yu 1,*, Xulin Guo 1 and Zhaocong Wu, (2104), Land Surface Temperature Retrieval from Landsat 8 TIRS—Comparison between Radiative Transfer Equation-Based Method, Split Window Algorithm and Single Channel Method, Remote Sensing, Vol. 6, PP. 9829-9852.

# Chapter 5

**The analysis of the in-situ observed and satellite image air temperature**

## 5.1 Introduction

Air temperature is one of the most important climatic elements and is one of the most important determinants of the climate of any geographical region. Our understanding of the heat and cold of our surroundings is measured as the "air temperature". The criteria for determining the proper temperature and inadequate temperature in human life and the types of activities, such as agriculture, industry and construction, are measured with air temperature. When we speak of the temperature changes and the factors affecting it in our environment, there is no doubt that all that is meant is the air temperature. Changes that humans create in their environment can directly or indirectly affect the temperature, most importantly, changes in land cover. Many researchers have studied the temperature of the land surface temperature and air temperature and its relation with land cover changes and found links between them, (Hung et al., 2005; Kataoka et al, 2008). Widyasamratri et, al. (2013) used the long term temperature statistical data from 1980 to 2010 of two ground stations and also two satellite images relating to 1989 and 2006 of that region, to analyse and compare the land surface temperature and the air temperature.

The aim of this research is to study the air temperature and its relationship with the land cover of the study area and this has been calculated and investigated.

### 5.2. Data and Methodology

The air temperature derived from land surface temperature of the satellite images and the observed air temperature in the field work are examined through the following steps:

a) The land surface temperature derived from the satellite imagery for 1990 to 2015 were calculated in chapter four. Then these temperatures were converted in to air temperature using (formulas 7).

b) The observed air temperatures in the fieldwork have been reviewed from October 2015 to June 2016.

c) The surface temperature of the satellite imagery for the above period are converted to air temperature and compared with the observed temperature of the same period.

## 5.3. Conversion of ground temperature to air temperature

The temperature registered by the thermal band of a satellite image is related to the temperature of the land surface. While in human life and activities, the aim is the air temperature measurement which provides a better understanding of temperature. For this purpose, methods have been proposed to convert ground surface temperature to air temperature. One of the easiest and most suitable models for this purpose is from Garcia – cueto (2006).

$$Ta = 14.6 + 0.44 * LST \quad (8)$$

Where, Ta is air temperature

LST, land surface temperature,

14.6 and 0.44 are constants,

The formula has been used in many studies on the conversion of surface temperature to air temperature, including; Ardakani et al. (2014), using the formula in the temperature study of Yazd city. Sadeghinia et al. (2015) also used this formula to compare the air temperature of the ground stations and the temperature taken from the satellite.

Here, using the above formula, first the surface temperature of the images of January relating to 1991, 2001, 2010 and 2015, were converted to air temperature and the temperature pattern was evaluated. Then, the surface temperature of the images of July relating to 1990, 2000, 2000, and 2014 were converted to air temperature and the temperature patterns were evaluated.

## 5.4 Evaluation of air temperature of January month 1991-2015

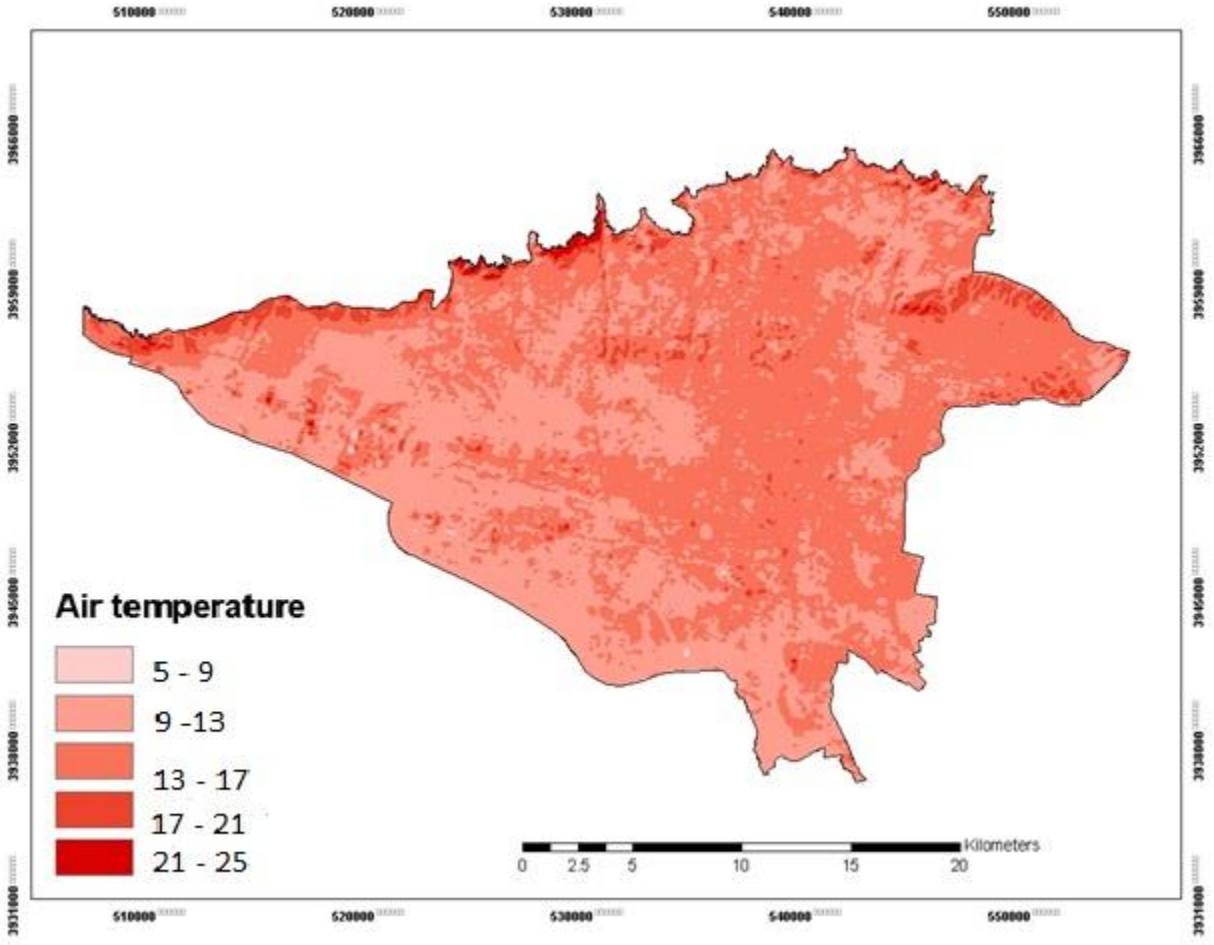


**Figure 5.48air temperatures in January 1991**

In the figure 5.48, most of central and eastern parts show temperatures between 14.9 - 8.15 ℃. In the western and southern parts, the minimum temperature is observed between 13 and 14.9 ℃ and the maximum temperature is observed in a very limited part of the extreme north. In the western half, temperatures are lower than eastern half.

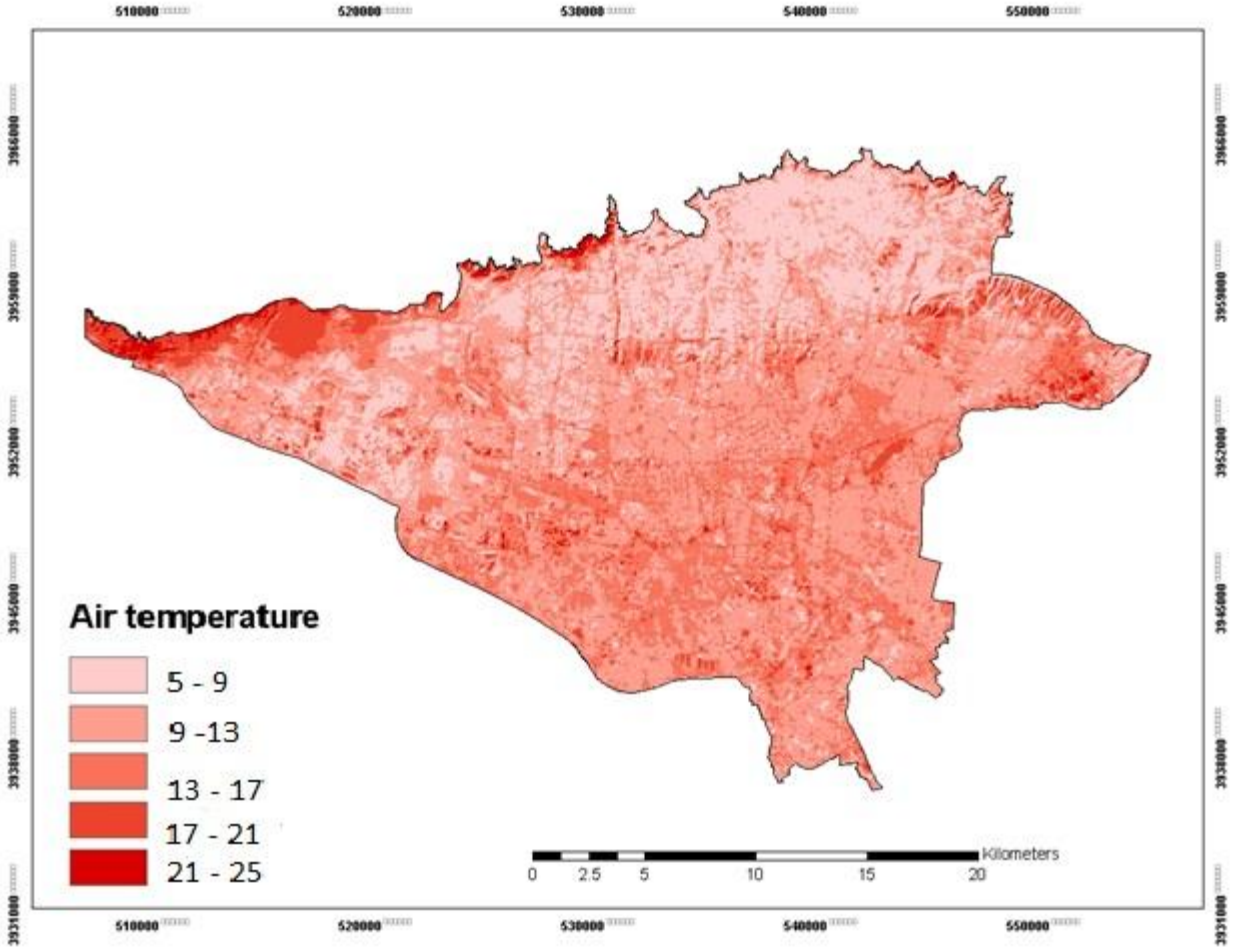


**Figure 5.49 air temperatures in January 2001**

The central area of the figure 5.49 to the south of the study area shows a temperature above 18 ° C. This temperature pattern shows an increase in temperature of over 4 ° C compared with the previous 10 year period. Also, the maximum temperature at the extreme north is more than 3 °C higher than the previous period. The minimum air temperature in this period is observed in the northern and north eastern parts of Tehran, in line with the highlands of this city.

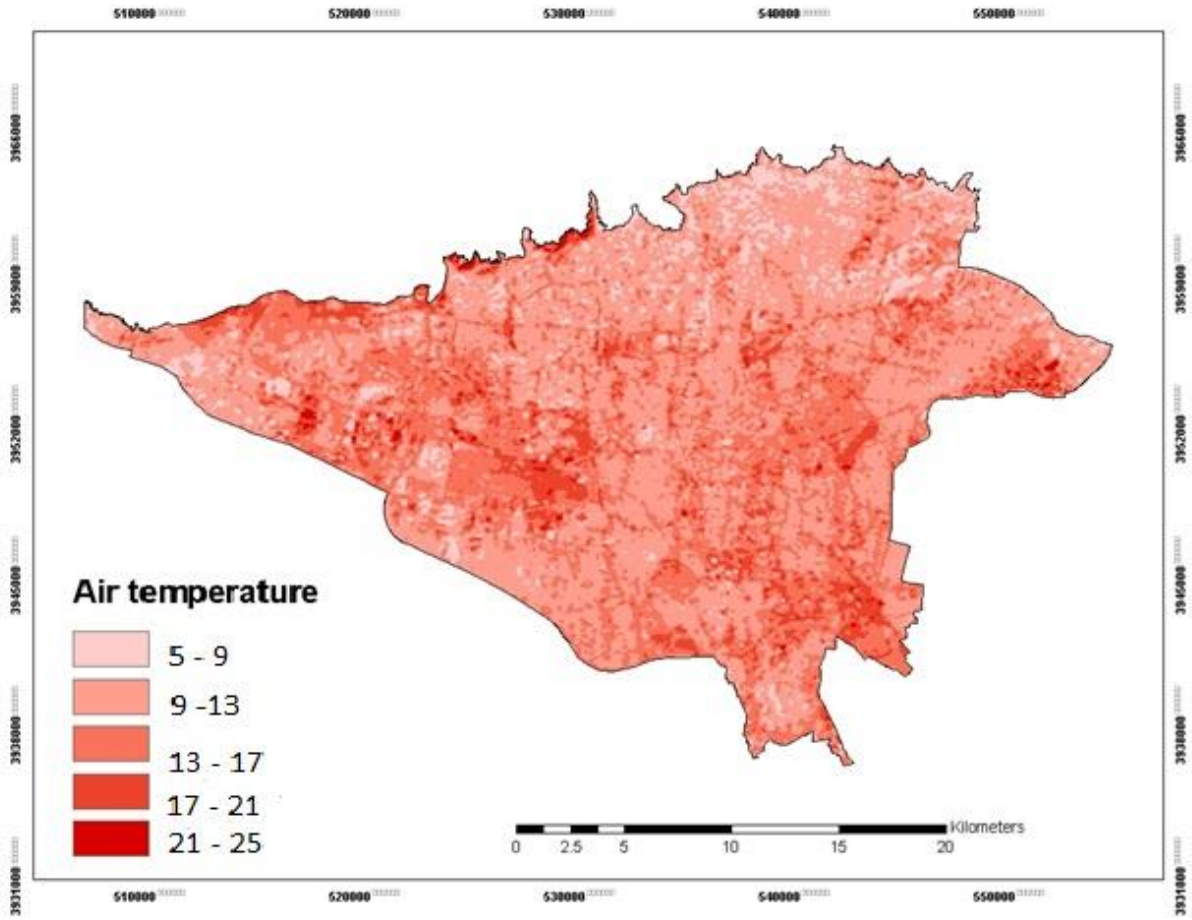


**Figure 5.50 air temperatures in January 2010**

In 2010, figure5.50, compared with the previous period of 2001, figure5.49, a decrease in the minimum and maximum temperature is observed. However, the maximum temperature pattern shows differences in that these temperature areas are now spread across the region. Temperatures over 17°C are over the west, where the axis of the industrial pole of the Tehran-Karaj has been formed. In this axis, a temperature of more than 17°C is also sporadically observed. The minimum temperature is more in the east of Tehran.

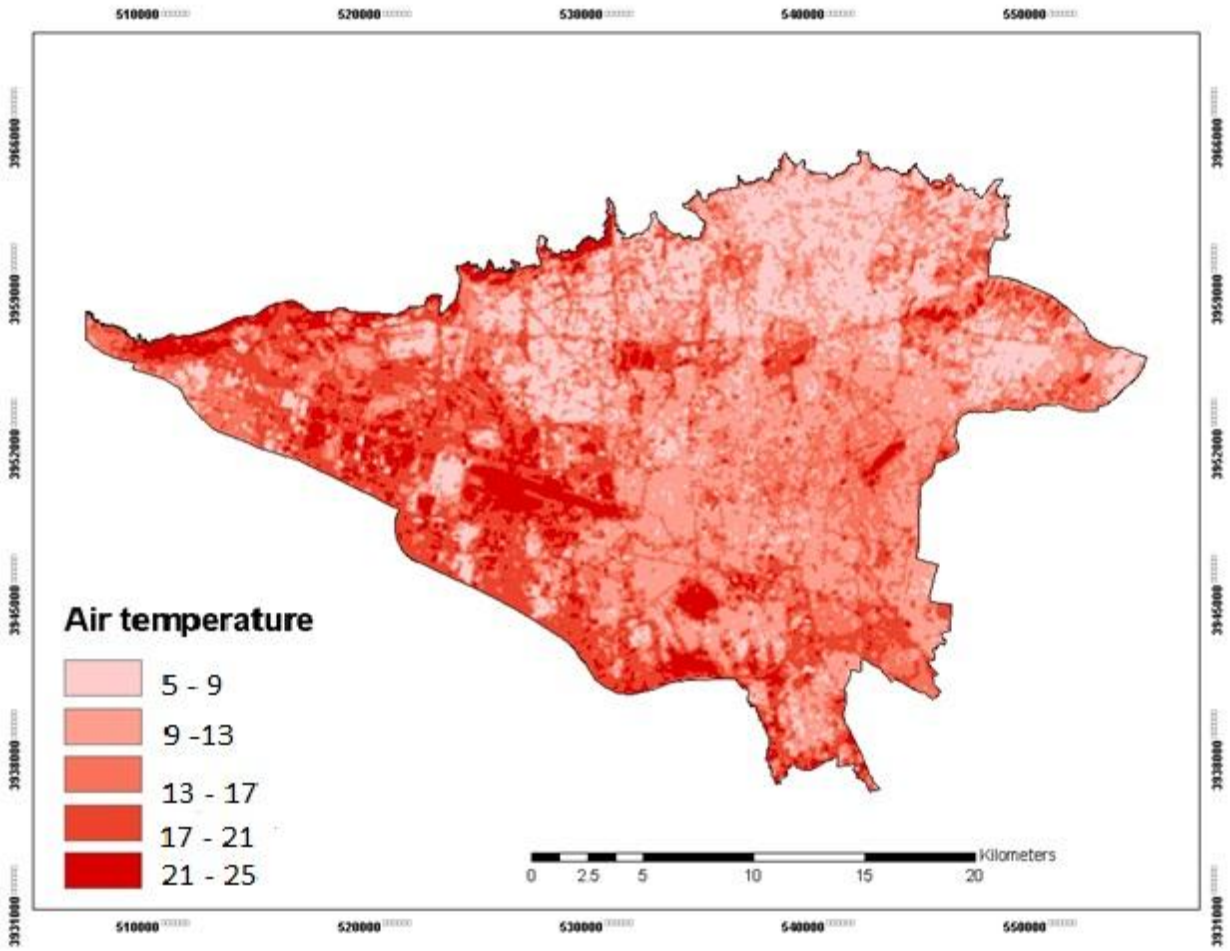


**Figure 5.51 air temperatures in January 2015**

The temperature pattern in 2015, figure 5.51, has changed considerably. The central parts of the study area, as in previous periods, show temperatures above 15°C in figure 5.50. But the maximum temperature, which in previous periods only included the northern extremes and a small part of the west, during this period, completely included the west of Tehran. This indicates the expansion of the industrial zone in the west of Tehran. Moreover, the maximum temperature is also seen in other parts including the central regions and parts of the south. Lowest temperatures are also observed in the northern half.

## 5.5. Evaluation of air temperature of July month 1990-2014

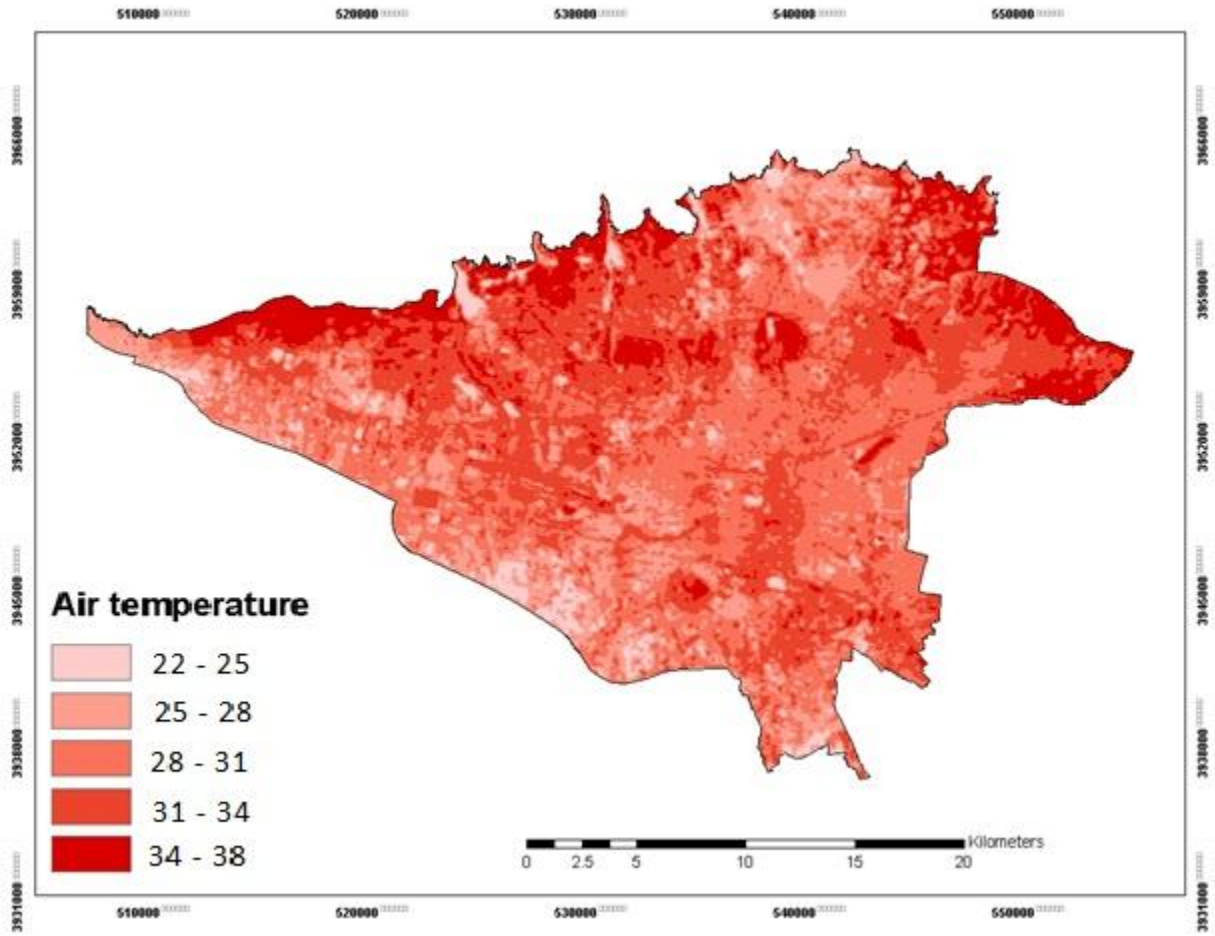


**Figure 5.52 air temperature in July 1990**

Maximum temperature is seen in the mid-north and the minimum temperatures are also observed in part of the west and northeast in figure 5.52. With the minimum temperature of over 22 °C and the presence of temperatures exceeding 34 °C in most areas of Tehran, it is clear that warm weather is predominant in this area.

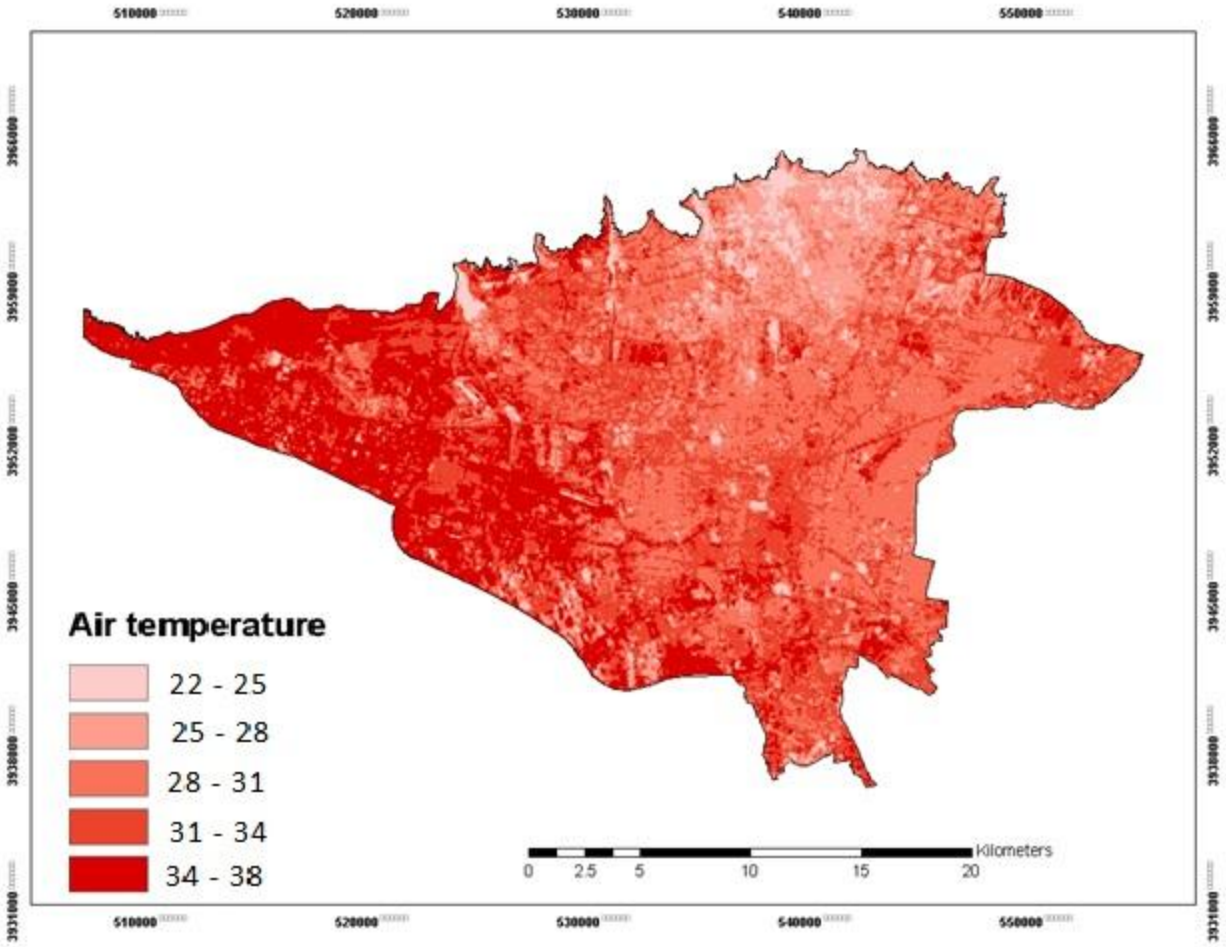


**Figure 5.53 air temperatures in July 2000**

The air temperature pattern in this year shows a marked change compared with the previous ten year period. The maximum temperature which in Fig. 5.52 was on the northern half, here is located on the south-west and most areas show temperatures of over 30 °C . These differences can be correlated with the increase in construction in the mid-west, which will be reviewed in chapter 6. In this year, the minimum and maximum temperatures each had a temperature increase of more than 1 and 2 °C, respectively. The northeast of the figure shows the lowest temperature.

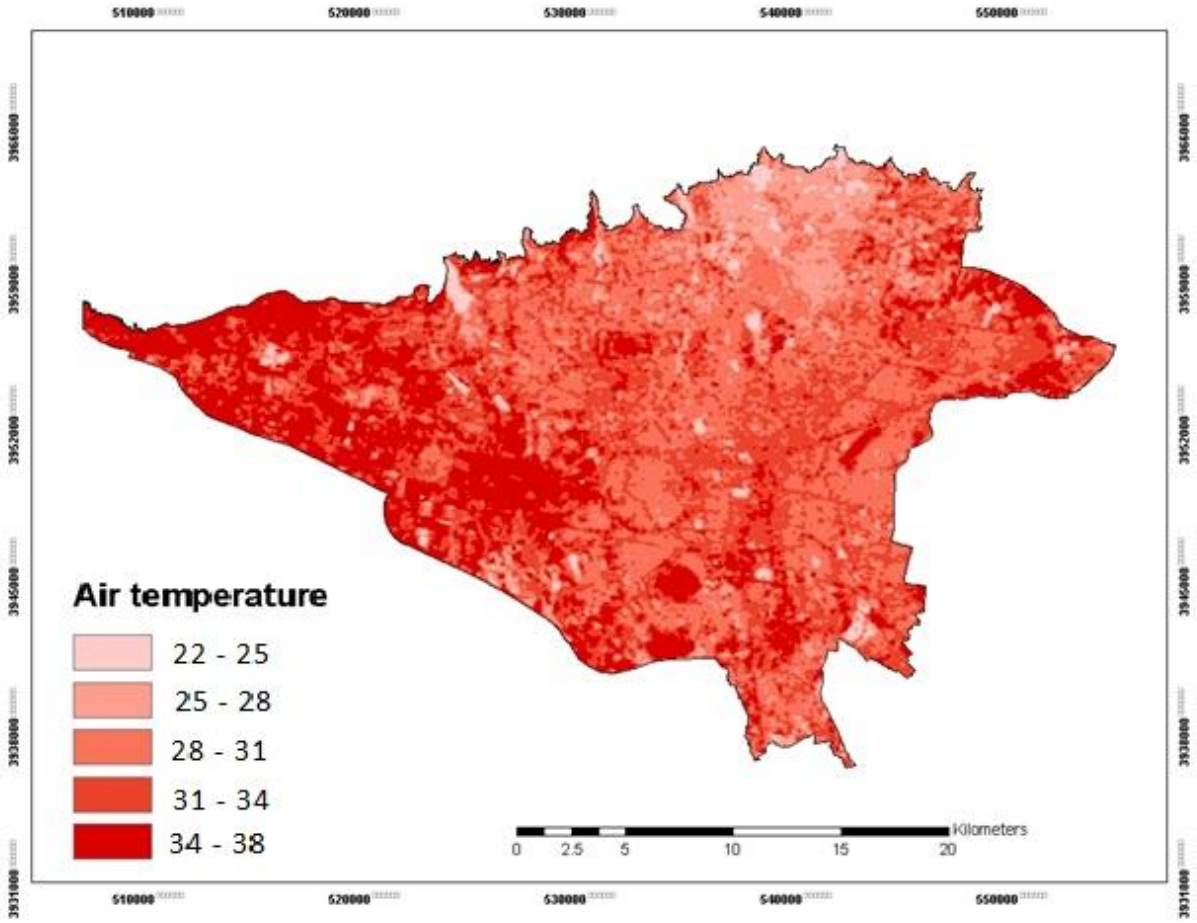


**Figure 5.54 air temperatures in July 2009**

In July 2009, figure 5.54 does not show a change in the air temperature pattern over the maximum and minimum temperatures of the previous ten year. In other words the mid-west is still at maximum temperature, and part of the northeast has the minimum temperature. However, in this year, minimum and maximum temperatures have increased by more than 2 ° C in comparison with the previous period. During this year, the highest degree construction and development took place in Tehran, and the most destruction of vegetation was at this time. This will be examined in detail in chapter 6.

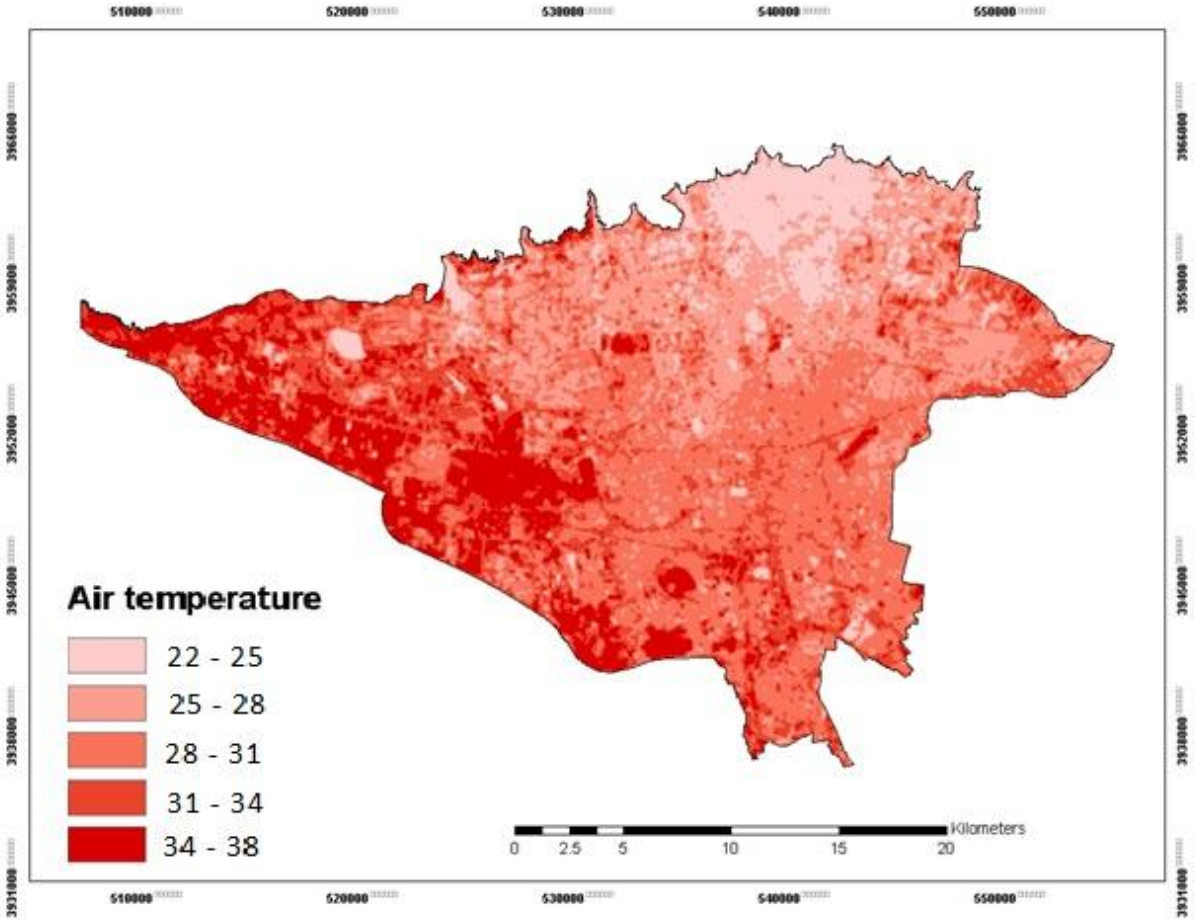


**Figure 5.55 air temperatures in July 2014**

The maximum and minimum air temperatures in figure 5.55 of 2014 shows more than 2°C increase. However, despite this, the temperature pattern continues to follow the pattern of temperature distribution in the 2000 (figures 5.53) and in 2009 (figure 5.54). As in the two previous periods, the highest temperature is observed in the west and the lowest temperature in the northeast. Also the average temperature is in the central, eastern and southern parts.

## 5.6. The field work frame

As mentioned previously, the temperatures of the January and July months studied in this chapter have been derived from the surface temperature maps. Meanwhile, the question of whether the air temperatures obtained from satellite images are reliable or whether the air temperatures recorded on the ground are the same or different from what is likely, is a subject to be considered. In order to determine the accuracy of the air temperature data obtained from satellite images, it is necessary to compare the temperature results of the satellite images and the temperatures recorded on the ground, to indicate how close or different the data are from each other. For this comparison, the ground data and satellite images must be prepared as much as possible simultaneously. In other words, the ground data for a particular time must be recorded at the same time as the satellite image taken. This topic of comparison of the air temperature from the satellite images (LST) and the observed air temperature on the ground was carried out in a field study in the study area (Tehran city), and will be explained here next.

From the geographical points, this city is situated in the geographical longitude of 51 degrees and 17 minutes up to 51 degrees and 33 minutes east with latitude of 35 degrees and 36 minutes up to 35 degrees and 46 minutes north. The area of the city is 730 kilometres square. The approximate east to west distance is 50 kilometres and from north to south is 30 kilometres. The highest altitude of it in the north is 2000 meters and in the south 1050 from the river surfaces.

In research works, many scholars have carried out field studies and one of the important issues in this type of study is the selection of sample points. Depending on the type of study, the number and manner of selecting it can be different. For example, Yang & et al. (2004) with "Estimation of Land Surface Temperature Using Spatial Interpolation and Satellite-Derived Surface Emissivity" in their study area of New England, USA, selected only one sample for their field data and recorded the daily temperature from July 2 to September 26. Also, Lam (2007) in his field study, selected three sample points and recorded his data and examined them. To select the sampling points, Tehran's land cover maps and the classified satellite images of 2014 were surveyed based on land cover types.

## 5.7. Field work data

Since the main goal in this research is to study the impact of land cover on temperature of the city of Tehran, therefore, this was investigate by selecting sample points in the region through a field work by recording the air temperature at these points to compare them with other data already obtained from other sources.The required data in this study are divided in to two parts: Measured temperatures from October until June, and the satellite images taken for the above period.

The overall design of this fieldwork is so that first the air temperatures from October 2015 until June 2016 were recorded continually on selected points on the ground. The next task after choosing the sample points was the recording of temperatures in each land cover type. The bulk of this field work is dedicated to analysing the air temperature as it is the main purpose of the thesis. Accordingly, in this study area field work, 4 regions were selected for sampling. These included : 1. east-north-east 2. west-northwest 3. Centre 4. South

This selection is based on the topography of the area to include the most possible number of land cover types. In each of these regions, land cover types that have the closest distances from each other and the furthest distance from other points were selected. On the other hand, the number of sample points was dictated by the availability of each land cover in the area. For example there are only two water bodies available in the entire study area and in selecting the sample pints in each region it has been endeavoured to include these nearest to other land cover points in each region. Since most of the land cover in Tehran is related to built-up, this type of coverage has the highest number of samples and the water body of the least number of samples. In this field study, 15 samples (figure 5.56) were selected from the types of land cover in the study area and the air temperatures were measured.

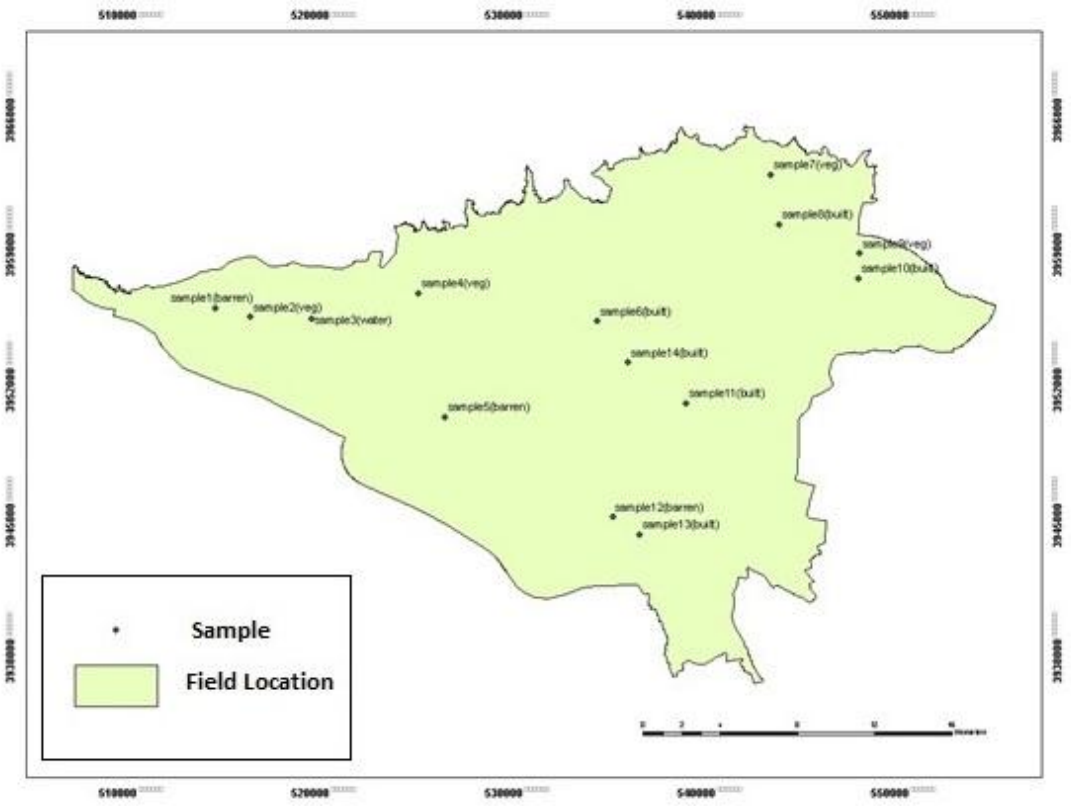


**Figure 5.56 field work location in city of Tehran**

### 5.7.1. Temperature measurement

The goal of recording the temperature in this fieldwork was for the purpose of comparing the temperature in various land cover types with the temperature obtained from the satellite. Also in this fieldwork the aim has been to record the various land cover temperatures on weekly basis over a five month period, using infra-red thermometer. This will be done on the same day and at approximately the same (allowing time to travel from point to point) time and the recorded measurements are shown in a tables 5.15 - 5.19. The temperatures observed for each month are shown in separate tables. In general, Tehran has all four seasons: spring, summer, autumn, and winter. For this fieldwork, (December and November) from the autumn, (February) from winter, (May) from spring and (July) from summer have been selected. The reason for this order has been the fact that satellite images from October 2015 to June 2016 were taken from the USGS website and it has only been possible to use those available with suitable quality. The minimum and maximum air temperatures recorded in each type of land cover have been compared with the minimum and maximum air temperatures obtained from the land cover types of satellite images.

In fact, the ultimate goal is to examine the difference between the temperatures obtained from two sources of observed data and the satellite data.

The temperatures recorded in October (Table 5.18) have been in the order of the highest temperature for barren land 26°C to 39°C, for the built-up between 23°C and 26°C, for vegetation between 21°C and 23°C, and the lowest temperature recorded 20°C to 21°C for water body.

**Table 5.18 air temperature derived from satellite data and Observed temperature in 8 October 2015**

| **October** | **Built up (6 samples)** | | | | | | | **Vegetation (4 samples)** | | | **Barren land (3 samples)** | | | **Water body (1 sample)** |
|---|---|---|---|---|---|---|---|---|---|---|---|---|---|---|
| 8.10.2015 *FT | 25 | 25 | 24 | 24 | 24 | 26 | 22 | 23 | 23 | 21 | 27 | 29 | 28 | 21 |
| 24.10 .2015 *ST | 24 | 23 | 24 | 24 | 23 | 25 | 21 | 21 | 22 | 22 | 26 | 27 | 26 | 20 |
| **Mean** | **24.5** | **24** | **24** | **24** | **23.5** | **25.5** | **21** | **22** | **22.5** | **21.5** | **26.5** | **28** | **27** | **21.5** |
| **Satellite air temperature** | **24** | **23** | **25** | **23** | **25** | **25** | **23** | **23** | **23** | **20** | **27** | **28** | **28** | **23** |

*FT and ST are first time and second time of measurement of temperature in month

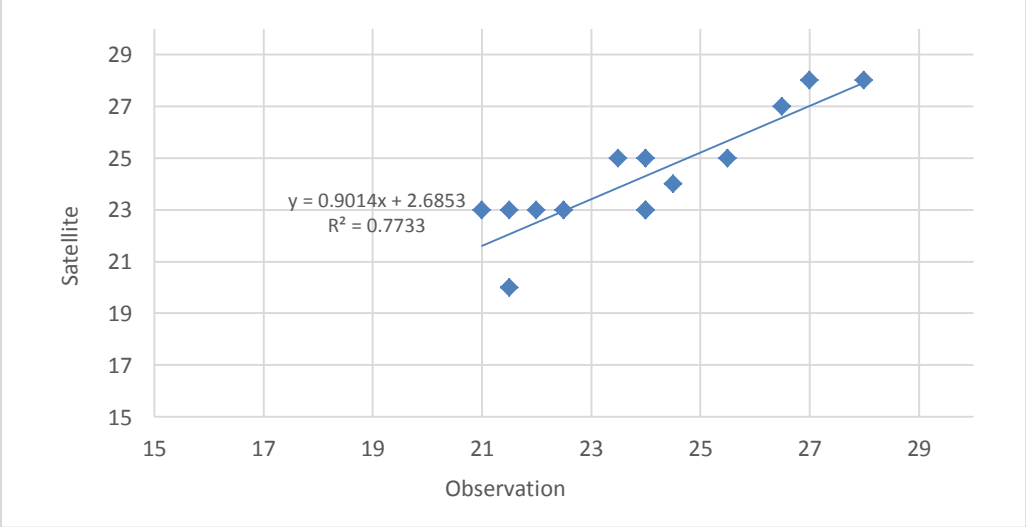


**Figure 5.57- Relationship between air temperature derived from satellite data and the observed temperature in October 2015.**

As the temperatures recorded for November (Table 5.19) show that barren land with between 20°C and 23°C has the highest temperature. After that, built-up with temperature of 18°C to 22°C and vegetation cover temperatures of 19 to 21 have been second and third respectively. The lowest recorded water temperature is 17°C to 18°C.

**Table 5.19 air temperatures derived from satellite data and Observed temperature in 25 November 2015**

| November | Built up (6 samples) | | | | | | Vegetation (4 samples) | | | | Barren land (3 samples) | | | Water body (1 sample) |
|---|---|---|---|---|---|---|---|---|---|---|---|---|---|---|
| 8.11.2015 *FT | 22 | 20 | 20 | 21 | 21 | 22 | 19 | 19 | 20 | 21 | 22 | 22 | 23 | 18 |
| 25.11.2015 *ST | 20 | 18 | 19 | 19 | 20 | 20 | 19 | 20 | 20 | 20 | 20 | 23 | 23 | 17 |
| **Mean** | **21** | **19** | **19.5** | **20** | **20.5** | **21** | **19** | **19.5** | **20** | **20.5** | **21** | **22.5** | **23** | **17.5** |
| **Satellite air temperature** | **19** | **18** | **19** | **19** | **19** | **20** | **19** | **20** | **20** | **20** | **22** | **22** | **23** | **19** |

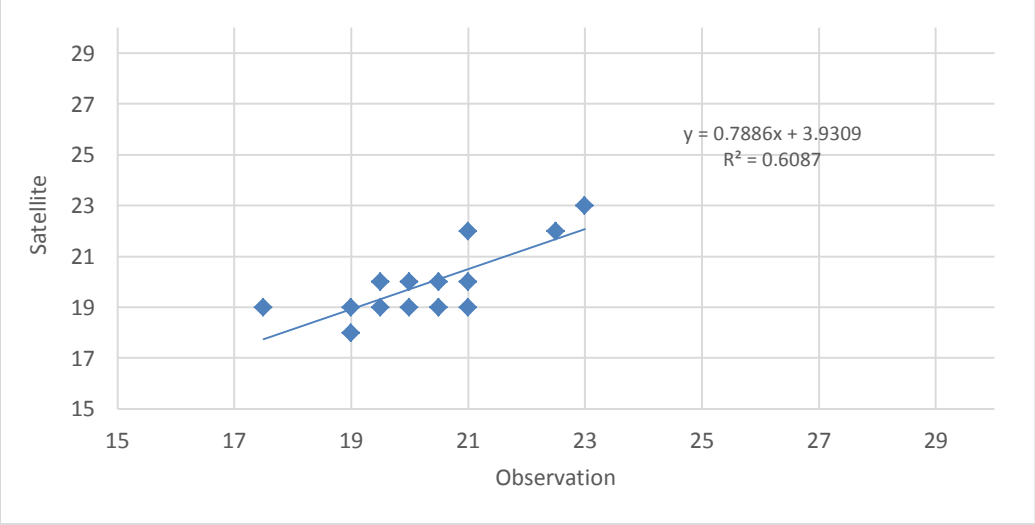


**Figure 5.58 Relationship between air temperature derived from satellite data and the observed temperature in November 2015**

February in Tehran is almost in line with the second month of winter in Persian calendar and after January is the coldest month of the season. As shown in Table 5.20, the recorded temperatures show a significant decrease compared to the previous two months (Tables 5.18 and 5.19). In this month, the highest temperature is related to the Barren land, which shows a temperature between 21°C and 22°C. After that, vegetation with temperature between 15°C and

17°C is in the second position and the built-up with temperatures ranging from 14°C to 16°C in the third place in February. As in the previous two months water body still has the lowest temperature at 15°C to 16°C.

**Table 5.20 air temperature derived from satellite data and Observed temperature in 13 February 2016**

| **February** | **Built up (6 sample)** | | | | | | **Vegetation (4 sample)** | | | | **Barren land (3 sample)** | | | **Water body (1 sample)** |
|---|---|---|---|---|---|---|---|---|---|---|---|---|---|---|
| | | | | | | | | | | | | | | |
| 13.2.2016 *FT | 15 | 16 | 16 | 14 | 14 | 14 | 17 | 16 | 17 | 16 | 21 | 22 | 22 | 15 |
| 25.2.2016 *ST | 14 | 14 | 15 | 17 | 16 | 16 | 18 | 16 | 15 | 15 | 21 | 22 | 22 | 16 |
| **Mean** | **14.5** | **15** | **15.5** | **15.5** | **15** | **15** | **17.5** | **16** | **16** | **15.5** | **21** | **22** | **22** | **15.5** |
| **Satellite air temperature** | **16** | **16** | **19** | **17** | **19** | **18** | **18** | **18** | **17** | **17** | **20** | **24** | **24** | **17** |

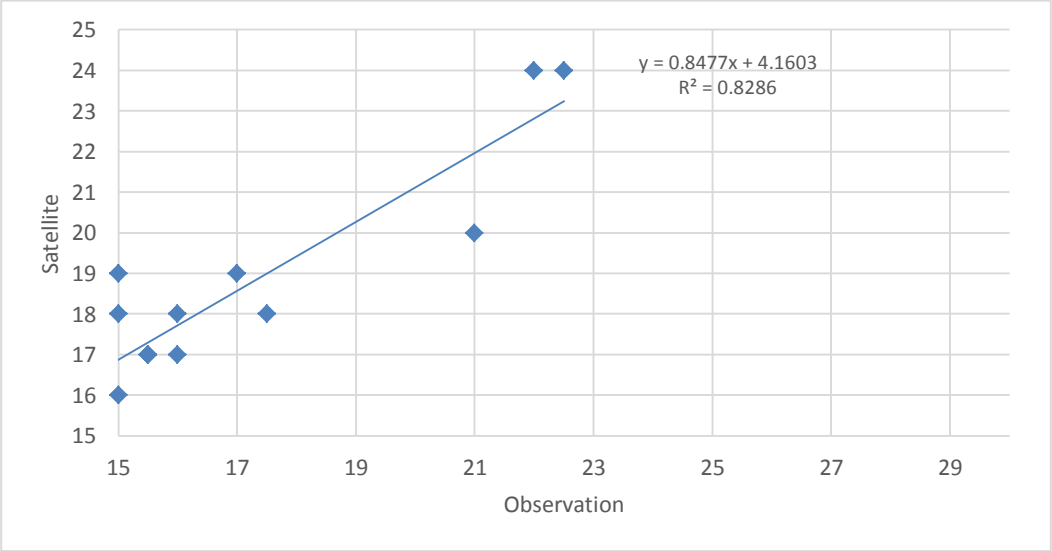


**Figure 5.59 Relationship between air temperature derived from satellite data and the observed temperature in February 2016**

May is the second month of the spring season in Tehran. The highest recorded temperature (Table 5.21) is for Barren lands with temperatures between 32°C to 35°C. The built-up also exhibits a temperature range of 29°C - 30°C and vegetation cover temperatures of 24°C - 26°C. The water body also has the lowest temperature of 21°C.

**Table 5.21 air temperature derived from satellite data and Observed temperature in 19 May 2016**

| May | Built up (6 sample) | | | | | | Vegetation (4 sample) | | | | Barren land (3 sample) | | | Water body (1 sample) |
|---|---|---|---|---|---|---|---|---|---|---|---|---|---|---|
| 5. 5.2015 *FT | 29 | 29 | 30 | 29 | 30 | 30 | 24 | 25 | 24 | 24 | 32 | 33 | 33 | 21 |
| 19.5.2016 *ST | 28 | 29 | 29 | 30 | 28 | 28 | 26 | 25 | 26 | 26 | 32 | 35 | 35 | 21 |
| **Mean** | **28.5** | **29** | **29.5** | **27** | **29** | **29** | **25** | **25** | **25** | **25** | **32** | **34** | **34** | **21** |
| **Satellite air temperature** | **27** | **27** | **28** | **27** | **28** | **27** | **28** | **27** | **26** | **28** | **32** | **34** | **34** | **23** |

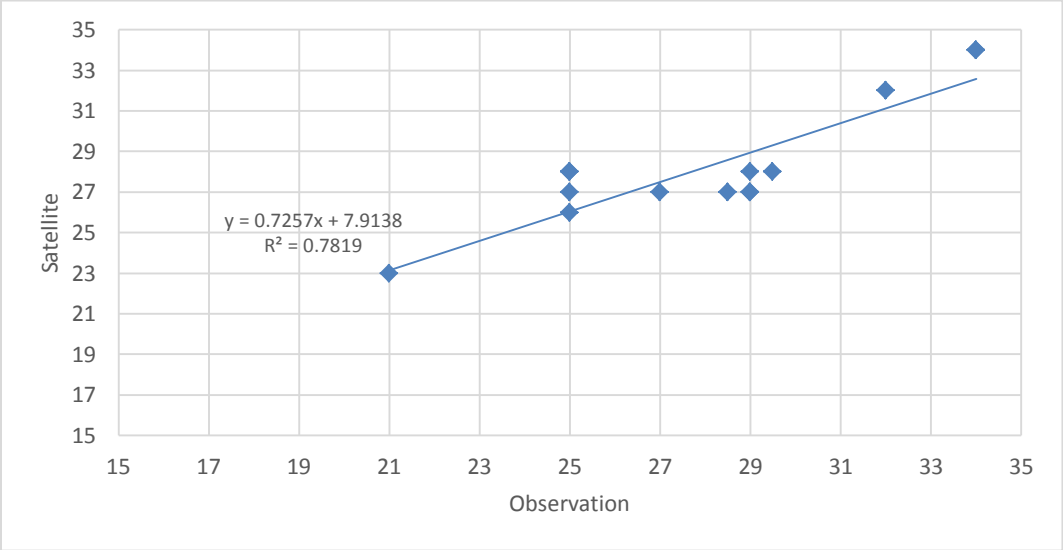


**Figure 5.60 Relationship between air temperature derived from satellite data and the observed temperature in May 2016.**

Summer heat begins from June in Tehran and peaks in July. In fact, June is the second hottest month after July. As in previous months, barren land has the highest temperature, which is between 35°C and 36°C (Table 5.22). After that, built-up with 30°C - 33°C, vegetation cover with 28°C - 30°C and finally water body with 21°C - 22°C are temperatures recorded this month in Tehran.

**Table 5.22 air temperature derived from satellite data and Observed temperature in 20 June 2016**

| June | Built up (6 sample) | | | | | | | Vegetation (4 sample) | | | Barren land (3 sample) | | | Water body (1 sample) |
|---|---|---|---|---|---|---|---|---|---|---|---|---|---|---|
| 5.6.2016 *FT | 31 | 31 | 32 | 32 | 32 | 33 | 30 | 28 | 28 | 28 | 35 | 36 | 35 | 21 |
| 20.5.2016 *ST | 32 | 31 | 33 | 33 | 32 | 33 | 31 | 30 | 30 | 30 | 35 | 36 | 36 | 22 |
| **Mean** | **31.5** | **31** | **32.5** | **32.5** | **32** | **33** | **30.5** | **29** | **29** | **29** | **35** | **36** | **35.5** | **22.5** |
| **Satellite air temperature** | **30** | **30** | **31** | **30** | **30** | **31** | **30** | **28** | **27** | **27** | **36** | **36** | **36** | **24** |

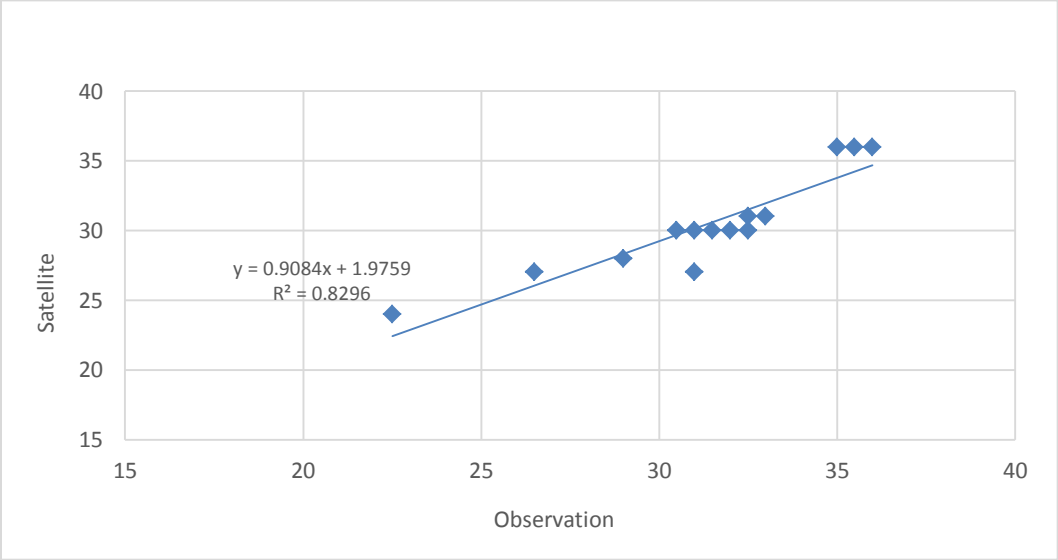


**Figure 5.61 Relationship between air temperatures derived from satellite data and the observed temperature in June 2016**

Investigating the temperatures recorded in Tehran showed that in all these months the barren land areas had the highest temperature. After that, the built-up areas showed the next highest temperature, and the vegetation comes after the two previous types of land covers. Only in February, which is considered to be one of the cold months of year, the vegetation temperature is slightly higher than the built-up. During the whole of this study period, the water body showed the lowest temperature. The next phase of this fieldwork is dedicated to examining and calculating the temperature of the satellite imagery of the same 5 months.

### 5.7.2 Satellite image of the field work

Thermal band of the 5 month's images were prepared in the same way as described in chapter 4 and their surface temperatures were calculated. The recorded temperature in each land cover in each month must be compared with the satellite images of the same month. This is where the question of, "can we compare the air temperature with land surface temperature?" arises. The comparison of measured air temperature with retrieved temperature from the satellite images does not give a reliable result. Therefore, with respect to the relationship of LST and air temperature which has already been established by some researchers, LST can be converted to air temperature. One of the simplest and most appropriate linear models is suggested by. (Garcia-cuto 2006).

$Ta = 14.6 + 0.44 \times LST$

Ta = temperature of air

Providing the land surface temperature is available from the measuring devices, using the above relationship the air temperature can be obtained. Then, the result can be compared with the recorded temperature from the fieldwork study.

In Figures 5.53-5.57 of the air temperatures, the position of each sample point measured in the fieldwork region has been determined. The goal here is to determine what temperatures are observed at which temperature range.

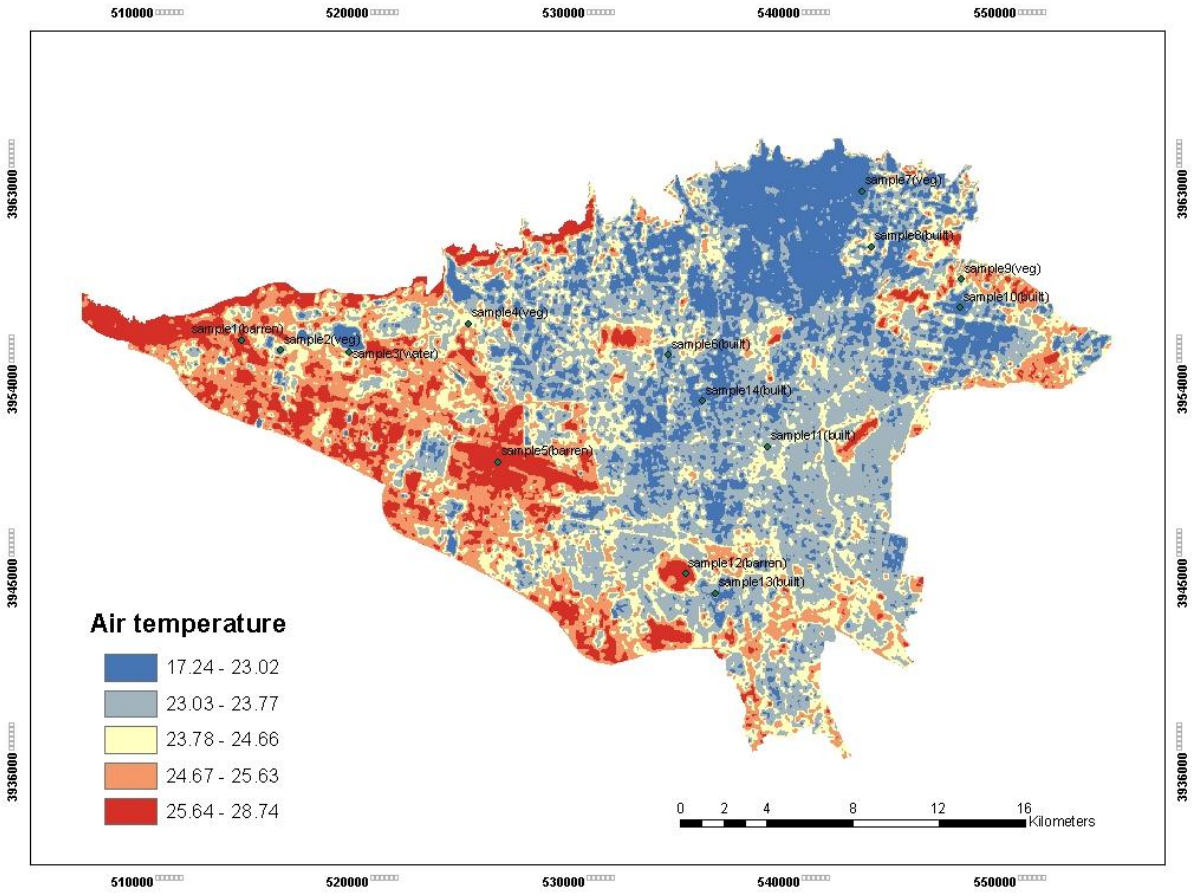


**Figure 5.62 air temperatures in October 2016**

In this month, all samples of barren lands are placed in the maximum temperature range. The figure 5.62 shows temperatures between 25 - 28.7 °C. The built-up in this figure is located at 23 - 23.7 °C range. Two samples out of four vegetation samples are located at 23 - 23.7°C and two others at the 23.7 - 24.6°C ranges. Water bodies are at the lowest temperature range.

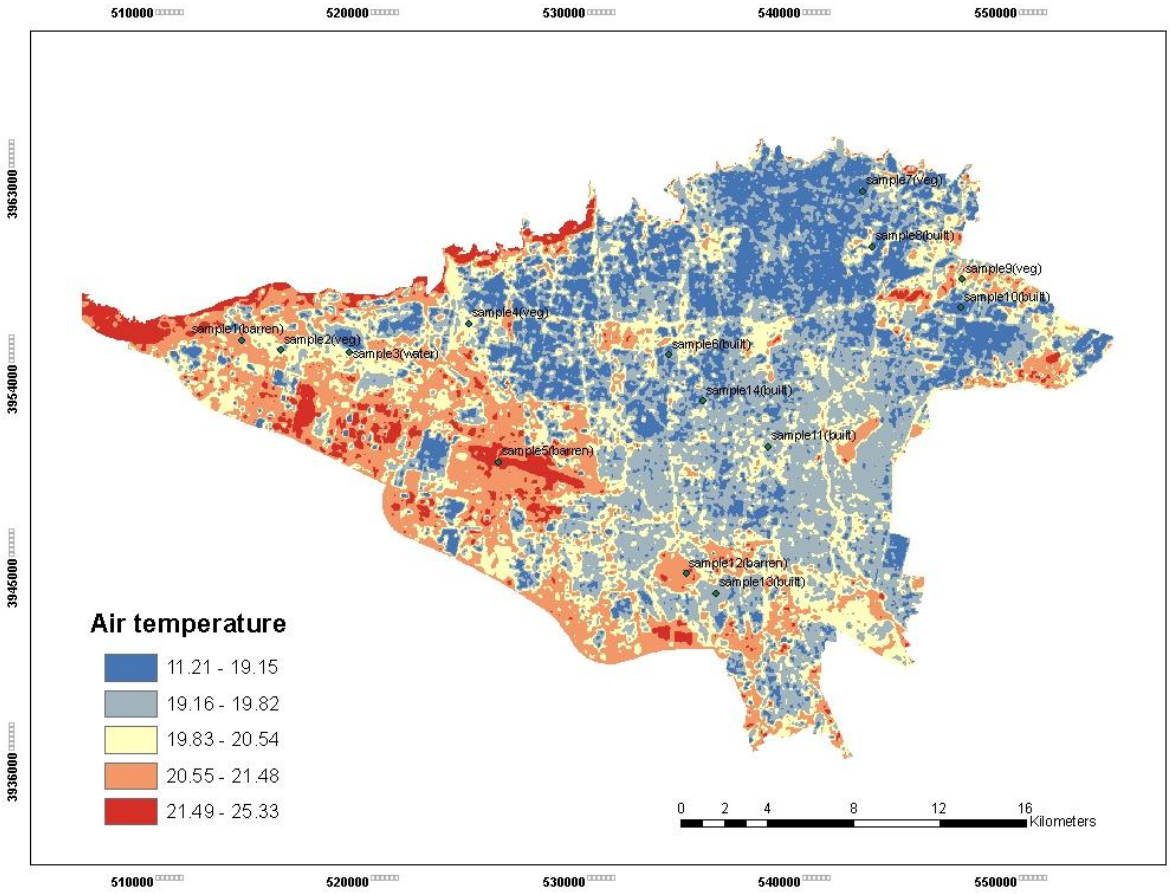


**Figure 5.63 air temperatures in November 2016**

The temperatures of barren land fall in the two temperature ranges which show the highest temperatures of 20.5 - 25°C, (figure5.63). After that, both the built-up and vegetation covers fall approximately in the same temperature range from 19°C to 20°C. The water body is also located in the minimum temperature range of 11 - 19°C.

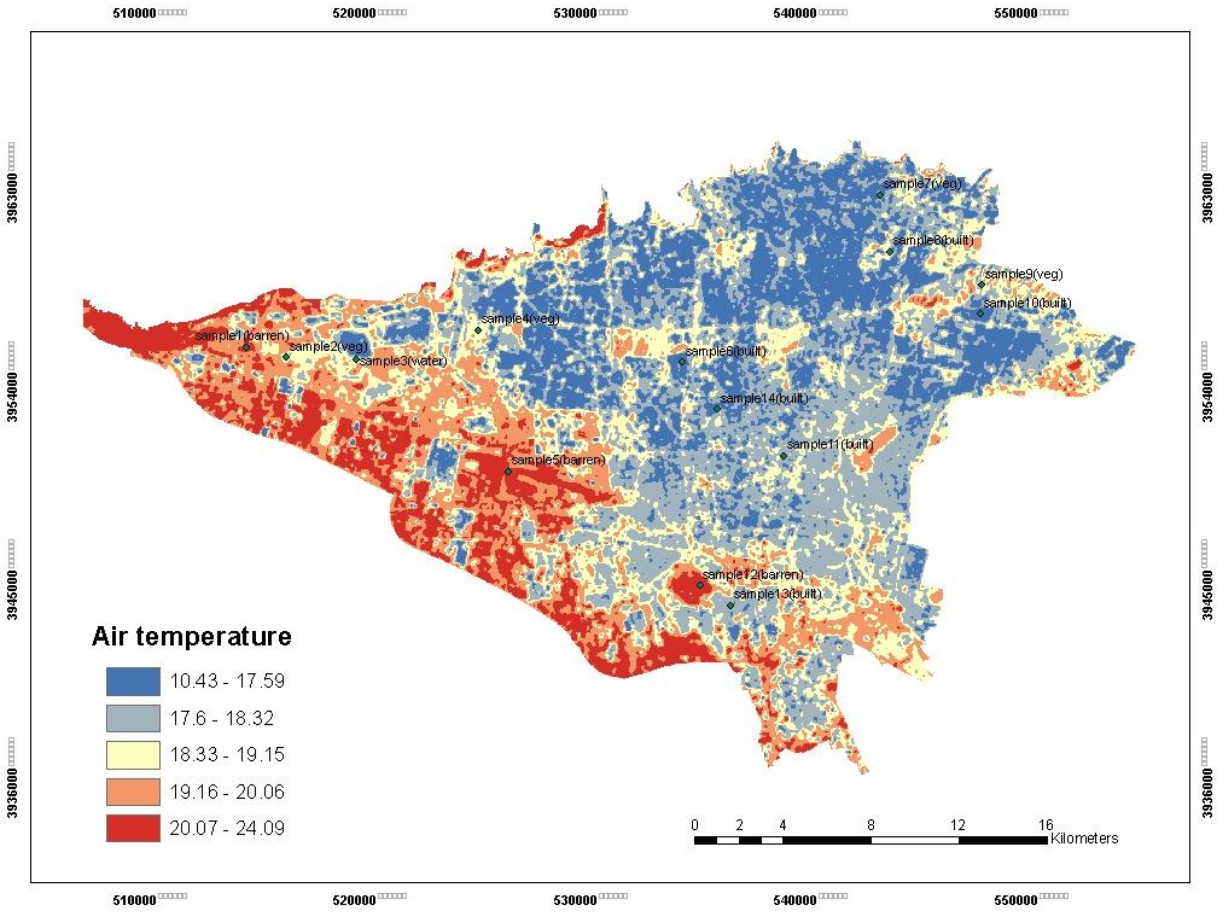


**Figure 5.64 air temperatures in February 2016**

In February, (figure 5.64) as well as in the two Figures of 5.62 and 5.63, barren lands are at the highest temperature range between 20 to 24°C. In this month, vegetation cover, except for one case, shows temperatures between 18 and 19°C, while the built-up are set at a temperature range of 17 to 18.3°C. The water body is located in the lowest temperature range, as in previous months.

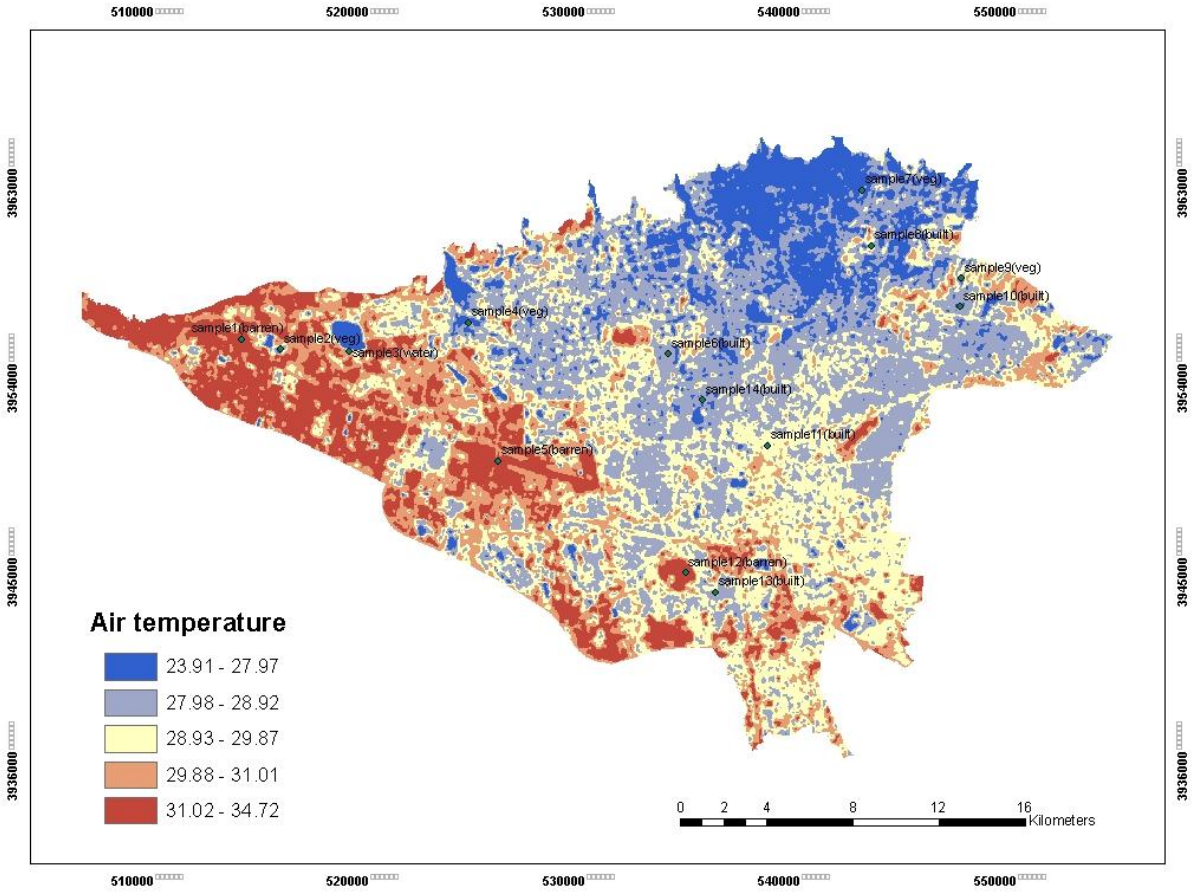


**Figure 5.65 air temperatures in May 2016**

Figure 5.65 shows the temperature of the samples during the month of May. In this month, barren lands like the previous months are at a maximum temperature range of between 31 and 34°C. The samples of the built-up fall in the range of between 27 and 29°C and vegetation are also shown in temperature range of 23 - 28°C. The water body is also at minimum temperature.

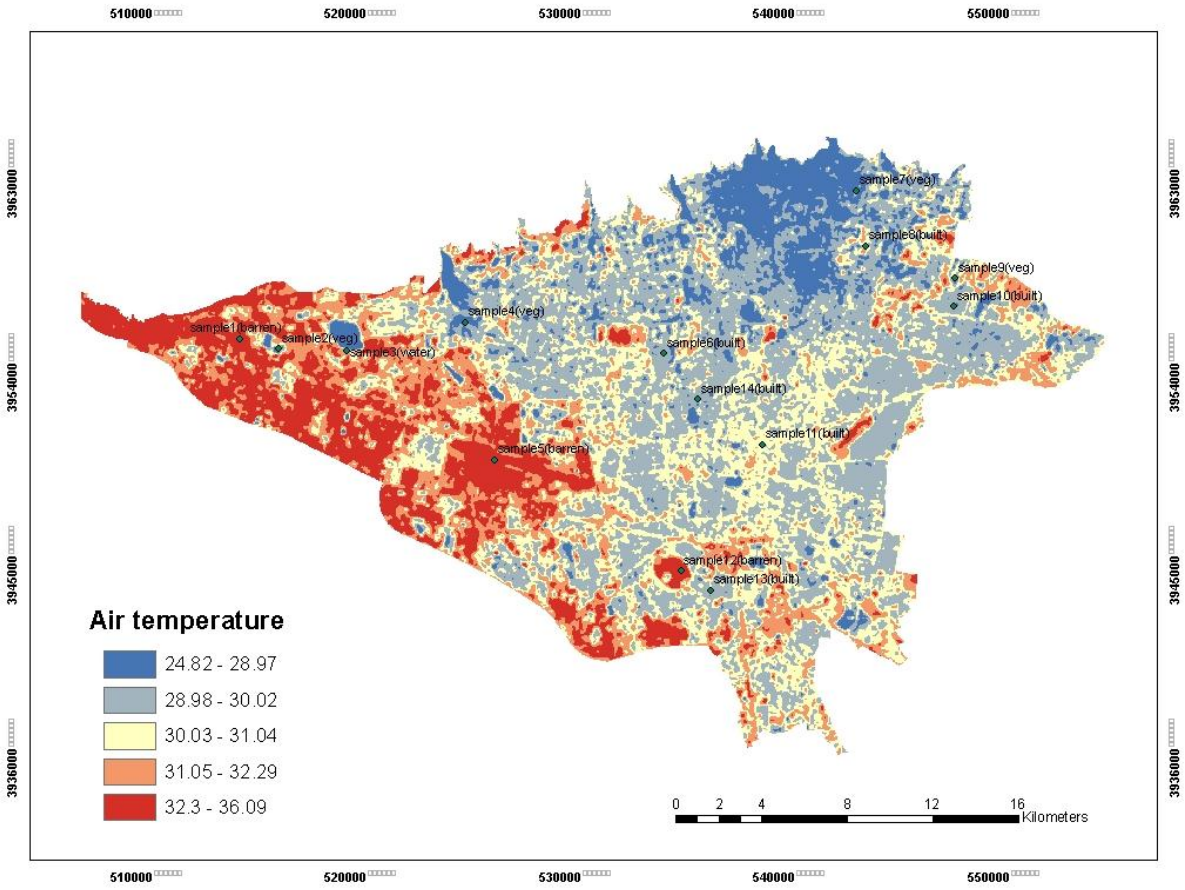


**Figure 5.66 air temperatures in June 2016**

In June, (figure5.66) barren lands are set at a temperature of 32 - 36°C, which is the maximum temperature, and the built-up also show temperature range of 30 - 31°C. Vegetation is also in the 24 - 28°C and 28 - 30°C ranges, and the water body is in the lowest temperature range, as in previous months.

## 5.8. Summary

As shown in figures 5.48to 5.51, the minimum January temperatures for all years were between 5 and 7°C. At maximum temperatures, there is a higher fluctuation between 19 and 24°C, which represents 5°C of difference in different years, and does not show regular trend but mostly shows maximum temperature fluctuations. In addition to temperature fluctuations, the study of air temperature maps for July 1991 to 2015 also showed that the pattern of air temperature distribution has changed over the course of three decades. The maximum temperature in 2015

(figure 5.51), temperature indicates a displacement from the north to the west. This change in temperature pattern can be related to land cover changes during this period. The maximum change in land cover and expansion of the city occurred, in 2015 (figure 5.51). In this figure the maximum temperature is in the southwest.

Figures (5.52 - 5.550) show the minimum and maximum temperatures for July from 1990 to 2014. In any of the cases (minima and maxima) there is no distinct sequence to indicate a regular increase or decrease in temperature during the study period. As for the January, temperature fluctuations are also observed during the study period.

The study of the air temperature in the figures of 5.62-5.66 in 215-2016 field work shows that the distribution of the temperature pattern in hot and cold months is similar to the distribution of the temperature pattern of January 2015 and July 2014. This means that the mid-west has the highest temperature and the northeast has the lowest. The central and southern regions of the city also show the temperatures between these maximum and minimum temperatures. In fact, in the last few years, the pattern of temperature distribution does not show a significant change.

Also, the comparison of the recorded temperatures (tables 5.18 to 5.22) and air temperatures drawn from the figures (5.62 to 5.66) indicate a temperature difference of 1°C -1.5°C between the observed air temperature and the air temperature drawn from the satellite images. The regression between the observed air temperatures and those from satellite images show a rather high correlation. This correlation for the month of October is 0.77, November 0.60, February 0.82, May 0.78 and June 0.82 (figure 5.57 to 5.61).

## Reference

1. Ardekani.M, Kousari, Esfandiari 2014, Assessment and mapping of desertification sensitivity in central part of Iran, International journal of Advanced Biological and Biomedical Research, Vol. 2, PP. 1504-1512

2. Kataoka, Kumi, Matsumoto, Futoshi., Ichinose, Toshiaki., & Taniguchi, Makoto. Urban warming trends in several large Asian cities over the last 100 years. Science of the Total Environment, Vol 407, PP. 3112– 3119.

3. Hung, Tran, Uchihama, Daisuke, Ochi, Shiro & Yasuoka, Yoshifumi. Assessment with satellite data of the urban heat island effects in Asian mega cities. International Journal of Applied Earth Observation and Geoinformation, Vol.8, PP. 34–48.

4. Sadeghinia.A, Bohloul Alijani. 2015. Spatial and Temporal Analysis of the relation of urban heat island with vegetation cover in Tehran. Journal of Tethys, Vol. 3, No. 3, PP. 237-250.

5. Widyasamratri 2013, A comparison of air temperature and land surface temperature to detect urbanization effect in Jakarta, Indonesia, Atmosphere & Oceanography & Climate change, University of Yamanashi, Japan.

# Chapter 6

## Concluding chapter

### 6.1 Changes Detection assessment

The land cover change matrix for the period 1990-2000 states the total variation in the land cover in the studied area (Table 3.8). One of the land covers that has changed a lot during this period is barren land. Barren land area, in 1995, was 32,410.31 hectares and out of all that area only 1539.14 hectares have remained unchanged. 28,988 hectares of the remainder being the majority have changed to built-up cover.1870 hectares have been changed to vegetation and 12 hectares to water body. An important consideration in comparing the total coverage of each land in the 1990s and 2000s is the shift in land use and vegetation cover in favor of the built-up cover. The survey of Barren land in 1990 and 2000 land cover (Fig. 3.23) clearly shows that an important part of the barren lands in the north and west of the city have been converted into built-up, with the total built-up area reaching 37,251.83 hectares from 15,780.18 hectares. From 1990 to 2000, barren land lands total shrunk by 25.9% to 19.3% of the total area of the city, vegetation from 21.5% to 19.8%. On the other hand the built-up cover has increased from 52% to 61% of the total area of the city.

Between 2000 and 2009, the most drastic conditions for land cover change occurred in Tehran. In this period vegetation reached its lowest level of 11.6% (Table 3.7). Unlike the previous period (1990-2000), the barren lands did not only show a decrease, but also increased by 23.9%. Similar to the previous period of 1990-200 the built-up area in this period increased by 64.3% (Table 3.7), which according to the change matrix this is 39445.47 hectares of the city area (Table 3, 9). In fact, a major part of the vegetation cover of the study area was converted to barren lands and built-up, which means that the decline of vegetation was from 12169.08 hectares to 7164.99 hectares. Figure 3.27 clearly shows the vegetation change to the built-up in the north-east of the study area.

The expansion of built-up continued to increase in 2009 to 2014 (Figure. 3.28) to reach 68.9% (Table 3.7). According to the change matrix in this period (Table 3.10), 42893.37 hectares

of the total land of the city are allocated to built-up. During 2009-2014, barren lands show a significant decrease compared to the previous period. In this period, the total of barren land area has reached 10.8%, which is the smallest amount in the whole of the study period (Table 3.7). During this period, we witnessed an increase in vegetation cover in the studied area, which has reached 12,159.27 hectares from 7,164.99 hectares (Table 3.10). A slight, but rather noticeable change occurred during this period in the land cover change, which is the creation of a lake in the area and this is one of the most important water bodies and situated in the northwest of the study area visible on the map (Figure. 3.21). In this period (2009-2014), barren land has fallen by 13% since the previous period, which means that barren lands have been converted to water body, built-up and vegetation cover.

In general, the results of land cover changes in Tehran indicate that during the study period of 1990 - 2014, a significant part of the barren land and vegetation have been converted in favour of built-up. The expansion of built-up has taken place in all directions from the north, south, west and east, from 1990 (Figure 3.18) to 2014 (Figure 3.22). In fact, like many other major cities in the world, Tehran with increasing population, especially migrant populations, from small towns and villages as well as industrialisation has faced urbanization. This factor has led to the increased building and construction and consequential encroachment and advance to barren land and vegetation land cover in and around the city. This change has been so severe that even the relatively steep slopes in the north of the city and the proximity to the semi-arid parts of the South and that of the Mehrabad Airport in the west of the city could not limit the expansion of the city to these areas and beyond. The largest part of this expansion and density has been in the western half of the city.

The study of the temperature time series of the city meteorological stations (Fig. 2.1), shows fluctuations in temperature (Figures 2.2 and 2.3.2.5). Also at one of the stations there is a sudden change in decreasing temperature (Figure 2.6). And on the time series there is no confluence of lines for one of the stations (fig. 2.4). These fluctuations and the sudden change of temperature were in the direction of increase of the minimum temperature. There was no significant trend seen in any of the time series for any station. Fluctuations (Figures 2.8 and 2.7) and sudden temperature changes (Figures 2, 10 and 2.9) are also seen in the mean maximum temperature time series. Only at the Chitgar Station (Figure. 2.11), a temperature increase trend

is observed. In sum, fluctuations and sudden changes in the time series of the monthly minimum and maximum temperatures of all five stations in Tehran show a rise in temperature. The dominant position in the long-term time series of Tehran's stations shows a disorder in the decrease and increase in temperature over the years and according to Prof. Alijani, these irregularities can be the beginning of climate change in this area. As well as these irregularities, the July air temperatures obtained from the satellite images do show any particular increasing or decreasing order in temperature during the study period. The study of the air temperatures retrieved from the images demonstrate high temperatures previously observed in the northern half, are now weakened and gradually drawn to the southwest. In fact, during the three consecutive periods under study, the air temperature distribution pattern has changed (figures 5.52-5.55). This is also the case for the January air temperatures. During this period, there is no specific increasing or decreasing order in temperature and what is certainty is the change in temperature distribution pattern (figures 5.48-5.51). During the study period, the highest temperature has gradually moved over to the southwest region. The analysis so far prove that the time series and satellite images represent temperature fluctuations and show no consistent trend that confirms the increase or decrease of temperature during the study period.

### 6.2 Study of classified lands air temperature

Minimum and maximum air temperatures for each land cover type for the months of January and July were calculated for all years (figures 6.67-6.74). The results indicate the effect of the land cover on the air temperature.

The study of July minimum temperature for the built-up from 1990, 2000, 2009 and 2014 shows a gradual increase during the study period (figure 6.67). During this period, the minimum temperatures are 23°C, 25°C, 27°C and 30°C. Simultaneous with minimum temperature, the distribution of built-up has been recorded from 52.4% -60.7% -64.3 to 68.9 (Table 3.7). In other words, built-up expansion has been accompanied by an increase in the minimum temperature in July throughout the study period.

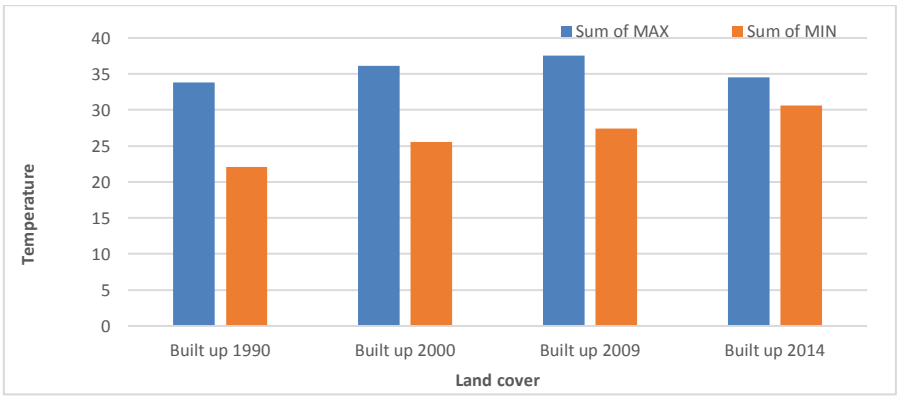


**Figure 6.67 built up air temperature in July (1990-2014)**

In the case of the minimum temperature in July for barren land (Fig. 6.68), this increasing temperature trend can be seen from 1990 to 2014. In fact, barren lands, same as the built-up, have experienced a rising trend in temperature. This temperature increase in barren land occurred while the total area of this land cover had decreased from 25.9% in 1990 to 10.8% in 2014(table 2.7) and (figures from 3.25to3.27).

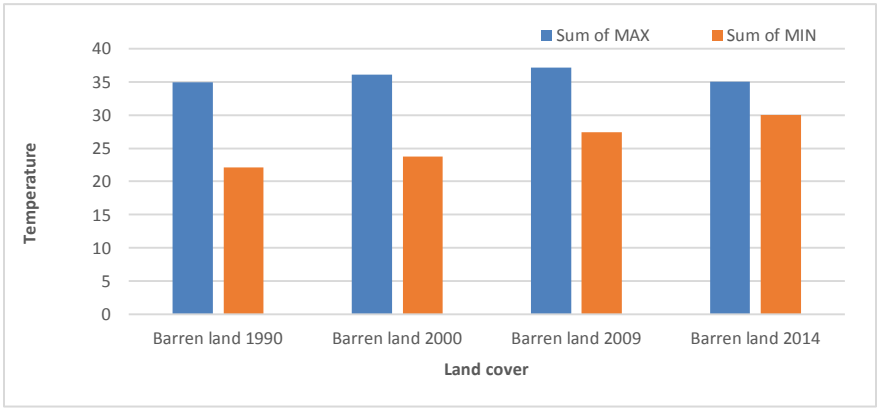


**Figure 6.68 barren land temperature in July (1990-2014)**

The maximum temperature in July for barren land and built-up has increased during the study period from 1990 until 2009. However, in 2014 the temperature has decrease and this disrupted the temperature increase trend.

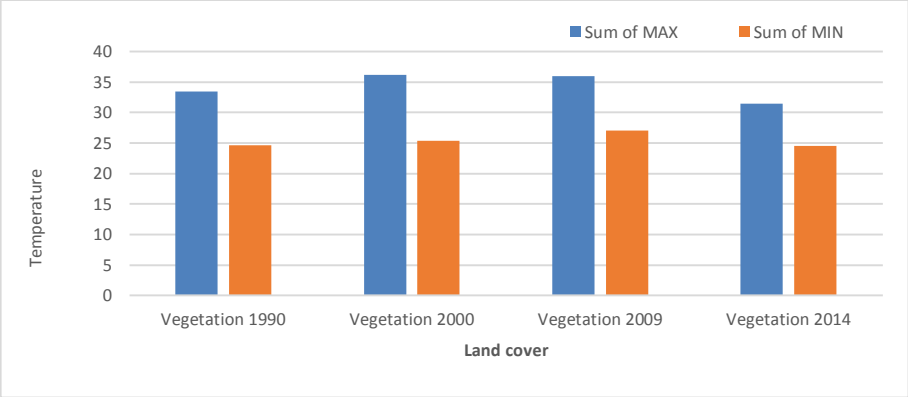


**Figure 6.69 vegetation air temperature in July (1990-2000)**

The minimum and maximum temperatures of July in vegetation cover have had the same trend during the studied period (figure. 6.69). The vegetation cover area in the years 1990, 2000 and 2009 was 21.5%, 19.8% and 11.6% (Table 3.7) and the minimum temperature was 24°C, 25°C and 27°C, respectively. Comparison of these figure shows that the decrease in vegetation has been proportional with an increase in temperature over three periods. In 2014, vegetation shows an increase of 8% compared to the previous period (Table 3.7). In the same time, a temperature drop of 2.5°C degrees since the previous period shows a temperature of 24.5°C. The maximum temperatures for the periods 1990, 2000 and 2009 for vegetation have increased, reaching 33.5°C, 36°C and 35.5°C. The maximum temperature which has been rising along with the minimum temperature until 2009, has decreased in 2014 and this change in temperature, corresponds to the decrease and increase in vegetation cover.

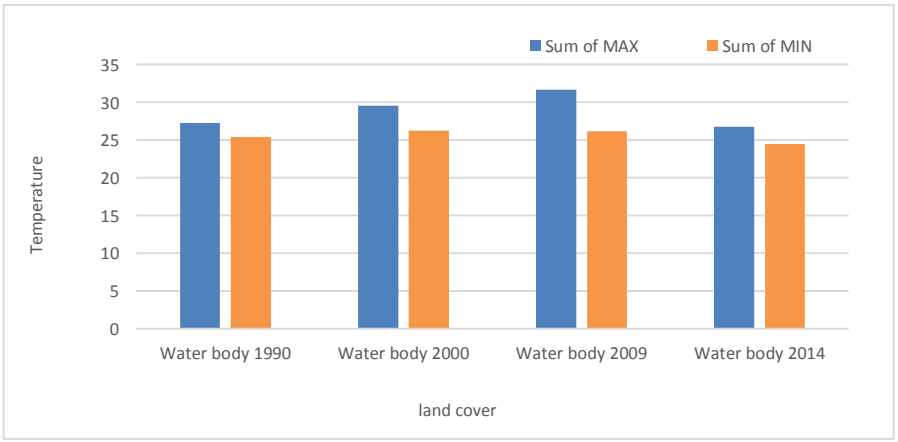


**Figure 6.70 water body air temperature in July (1990-2000)**

Water body in Tehran occupies a very small area including several small lakes, the largest of which was built in 2013 in the west of Tehran (figure 3.22). During the studied years, water body has had a near constant temperature, except in 2009, which shows the highest temperature (figure 6.70).

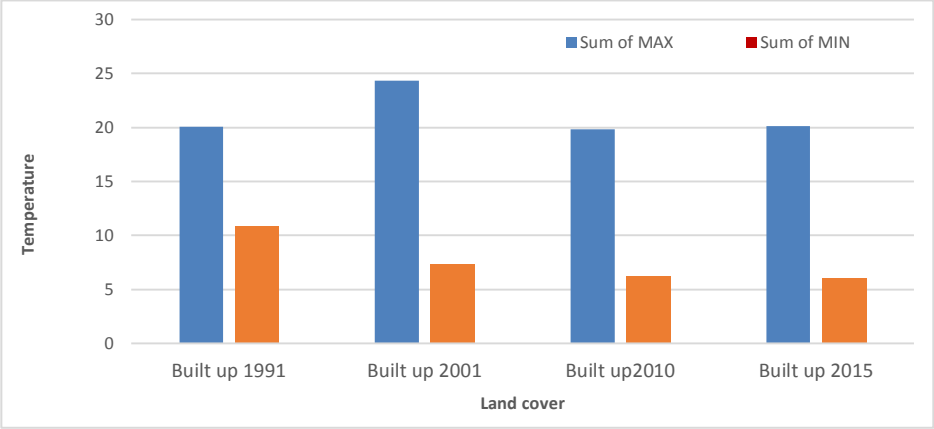


**Figure 6.71 built up air temperature in January (1990-2014)**

The figure 6.71 shows the minimum and maximum temperatures of January for the built-up from 1991 until 2015. The minimum temperatures in January of the years of 1991- 2001-2010 and 2105 were 10°C, 7°C, 6°C, and 6°C s, respectively. The maximum temperatures for the built-up during the years of 1991-2001-2010 and 2015 were 20°C, 20°C, 24 and 20°C respectively and the highest temperature occurred in 2001. In general, there is no specific increasing or decreasing pattern in the minimum and maximum temperatures.

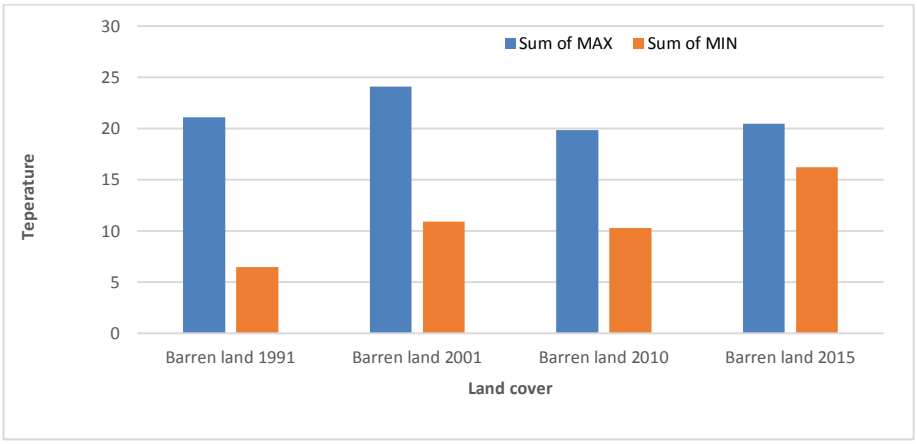


**Figure 6.72 barren land air temper in January (1990-2014)**

In the Barren lands, the minimum temperatures in the years 2001-2010, 1991, and 2015 are respectively 6.5°C, 10.8°C, 10.3°C, and 16°C, indicating an increase in the minimum temperature (figure 6.72). The maximum temperature of January for barren lands relates to 2001.

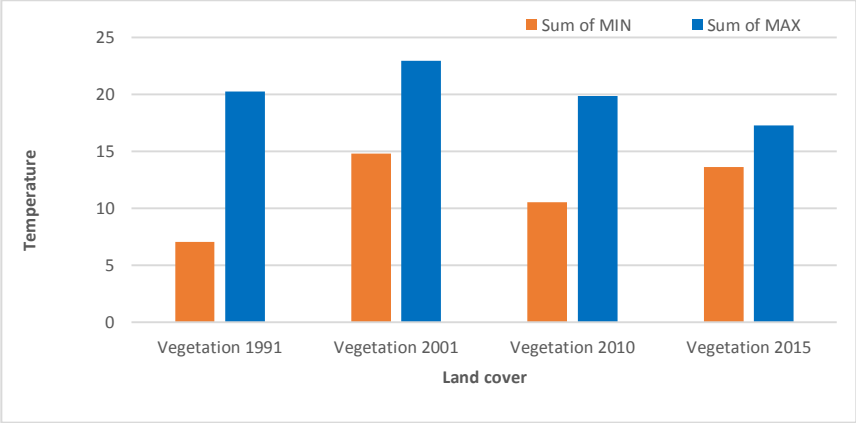


**Figure 6.73 vegetation air temperature in January**

The temperature status of January and the vegetation cover during the study period (figure 6.73) is similar to the temperature in July months (figure 6.69). As discussed earlier in this chapter, the decrease and increase in minimum and maximum temperature has had an opposite relationship with the decreases and increase in vegetation cover over the years. During the years when vegetation has decreased, the temperature has increased and the temperature has decreased with increasing vegetation. The highest temperature of January was recorded for vegetation in 2001, which according to (figure 3.27) is the year with the largest vegetation ruin in the period 2000-2009. In 2015, with the increase in vegetation cover, temperature has dropped.

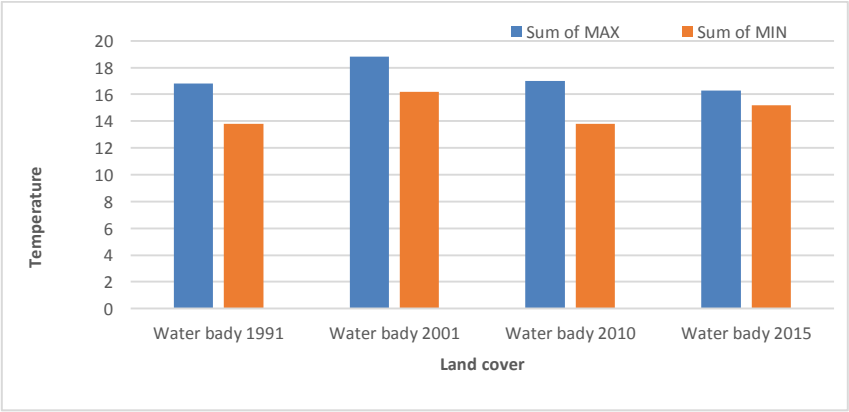


**Figure 6.74 water body air temperature in January**

As already mentioned, water body has a very small share of land cover in the region. The water body temperature of January has fluctuated in the studied years with the least temperature less than 13°C and the maximum has not exceeded 18.8°C.

## 6.3. Conclusion

The survey of the land cover in Tehran from 1990 to 2014 indicates significant changes in the land cover of the study area. This change in land cover was in line with the conversion of barren land and vegetation to Built-up. Nevertheless, the land cover change matrix indicates that during the studied periods parts of the Built-up were turned into other lands such as barren land and vegetation, which could be questionable. The reason for this is that in this research all buildings and constructions such as industrial centers, small airport buildings and military barracks have correctly been included in the built-up category. However, Bearing in mind that during the last few decades, many efforts have been undertaken by the municipality to shut down these centers or move them around or to the outskirts of the city, the result was that a major part of these old buildings and constructions were demolished. The main objective was to create parks, green spaces and playgrounds, since Tehran had a shortage of space with more than 11,000 people per square kilometer. One of the last of these widespread changes has been the conversion of a large military base and a huge airport into a district park as well as the construction of a lake. To this list, the demolition of worn buildings and the conversion of green spaces should also be added. In contrast, the barren lands around the city were converted to built-up. Also vegetation around the city changed, either due to drought or due to unauthorized constructions, especially in the highlands of the north and northeast of this city.

The fact is that as a result of the expansion of urbanization and the increase in construction, there have been widespread changes in the land covers of this city, which has changed the pattern of urbanization. In fact, the increase in construction, especially in the south-western part of the city, has caused an increase in maximum temperature in the southwest. It should be mentioned that the existence of an important highway in the western part between Tehran and the industrial city of Karaj is considered the most important industrial axis surrounding most of

the light and even heavy industry such as several automotive manufacturing plants with the need to easy transit access is located here.

These changes in land cover has not only changed the pattern of temperature distribution on the city, but also has increased the temperature in built-up areas and barren lands and this change in the pattern of temperature distribution correlates with the change in land cover.

In all, the results of the air temperature time series studies, as well as the simultaneous comparison of the temperature from the satellite images and the observed temperature (what was done in the fieldwork), support each other in confirming the existence of irregularities and fluctuations. Ultimately, the final analysis of temperature status and land cover situation can be concluded as the following:

1- The minimum temperature in July has increased in all the years in Built-up and barren lands.
2- The maximum temperature in July on Built-up and barren land is irregular and fluctuating.
3- The minimum and maximum temperature of vegetation in July and January has changed proportional to the increase or decrease in the surface area of this land cover. That is, by increasing the vegetation, a temperature drop has been observed and the temperature has increased by reduction in vegetation.
4- The minimum temperature of July has increased in barren lands.
5- The minimum temperature of July has decreased in built-up areas.
6- The minimum and maximum temperatures of water body in July and January has shown the lowest fluctuation.
7- The regression between the air temperature from satellite images and the observed temperature shows a correlation between 60% -82%.
8- There were no incremental or decreasing trends in the time series of the minimum and maximum temperature of ground station data. There are sudden fluctuations in all stations.

In sum, the study of air temperature from ground based stations and satellite images indicates fluctuations and irregularities. The air temperature results obtained from satellite

images are consistent with the results obtained from the time series. The relationship between temperature distribution pattern change and land cover change is well evident. Changes in land cover and expansion of built-up areas have caused a change in the temperature distribution pattern, more than being the cause of incremental temperature trend. These irregularities can be considered as an introduction to the beginning of change in the study region.

This is a warning to prevent actions that exacerbate temperature disruptions. The city of Tehran and other large cities of Iran, which have almost the same situation with land cover changes, must reduce the impact of irregularities and even climate change by controlling these changes. The impact of temperature fluctuation, which is more in the direction of increase in temperature, can have adverse effects on other climatic factors. The consequential effects of these on a semi-arid land such as Iran can lead to irreparable damage, which is beyond the scope of this thesis.